DEVELOPMENT AND APPLICATION OF SURFACE COATINGS FOR MICROCHIP CAPILLARY ELECTROPHORESIS-ELECTROSPRAY IONIZATION-MASS SPECTROMETRY ANALYSIS OF BIOLOGICAL ANALYTES

Nicholas G. Batz

A dissertation submitted to the faculty at the University of North Carolina at Chapel Hill in partial fulfillment of the requirements for the degree of Doctor of Philosophy in the Department of Chemistry.

Chapel Hill
2014

Approved by:

J. Michael Ramsey

James W. Jorgenson

Nancy L. Allbritton

R. Mark Wightman

Anne M. Taylor

ABSTRACT

Nicholas G. Batz: Development and Application of Surface Coatings for Microchip Capillary Electrophoresis-Electrospray Ionization-Mass Spectrometry Analysis of Biological Analytes
(Under the direction of J. Michael Ramsey)

This work describes the development of improved surface coating methods for microchip capillary electrophoresis-electrospray ionization-mass spectrometry (CE-ESI-MS) and their application for the analysis of biological analytes. A new coating method based on chemical vapor deposition (CVD) of aminopropyl silane (APS) reagents is demonstrated. The method improved the efficiency of separations over previously used surface coatings while also promoting batch processing of multiple devices at once. The separation performance was quantified using a new efficiency metric based on CE theory. Microchips coated via CVD produced the most efficient liquid phase separations coupled to MS reported to date.

The CVD method was found to produce a base layer well suited for subsequent modification. APS surfaces administered via CVD were modified with n-hydroxy succinimide (NHS) esters of polyethylene glycol (PEG) with varying PEG chain lengths. These coatings were found to produce highly efficient separations while offering a range of electroosmotic flow (EOF) values. PEGylation resulted in increased peak capacity and resolution as compared to APS coatings for the separation of intact proteins and digested proteins using CE-ESI microchips coupled with MS.

Microfluidic CE-ESI devices with separation channels of 1 cm and 3 cm in length were coated with APS via CVD and used for high speed (HS) CE-ESI-MS of peptides and proteins.

These devices were capable of CE separation times ranging from 10 s to < 1 s. To adequately sample the temporally narrow peaks generated by these devices a new MS data collection with increased data acquisition rates was developed. Both MS and tandem MS analyses were demonstrated using this high speed MS data acquisition method. The HSCE-ESI-MS separations performed on the 1 cm microchip are the fastest liquid phase separations coupled to MS reported to date.

Finally, the performance limits of both the APS and PEG surface coatings were investigated. APS was applied to a CE-ESI device with a 1 m separation channel to test the ability of the CVD method to coat long channels. This device achieved > 1.4 million theoretical plates for the separation of peptide standards. A PEG surface coating was used to analyze an intact monoclonal antibody to determine structural charge variants as well as variants arising from glycosylation differences. Additionally, this PEG surface was used to inhibit the effects of sample matrix components that were deleterious to CE-ESI-MS through on-chip mobility-based sample clean-up. This approach facilitated the analysis of biological samples in matrices that would otherwise be incompatible with microchip CE-ESI-MS.

TABLE OF CONTENTS

LIST OF TABLES

LIST OF FIGURES

LIST OF ABBREVIATIONS

APDIPES	(3-aminopropyl)di-isopropylethoxysilane
APS	aminopropyl silane, general
APTES	(3-aminopropyl)triethoxysilane
BGE	background electrolyte
BSA	bovine serum albumin
CCD	charge-coupled device
CE	capillary (zone) electrophoresis
cm	centimeter, 10^{-2} meters
CVD	chemical vapor deposition
D	true diffusion coefficient
D_{app}	experimentally apparent diffusion coefficient
Da	Dalton, mass unit defined as grams per mole
DAQ	data acquisition
E	electric field strength
EOF	electroosmotic flow
ESI	electrospray ionization
HSCE	high speed capillary electrophoresis

Hz	Hertz, defined as 1/second
IMS	ion mobility spectrometry
kDa	kilo-Dalton, defined as 10^3 Daltons
KOH	potassium hydroxide
kV	kilo-Volt, defined as 10^3 Volts
LC	liquid chromatography
L_d	separation distance
LIF	laser-induced fluorescence
mL	milli-liter, defined as 10^{-3} liters
mM	milli-molar, unit of concentration defined as 10^{-3} moles per liter
MS	mass spectrometry
mg	milli-gram, unit of mass defined as 10^{-3} grams
mW	milli-Watt, unit of power defined as 10^{-3} Watts
NHS	n-hydroxy succinimide/succinimidyl
N	theoretical plate count
N/m	theoretical plates per meter
PEG	polyethylene glycol
R6G	rhodamine 6G

RMS	root mean square
R_s	electrophoretic resolution
RSD	relative standard deviation
s	seconds
t	time
V	Volt

LIST OF SYMBOLS

°C	degrees Celsius
σ	sigma, used to denote the statistical standard deviation of a peak
σ_l^2	spatial variance
μ	mobility, general
μ_{eo}	mobility, electroosmotic
$\bar{\mu}_{ep}$	mobility, average electrophoretic
μm	micrometer, 10^{-6} meters
Δ	"delta", defined as the quotient of the experimental diffusion coefficient and the true diffusion coefficient of a peptide or protein

CHAPTER 1: INTRODUCTION TO BIOANALYSIS VIA MICROCHIP CAPILLARY ELECTROPHORESIS-ELECTROSPRAY IONIZATION-MASS SPECTROMETRY

1.1 Capillary zone electrophoresis theory and practical considerations

Capillary zone electrophoresis (CE) is an analytical separations technique that separates molecules based on differences in their electrophoretic mobility (μ_{ep}) under the influence of an electric field.[1-4] The glass or fused silica capillaries with which CE is often performed have a charged surface giving rise to bulk fluid flow due to electroosmosis (EOF).[2] The summed vector of both the EOF (μ_{eo}) as well as an analyte's μ_{ep} dictates the analyte's apparent mobility (μ_{app}) as defined in eq 1.1.

$$\mu_{app} = \mu_{ep} + \mu_{eo} \tag{1.1}$$

Differences in μ_{app} between analytes leads to separation in CE. The extent of resolution (R_s) in CE is dependent on the applied voltage (V), μ_{eo}, and the average electrophoretic mobility of the analytes ($\bar{\mu}_{ep}$), according to eq 1.2:[5]

$$R_s = 0.177\left(\mu_{ep,1} - \mu_{ep,2}\right)\left[\frac{V}{D(\bar{\mu}_{ep} + \mu_{eo})}\right]^{1/2} \tag{1.2}$$

The resolution (R_s) is also influenced by the diffusivity (D) of the analyte molecules, and the magnitude of the voltage applied (V). These properties also greatly influence the efficiency of a CE separation. CE separation efficiency, in terms of theoretical plates (N), is defined in eq 1.3:[6]

$$N = \frac{(\mu_{ep} + \mu_{eo})V}{2D} \tag{1.3}$$

The magnitude of $\mu_{eo}$is dictated by both the static charge at the walls of the CE conduit as well as the thickness of the electrical double-layer that is formed due to charged species in solution.[6] Figure 1.1 is a cartoon of the conditions that give rise to EOF in CE. The cartoon describes the electrical double layer and the approximate nature of the potential drop across this layer localized near the surface, into the bulk solution of the conduit.[7]

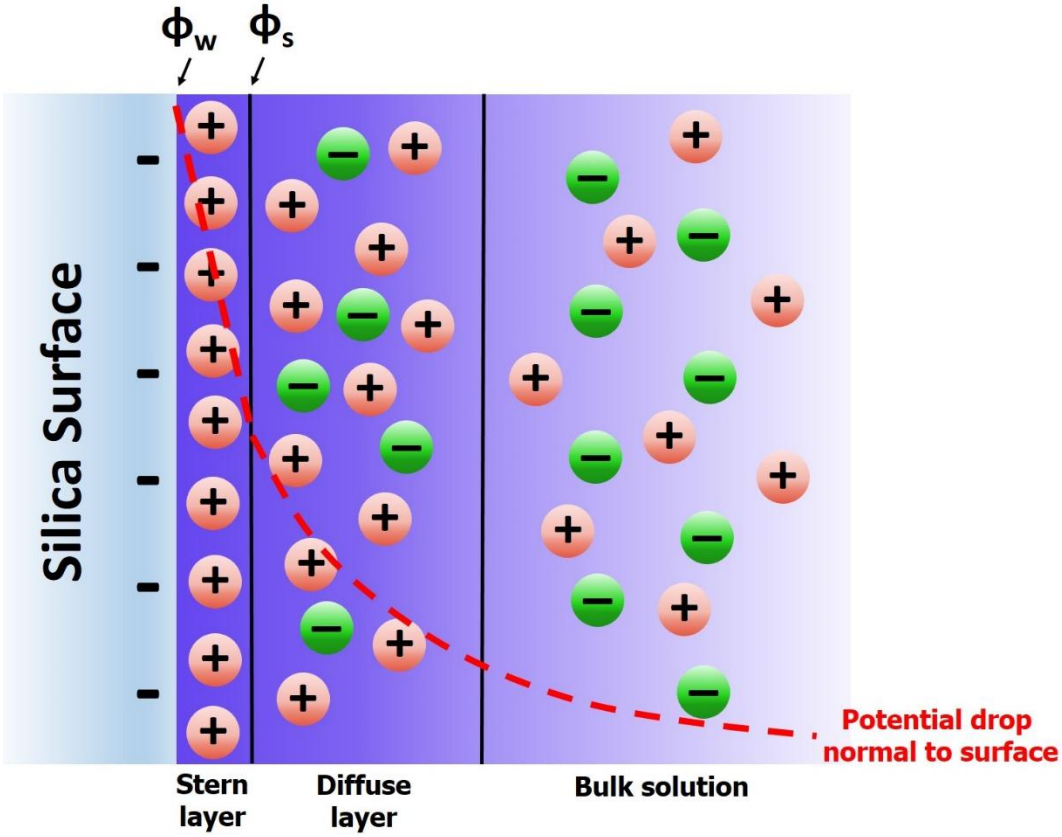

Figure 1.1 Double layer cartoon depicting relative ion ratios and the potential drop across the Stern layer, diffuse layer, and into the bulk solution.

A negatively charged silica surface is shown on the left with a negative surface potential (ϕ_w). Cations in solution (red) electrostatically adsorb to the negatively charged surface forming a static layer known as the Stern layer. The potential drop across the Stern layer is linear in nature as depicted by the red dashed line. The potential (ϕ_s) at the Stern layer boundary is known as the ζ-potential. Beyond the Stern layer cations exist in an overabundance relative to anions forming

a mobile diffuse layer. Net flow of cations in the diffuse layer gives rise to EOF. The electrical potential drops in an exponential fashion across the diffuse layer into the bulk solution where charge neutrality exists. The size of the diffuse layer is impacted by the ionic strength of the BGE as well as the ζ-potential. The higher the ionic strength of the BGE, the smaller the diffuse layer will be. The larger the electrical double layer the greater the electromotive force and the higher the EOF. The magnitude of the EOF impacts both the separation resolution as well as the analysis time in addition to the resolution and efficiency contributions described in eq 1.1 and eq 1.2, respectively.

Reducing the analysis time minimizes band broadening because in CE band broadening is ideally due to axial-diffusion only. A system with a high ζ-potential and low ionic strength BGE will result in high EOF and a short analysis time. This high EOF condition also reduces the relative differences in μ_{app} leading to limited resolution. From eq 1.2 it is evident that increasing the voltage applied is one method by which the resolution can be improved. All of these conclusions are supported by CE theory under the assumption that there is zero interaction between analyte bands and the walls of the CE conduit. Any analyte-wall interactions introduce mass transfer effects and non-diffusional band broadening which is not accounted for in the above equations. With analyte-wall interactions present the benefits of reducing analysis time in CE, with respect to efficiency, are negated as band broadening is no longer diffusion-limited. Additionally, increasing the voltage will exacerbate non-diffusion band broadening effects further decreasing separative performance.

1.2 Motivations for microfluidic CE-ESI-MS for bioanalysis

Microfluidic devices are a unique analytical platform capable of integrating multiple processes into a single device.[8-18] Biological samples often necessitate multiple analysis steps

due to their intrinsic complexity as well as the analytically challenging nature of the matrices in which they are found. Often the complexity of bioanalytes necessitates sample preparation as well as separation steps prior to analysis. Capillary electrophoresis (CE) is capable of highly efficient separations with short analysis times and microfluidic devices have emerged as an excellent platform for CE.[8, 13, 19-21] Microfluidic devices have achieved separation efficiencies of greater than 1 million theoretical plates[22] and sub-second analysis times.[21] Prior work utilizing microfluidic CE has often relied on optical detection methods which are inherently fast and well suited to optically transparent microchips.[15-16, 19, 21] However, optical detection methods such as laser induced fluorescence (LIF) are information-limited when compared to mass spectrometry (MS). For microfluidic devices to be truly impactful in the field of bioanalysis it is imperative that they be coupled with MS due to the information rich nature of MS and the increasing complexity of biological analytes of interest.

Previously, integrated CE-ESI microchips have been used by the Ramsey group to analyze a range of biological analytes of varying complexity. These analytes have included complex mixtures of peptides resulting from protein digests, mixtures of intact proteins, and contents from red blood cells lysed on-chip.[8, 12-13] Liquid chromatography (LC)-MS has been used predominantly in the literature to investigate similar classes of analytes however CE-ESI-MS, particularly in the microchip format, offers potential advantages over LC in multiple ways. CE is a promising separations method for intact proteins due to their intrinsically low diffusion coefficients and the theoretically diffusion-limited nature of band broadening in CE. CE also presents potential advantages for the analysis of peptide mixtures which are commonly analyzed in bottom-up proteomics and peptide mapping experiments. For these types of experiments protein digests are analyzed to elucidate their amino acid sequences as well as the location of

post-translational modifications which may affect protein function.[23-24] Ideally, peptide mapping experiments achieve 100% sequence coverage. Due to its reliance on hydrophobic retention mechanisms, hydrophilic peptides with low molecular weight are often excluded from reverse phase LC-MS analyses.[23] CE, as opposed to LC, does not depend on the hydrophobicity or hydrophilicity of analytes and as such offers an orthogonal and potentially improved separation approach to LC for peptide analyses.

Despite the potential advantages of increased efficiency, increased sequence coverage, and reduced analysis times offered by CE-ESI-MS, adoption of the method by the scientific community has been slow. This can be attributed to multiple practical drawbacks associated with CE. One major hurdle to the realization of theoretical CE-ESI-MS performance for biological analytes is the integration of CE with ESI. The integration capabilities of microfluidic devices have proven to be particularly effective at overcoming this challenge when compared to CE-ESI performed in traditional fused-silica capillaries.[8, 23] Another aspect of CE that has been detrimental to its wide spread use is surface adsorption of analytes. Biological analytes, such as intact proteins especially, have a tendency to interact with surfaces. These surface interactions, which are critical for the selectivity of LC, inhibit the efficiency of CE substantially. Surface control can be particularly challenging for CE methods that are ESI-MS compatible due the simple background electrolytes (BGEs) commonly used for sensitive ESI-MS. Finally, a third mitigating factor limiting the applicability of CE-ESI-MS to biological analytes commonly analyzed by LC-MS is the lack of preconcentration which often limits CE-ESI-MS sensitivity.

Recent work by the Ramsey group has successfully coupled high speed, high efficiency CE with electrospray ionization- mass spectrometry (ESI-MS) using a monolithic microfluidic device.[8-9, 11-13] These devices have been used for the analysis of metabolites, amino acids,

peptides, partially digested proteins, and intact proteins with masses of approximately 150 kDa. The separation efficiency of these devices was improved using new surface coating technologies developed in lab.[8] In addition to integrating highly efficient CE separations with sensitive ESI-MS analysis, additional surface coating technology developments have enabled in-line sample clean-up in an effort to minimize bench top sample preparation methods for bioanalytes and improve CE sensitivity. These advancements have opened up new application space for the analysis of complex biological analytes of interest using microfluidic devices or so called micro-total analysis systems.[18]

1.3 Work described in this dissertation

In this dissertation the development of surface coating technology for microfluidic CE-ESI-MS of biological analytes is reported and discussed. Surface coatings play a vital role in achieving the theoretical performance advantages of CE while maintaining ESI-MS compatibility. Despite their importance, surface coating methods in the literature were found to offer performance that was poor relative to theoretical expectations for CE. Chapter 2 discusses the current state of coating methodologies in the literature, their short-comings, and the requirements that must be met for the successful application of CE-ESI-MS to complex biological analytes. The development of a new efficiency metric that facilitates comparisons of CE coating performance as well as a new coating method based on chemical vapor deposition (CVD) is described. Chapter 3 discusses a suite of coating methods intended to further improve the applicability of CE-ESI-MS to biological mixtures of increasing complexity. To improve the resolution of complex mixtures these coatings were designed for the reproducible generation of a range of electroosmotic flow (EOF) magnitudes. Chapter 4 describes efforts to maximize the analysis speed of CE-ESI-MS using the previously developed coating technologies. The

temporally narrow peaks generated from high speed CE-ESI microchips required changes to the fundamental operation of a mass spectrometer to increase the rate of MS data acquisition. Chapter 5 describes the future applications for the microfluidic CE-ESI-MS technologies developed in the Ramsey lab and highlights the analysis of intact monoclonal antibodies in particular.

1.4 References

1. Jorgenson, J. W., Lukacs, K. D., *Clin. Chem.* **1981**, *27*. 1551-1553.

2. Jorgenson, J. W., Lukacs, K. D., *J. Chromatogr.* **1981**, *218*. 209-216.

3. Jorgenson, J. W., Lukacs, K. D., *Anal. Chem.* **1981**, *53*. 1298-1302.

4. Jorgenson, J. W., Lukacs, K. D., *Science* **1983**, *222*. 266-272.

5. Jorgenson, J. W., *Trac-Trends in Anal. Chem.* **1984**, *3*. 51-54.

6. Lukacs, K. D., Jorgenson, J. W., *HRC & CC, J. High Resolut. Chromatogr. Chromatogr. Commun.* **1985**, *8*. 407-411.

7. Kirby, B. J., Hasselbrink, E. F., *Electrophoresis* **2004**, *25*. 187-202.

8. Batz, N. G., Mellors, J. S., Alarie, J. P., Ramsey, J. M., *Anal. Chem.* **2014**, *86*. 3493-3500.

9. Mellors, J. S., Black, W. A., Chambers, A. G., Starkey, J. A., Lacher, N. A., Ramsey, J. M., *Anal. Chem.* **2013**, *85*. 4100-4106.

10. Flangea, C., Schiopu, C., Capitan, F., Mosoarca, C., Manea, M., Sisu, E., Zamfir, A. D., *Centr. Euro. J. Chem.* **2013**, *11*. 25-34.

11. Chambers, A. G., Mellors, J. S., Henley, W. H., Ramsey, J. M., *Anal. Chem.* **2011**, *83*. 842-849.

12. Mellors, J. S., Jorabchi, K., Smith, L. M., Ramsey, J. M., *Anal. Chem.* **2010**, *82*. 967-973.

13. Mellors, J. S., Gorbounov, V., Ramsey, R. S., Ramsey, J. M., *Anal. Chem.* **2008**, *80*. 6881-6887.

14. Haeberle, S., Zengerle, R., *Lab Chip* **2007**, *7*. 1094-1110.

15. Jacobson, S. C., Koutny, L. B., Hergenroder, R., Moore, A. W., Ramsey, J. M., *Anal. Chem.* **1994**, *66*. 3472-3476.

16. Jacobson, S. C., Hergenroder, R., Moore, A. W., Ramsey, J. M., *Anal. Chem.* **1994**, *66*. 4127-4132.

17. Jacobson, S. C., Hergenroder, R., Koutny, L. B., Warmack, R. J., Ramsey, J. M., *Anal. Chem.* **1994**, *66*. 1107-1113.

18. Reyes, D. R., Iossifidis, D., Auroux, P. A., Manz, A., *Anal. Chem.* **2002**, *74*. 2623-2636.

19. Culbertson, C. T., Jacobson, S. C., Ramsey, J. M., *Anal. Chem.* **2000**, *72*. 5814-5819.

20. Culbertson, C. T., Jacobson, S. C., Ramsey, J. M., *High efficiency separations on microchip devices*. 2000; p 221-224.

21. Jacobson, S. C., Hergenroder, R., Koutny, L. B., Ramsey, J. M., *Anal. Chem.* **1994**, *66*. 1114-1118.

22. Culbertson, C. T., Jacobson, S. C., Ramsey, J. M., *Anal. Chem.* **2000**, *72*. 5814-5819.

23. Ramautar, R., Heemskerk, A. A. M., Hensbergen, P. J., Deelder, A. M., Busnel, J.-M., Mayboroda, O. A., *J. Proteomics* **2012**, *75*.

24. Kleparnik, K., *Electrophoresis* **2013**, *34*. 70-85.

CHAPTER 2: CHEMICAL VAPOR DEPOSITION OF AMINOPROPYL SILANES IN MICROFLUIDIC CHANNELS FOR HIGHLY EFFICIENT MICROCHIP CE-ESI-MS

2.1 Introduction

Electrospray ionization (ESI) has revolutionized the study of large biological molecules by combining the power of mass spectrometry (MS) with liquid phase separation methods. The most successful embodiment of this concept is liquid chromatography (LC)-ESI-MS of enzymatically digested proteins. For applications such as drug development and proteomics, LC-ESI-MS has become the gold standard for analysis. Much work has also been put forth to couple capillary electrophoresis (CE) with ESI-MS,[1] but CE-ESI-MS has achieved less widespread use at this time. CE offers some potential advantages over LC, particularly for separating intact proteins.[2-7] In practice, however, most CE-ESI-MS separations do not achieve theoretically achievable separative performance, thus allowing potential for significant improvements. Efficient ESI of peptides and proteins requires the use of acidic, low ionic strength background electrolytes (BGE).[1, 8] Under these conditions the native silica or glass surfaces of typical CE capillaries/channels exhibit poor electroosmotic flow (EOF) stability and analyte bands can be broadened by surface interactions. To counteract these deficiencies, surface coatings are commonly employed.[9] For compatibility with cationic analytes and positive ESI, static, positively charged surface coatings are desired.[8-9] Many such coatings, ranging from covalently attached silanes to ionically associated polymers have been described previously, but few, if any have approached diffusion-limited separative performance for CE-ESI-MS of peptides and proteins.[5, 9-21]

A recent example from the literature provides an excellent benchmark for the type of work being done in this field. Faserl et al. investigated the performance of three different coatings (polyethyleneimine, PolyE-323, and M7C4I) for CE-ESI-MS of peptides.[11] They used meter-long fused silica CE capillaries with porous tip emitters for sensitive sheathless ESI. The best separation performance was achieved using the covalently-attached M7C4I coating. The results reported are superior to most CE-ESI-MS analyses of peptides found in the literature, however, a detailed analysis of band broadening was not included. A comparison of experimental performance to theoretical limits is uncommon in CE-ESI-MS literature, making it difficult to quantitatively compare different systems. This paper did report an average peak width of 3.8 seconds for an approximately 6 min separation window centered at a migration time of 9 min. Using these data we calculate an average separation efficiency of 295,000 theoretical plates and a peak capacity of 95. While these values are impressive when compared to other reports of CE peptide separations, a more rigorous evaluation is necessary to determine whether or not performance could be improved.

The number of theoretical plates (*N*) that can be generated in a diffusion limited CE separation is given by:

$$N_{optimal} = \frac{\mu E L_d}{2D} = \frac{\mu V}{2D} \tag{2.1}$$

where μ is the effective analyte mobility, *E* the electric-field strength, L_d the separation distance,D the molecular diffusion coefficient and *V* the applied voltage. Because the value of *N* is affected by multiple parameters this metric is not easily used to compare performance to what is possible theoretically. Many have adopted the use of theoretical plates per meter to normalize results with respect to column length, but this metric does not address differences in applied voltage or analyte mobility and diffusivity. Reporting efficiency in this way can be misleading as

the efficiency is theoretically independent of separation distance. Under ideal conditions freely migrating bands will broaden due to molecular diffusion only.[22-24] An ideal CE separation can therefore be described as diffusion-limited. For a diffusion-limited separation the time-dependent axial spatial variance (σ_l^2) of the analyte band is governed by the Einstein-Smoluchowski equation.[25]

$$\sigma_l^2 = 2Dt \tag{2.2}$$

From eq 2.2 we can determine an apparent diffusion coefficient (D_{app}) for any analyte band within a CE separation where:

$$D_{app} = \frac{\sigma_l^2}{2t} \tag{2.3}$$

Highly efficient separations will yield a D_{app} value that is comparable to the molecular diffusion coefficient of the analyte indicating that axial dispersion is limited to diffusion. Separations suffering from Joule heating,[26] analyte-wall interactions,[27] Taylor dispersion[28] or other sources of extraneous band broadening will display D_{app} values that are elevated relative to D. The ratio of the apparent diffusion coefficient, determined from a migrating band, to the molecular diffusion coefficient provides a clear measure of the quality of the separation. In this work we define this metric as Δ:

$$\frac{\mathrm{D_{app}}}{D} \equiv \Delta \tag{2.4}$$

A theoretically optimal CE separation will have a Δ value of 1. Larger values of Δ indicate greater deviation from ideal separation performance, and thus room for improvement. From eq 2.1 and eq 2.3 the theoretically optimal separation efficiency can be related to the experimentally observed separation efficiency by:

$$N_{optimal} = \Delta \cdot N_{observed} \tag{2.5}$$

We therefore, refer to the Δ value as the "efficiency coefficient" of a CE separation. This value directly indicates how efficient a CE separation would be if all extraneous sources of band broadening were removed.

The results for average peptide separation performance reported by Faserl et al. can be used to determine the Δ value of their separation. Using a conservative estimate for the molecular diffusion coefficient of peptides (5×10^{-6} cm^2/s) we calculate an average Δ value of 8, or the possibility of improving the separation performance by eight fold. The optimized separation efficiency would increase from 300,000 to 2.4 million theoretical plates and the peak capacity would be improved from 95 to 268.[24, 29]

The microfluidic CE-ESI devices reported here feature an integrated ESI interface with virtually zero dead volume and the ability to inject sample bands with temporal widths as narrow as 10 ms.[5] These devices minimize extra-column band broadening such that the quality of the surface coating is the efficiency-limiting component of the platform. Attempts to optimize the performance of these devices led us to develop improved surface modification methods. Surface coatings administered in the liquid phase, both in our lab[5, 14, 30-31] and in the literature,[9-12, 17-18, 20, 32], fall short of theoretically optimal performance. Microscopic examination of the movement of fluorescent analyte bands in our microfluidic devices coated with a liquid phase reagent (PolyE-323)[5, 14] revealed Taylor dispersion attributed to non-uniform surface coating as a cause of extraneous band broadening. Spatial heterogeneity of ζ-potential, has been shown to induce band broadening in CE.[13, 33-37] Chemical vapor deposition (CVD) has been used to form highly uniform coatings on external wafer surfaces[38-41] and therefore seems ideally suited for coating microfluidic channels for CE. In addition to improving coating uniformity, CVD offers advantages for coating complex microfluidic channel networks as well as batch processing of

multiple devices. Moreover, this approach could be beneficial for the modification of nanofluidic devices as the small dimensions often mitigate liquid flushing methods.

In this work microfluidic CE devices were coated by CVD of aminopropylsilane (APS) reagents. We describe a microfluidic CE method for rigorously evaluating the performance of the surface coatings with regard to EOF, separation efficiency, and stability. In particular, we measured the performance and EOF of three different devices at pH 2.8 and pH 7.5 for comparison to liquid-phase APS coatings described in the literature. Device-to-device reproducibility of the coating method was evaluated for 20 different devices coated over an 80-day period. Stability of coatings formed with two different APS reagents was measured over a 1-week period. In addition to these evaluations of coating performance, a device with an integrated ESI interface was coated using the CVD method and used for microfluidic CE-ESI-MS of peptides and intact proteins.

2.2 Experimental

2.2.1 Reagents and materials

MS-grade organic solvents (acetonitrile, methanol, 2-propanol), formic acid (99.9%), ammonium acetate, and potassium hydroxide were obtained from Fisher Chemical (Fairlawn, NJ). Water was purified with a Nanopure Diamond water purifier (Barnstead International, Dubuque, IA). Fluorescein, rhodamine 6G (R6G), and (3-Aminopropyl)triethoxysilane (APTES) were obtained from Sigma-Aldrich (St. Louis, MO). (3-Aminopropyl)di-isopropylethoxysilane (APDIPES) was obtained from Gelest (Morrisville, PA). Peptide analytes bradykinin, methionine-enkephalin, thymopentin and angiotensin II were obtained from American Peptide Company (Sunnyvale, CA). MassPrep™ enolase tryptic digest and intact protein standards were provided by Waters Corporation (Milford, MA).

2.2.2 Microfluidic device designs

Schematics of the two microfluidic designs used for this work are shown in Figure 2.1. The device used for rigorous analysis of band-broadening and EOF of aminopropyl silane coatings was a simple cross design. This design incorporates two functional elements: an injection cross and a 3 cm separation channel. Laser induced fluorescence (LIF) detection was used with this chip design. The CE-ESI device includes four functional elements: an injection cross, a serpentine separation channel (23-cm long), an electroosmotic pump, and an ESI orifice. The reservoir labels indicate sample (S), background electrolyte (B), sample waste (SW), waste (W, CE-LIF only), and electroosmotic pump (EO, CE-ESI only) reservoir locations. Microchannel dimensions for both devices were 10 μm deep and 70 μm wide. The serpentine turns of the CE-ESI device were asymmetrically tapered to a width of 25 μm to minimize geometrical band broadening.[5, 42-43]

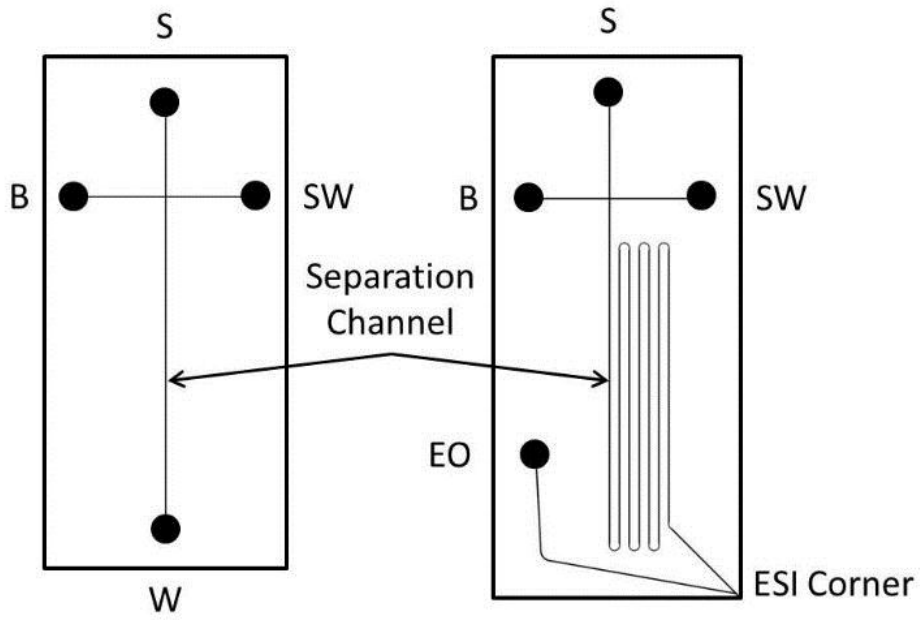

Figure 2.1 Schematics for the microfluidic chip designs used for CE-LIF and CE-ESI, respectively. Microchannel depths were 10 μm for all devices. All other dimensions presented in the text.

2.2.3 Fabrication of microfluidic devices

Devices for microfluidic CE with LIF detection were fabricated in-house from 0.9 mm thick B270 glass purchased from Telic Company (Valencia, CA). Previously described photolithography and wet chemical etching techniques were used.[5, 44] A total of 27 of these devices were used for the work presented here. The device used for microfluidic CE with integrated electrospray ionization (ESI) was fabricated by Caliper Life Sciences (Hopkinton, MA) using our mask design. This device was made with 0.5 mm thick B270 glass. The corner of the device used for ESI was polished in-house to remove dicing imperfections using a lapping wheel with 3 μm lapping paper from Ultra Tec (Santa Ana, CA). Glass cylinders, 8 mm in diameter, were attached to all devices for use as solvent reservoirs with a chemically resistant epoxy (Loctite E-120HP, Henkel Corporation, Germany).

2.2.4 Chemical Vapor Deposition coating procedure

APS coatings were administered in the gas phase at low pressure using a commercially available LabKote CVD system (Yield Engineering Systems, Livermore, CA). Prior to CVD coating, devices were pretreated by flushing for 15 min with a mixture of 1 g of potassium hydroxide (KOH) dissolved in 25 mL of 80% 2-propanol-20% water solution. Flushing was accomplished by applying suction to the waste port of CE-LIF devices or the ESI corner of CE-ESI devices (Figure 2.1). The pretreatment step was followed with a rigorous rinsing of the microfluidic channels as well as all other surfaces of the chip and fluid reservoirs with deionized water. After rinsing, pretreated channels were dried by applying suction to the channel inlet reservoirs using house vacuum on the bench top.

After pretreatment, dried devices were ready to be coated using the automated CVD system. The general protocol for this instrument involved four steps; 1) dehydration of the

vacuum chamber, 2) injection and subsequent vaporization of the APS reagent, 3) "soak" period in which reagent vapor is held in the chamber, 4) evacuation purges to remove all reagent vapors. Steps 1-4 were repeated a total of three times for each coating procedure before removing the devices from the CVD system. Each dehydration purge consisted of three pressure cycles in which the chamber was pumped down to a pressure of 0.1 Torr then refilled with dry nitrogen gas. Evacuation purges consisted of four pressure cycles to ensure minimal residual APS vapor was present. After dehydration 0.3 mL of reagent was injected and vaporized resulting in a pressure rise from 0.1 Torr to 2.0 Torr. Each injection was followed by a 15 min soak period. The chamber was held at 130 °C for APTES depositions and 160 °C for APDIPES depositions. All other instrument parameters were the same for each reagent used. The total time for the coating procedure was approximately 1 hour. Coated devices were allowed to cool to room temperature prior to use. Anyone attempting to build a CVD system or working with silanes should be careful to avoid releasing harmful vapor into the ambient air of the laboratory. Note, the CVD process coats both the internal and external surfaces of microfluidic devices; appropriate personal protective equipment should be worn when handling silanized devices.

2.2.5 Operation of microfluidic devices

Both CE-LIF and CE-ESI devices were operated by application of voltages to the solvent reservoirs. Polyethylene caps (Grace Davison Discovery Sciences, Bannockburn, IL) were placed on each reservoir to reduce solvent evaporation. Platinum wire (Alpha Aesar, Ward Hill, MA) electrodes were inserted through small holes in the reservoir caps into each reservoir. For CE-LIF the electrodes were powered by a custom-built Bertan Model 2866, fast-switching, 6-channel power supply capable of supplying 0 to +10 kV to each reservoir independently. For CE-ESI a home-built power supply was used that contained five individual power supply modules

from UltraVolt Inc. (Ronkonkoma, NY). Three of the modules (10A12-N4) could supply 0 to -10 kV while the other two modules (10A12–П4) could supply 0 to +10 kV. The power supplies were controlled *via* an SCB-68 breakout box connected to a PC *via* a PCI 6713 DAQ card. A LabVIEW program was used to control voltage outputs. For CE-LIF the voltages applied to the S, B, SW, and W reservoirs were 0, 0, 1.4, and 2 kV, respectively (Figure 2.1). To open the electrokinetic gate for sample injection the voltages were switched to 0, 0.6, 0.8, and 2 kV for 20 ms. These voltages yielded an electric field strength of 550 V/cm in the separation channel. For CE-ESI the voltages applied to the S, B, SW, and EO reservoirs were -6, -6, -5, and 6.2 kV respectively. To open the electrokinetic gate for sample injection the voltages were switched to -6, -5.5, -5.5, and 6.2 kV for 200 ms. These voltages yielded an electric field strength of 410 V/cm in the separation channel and an ESI voltage of +4.8 kV relative to the MS inlet.

2.2.6 CE-LIF data collection and analysis

Laser induced fluorescence was performed on a Nikon Eclipse Ti-U inverted microscope (Rochester, NY) equipped with a dual filter turret using a 20x objective. The 488 nm beam from a continuous wave, tunable argon ion laser from Melles Griot Laser Group (Carlsbad, CA) was directed into the back of the microscope at a power of 2 mW and diverted towards the stage using a Nikon filter cube containing a Semrock dichroic mirror. Fluorescence was collected in an epifluorescence setup through a 488 nm Semrock BrightLine long pass filter and detected using a photomultiplier tube from Hamamatsu (Bridgewater, NJ, model H6780). The signal was then routed through a low-noise current preamplifier from Stanford Research Systems (model SR570, Sunnyvale, CA) prior to data collection *via* a DAQ board (PCI-6251) and LabVIEW software from National Instruments (Austin, TX). To aid in establishing appropriate gating potentials and visual monitoring of fluids on-chip, the microscope was equipped with a Sony Exwave HAD 3

CCD color video camera, Model DXC-390 (Sony Corp, Japan) and a Nikon Intensilight mercury arc lamp. Devices to be analyzed were filled with background electrolyte (BGE) by applying suction at the waste port using house vacuum. Once filled with BGE the device was mounted on the microscope using a custom polycarbonate stage (to minimize the chance of electrical arcing). Sample was loaded into the sample reservoir using a micropipette. Voltages were applied to electrokinetically gate and inject sample as described previously.[43] Electronic injection profiles were constructed in LabVIEW to automatically perform a series of five replicate CE injections. Prior to initiating the injection profile, 3-5 test injections were performed to ensure that the migration times were stable. The profile of replicate injections was performed with LIF detection at each of six different locations starting at a separation distance of 2.2 cm and terminating at a distance 0.35 cm from the injection cross. Data files were exported from LabVIEW to IGOR Pro (version 6.22A, wavemetrics.com) for peak fitting analysis.

2.2.7 CE-ESI data collection and analysis

The CE-ESI device was mounted on a custom built stage with the ESI corner approximately 5-10 mm from the sample cone inlet of a Synapt G2 quadrupole-ion mobility-time of flight mass spectrometer (Waters Corporation, Milford, MA). A 1/16th inch thick, 4 cm by 5 cm, single-sided copper clad circuit board (M.G. Chemicals, Burlington, Ontario, Canada) was used to shield the electrospray orifice from the high voltages applied to the microfluidic reservoirs. A thin slit was cut into the rectangular board such that the ESI corner could protrude 3-5 mm through the slit. Positive voltage (0.5 kV) was applied to the copper plate that was oriented to face the MS inlet. The MS was operated in sensitivity mode at an acquisition rate of 90 ms per summed scan with an inter-scan delay of 24 ms. Data were acquired from 300 to 3000 m/z. MassLynx software on the MS control computer was used for data acquisition, triggered by

the LabVIEW program used for electrokinetic control of the microfluidic device. Electropherograms collected in MassLynx were exported to IGOR Pro for peak fitting analysis. Data from the CE-ESI-MS analysis of enolase tryptic digest was additionally processed by BiopharmaLynx (version 1.2, Waters Corporation) to match observed peak masses with the amino acid sequence of yeast enolase obtained from the UniProt database. The analysis parameters allowed for tryptic digestion with no missed cleavages and no modifications.

2.3 Results and discussion

2.3.1 Characterization of CVD deposited aminopropyl silane coatings by CE-LIF

The performance of the CVD deposited aminopropyl silane coatings was evaluated using CE-LIF. The purpose of this analysis was to measure the electroosmotic mobility and electrophoretic band broadening with high accuracy. This method removes sources of extra-column band broadening by observing analyte bands at multiple locations along the separation channel. Data exemplifying this type of analysis is shown in Figure 2.3. This figure shows the separation of fluorescein and rhodamine 6G (R6G) on an APS coated device, with LIF detection at six different detection points ranging from 0.35 cm to 2.2 cm from the injection cross. Using these data one can determine the apparent diffusion coefficient of the separation according to eq 2.3. The apparent diffusion coefficient can be used in conjunction with the molecular diffusion coefficient, D, to determine the efficiency coefficient Δ, according to eq 2.4.

In this work the stopped-flow method was used to determine D.[58] The experiments were performed by simple modification of the normal CE-LIF or CE-ESI methods. Sample bands were injected and allowed to migrate under electrokinetic flow until the analyte bands reached a point approximately midway between the injection and detection points. Voltages were then turned off for periods of time (dwell time), stopping the flow and allowing the bands to broaden

by diffusion alone. After the stopped-flow period, the voltage was reapplied to complete the run. The results can be seen in Figure 2.2 where the spatial variance (σ_l^2) of the analyte bands is plotted as a function of time (t).

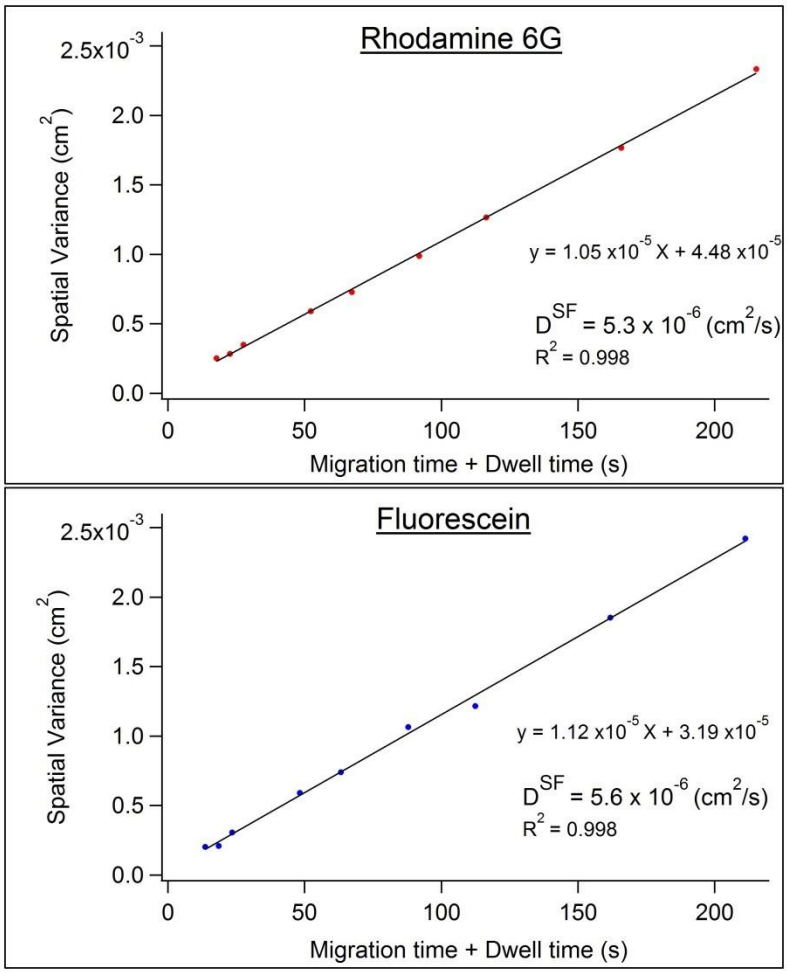

Figure 2.2 Data from stopped-flow LIF experiments performed in 50% acetonitrile, 0.1% formic acid using a mixture of fluorescein and rhodamine 6G. The slope of each plot indicates the rate of band broadening and is used to determine the molecular diffusion coefficient.

The slope of this plot (σ_l^2/t) provides a measure of diffusion via equation 2.3 ($D_{app} = \sigma_l^2/2t$), and can be used to determine the apparent diffusion coefficient for each dye. The apparent diffusion coefficient generated from stopped-flow data is an accurate representation of the true molecular diffusion coefficient and is listed in each panel of Figure 2.2 as D^{SF}.[58]

Once the molecular diffusion coefficient of an analyte is known it can be used to determine Δ values for all future CE analyses performed using that combination of analyte, BGE, and temperature. The stopped-flow time ranged from 0 to 200 s for CE-LIF analysis of fluorescein and R6G. For CE-ESI of fluorescein and the peptide analytes the stopped-flow period was varied from 5 to 20 min. Results from all stopped-flow analyses can be found in Table 2.1. This stopped-flow method can be applied to any CE system, but special care should be taken to prevent pressure-driven transport during the stopped-flow period, particularly for capillary systems.

Table 2.1 Diffusion coefficients measured by stopped-flow in 50%acetonitirile, 0.1% formic acid

Analyte	[a]CE-LIF	[a]CE-ESI-MS
Fluorescein	5.6 ± 0.1	5.4 ± 0.5
Rhodamine 6G	5.3 ± 0.1	-
Methionine Enkephalin	-	3.3 ± 0.4
Angiotensin II	-	3.1 ± 0.6
Bradykinin	-	3.3 ± 0.6
Thymopentin	-	4.0 ± 0.5

[a]all values (x $10^{-6}$$cm^2$/s)

Table 2.2 lists the results of this type of analysis for three different devices, CVD-coated with APDIPES at different times. Table 2.2 lists the EOF mobility, along with the efficiency coefficient (Δ) of R6G, and the common metric of plates per meter. Experiments were performed at two different pH levels spanning the range commonly used for positive ESI.

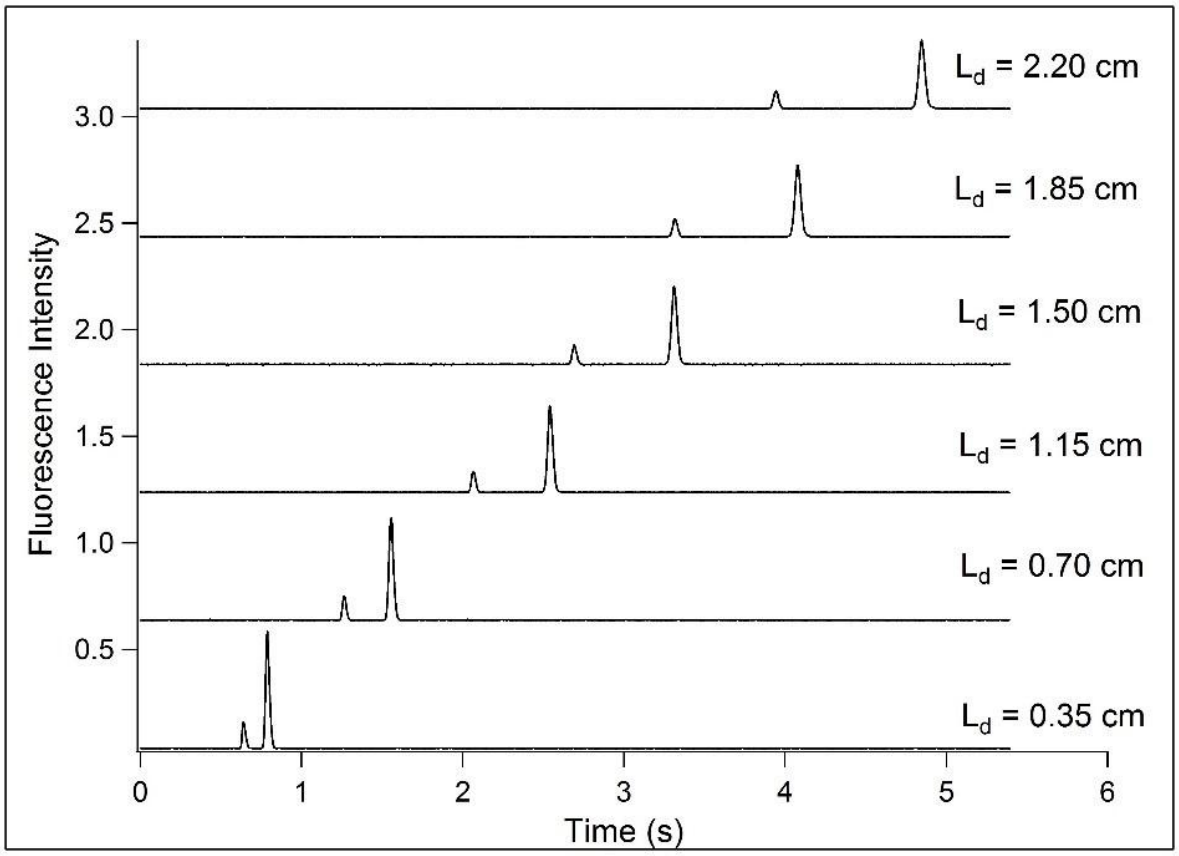

Figure 2.3 Representative data for CE-LIF performance analysis using a cross-channel microfluidic device with a separation channel length of 3 cm. Electropherograms for a mixture of fluorescein and rhodamine 6G were acquired at the separation distances indicated.

The BGEs used for this study contained 10 mM ammonium acetate and 50% acetonitrile (by volume), adjusted to lower pH using formic acid. The pH of each solution was determined directly using a pH probe (InLab 413 pH probe, Mettler Toledo, Columbus, OH) with polymeric electrolyte for compatibility with low ionic content media and organic solvents. R6G was used as a model analyte to determine band broadening at both pH 2.8 and pH 7.5. At pH 7.5 R6G was also used to determine the EOF as it is neutral at this pH. Because R6G is positively charged at pH 2.8 fluorescein was added to this mixture for use as a neutral dead-time marker.

Table 2.2 Performance of APDIPES coated microfluidic devices

	pH 2.8	pH 7.5
EOF ($cm^2V^{-1}s^{-1}$)	-6.36E-04 (0.7%)[1]	-5.79E-04 (4%)
Δ	1.09 (3%)	1.49 (13%)
Plates/m	1.86E+06 (5%)	1.28E+06 (15%)

[1]Percentages listed in parenthesis are relative standard deviations (n = 3).

At pH 2.8 the separation approached the theoretically limiting efficiency (Δ_{R6G} = 1.09) with a strong anodic EOF. At pH 7.5, we observed a 9% decrease in EOF along with a decrease in separation efficiency (Δ_{R6G} = 1.49). These changes could indicate the presence of silanol groups not fully covered by the APS coating. Liquid phase APS coatings have been reported in the literature for which the EOF not only decreased at elevated pH levels but changed from anodic to cathodic at pH values greater than 5.5.[45] This reversal of EOF at elevated pH is not seen in our CVD-coated devices up to pH 7.5. This result is in good agreement with previously reported comparisons of liquid and vapor phase silanization of surfaces in which vapor phase methods were found to produce surfaces with more uniform coverage[46] and greater hydrolytic stability.[47]

2.3.2 Device-to-device reproducibility of the CVD coating method

The reproducibility of the APDIPES surface coating method, was evaluated in terms of EOF and band broadening performance for 20 different microfluidic devices coated over a 2-week period in batch sizes ranging from 1 to 3 devices. The devices with separation channels of 3 cm in length were evaluated using the CE-LIF method described above, but with a BGE fully optimized for ESI sensitivity (50% acetonitrile, 0.1% formic acid by volume). The anodic EOF in this BGE was significantly greater than that observed during the initial characterization using ammonium acetate buffered BGE due to the decreased ionic strength. The average electroosmotic mobility across all 20 devices was -1.06 x 10^{-3} $cm^2V^{-1}s^{-1}$ with a relative standard deviation (RSD) of 2.6%. The average values of Δ were 1.17 (12% RSD) for fluorescein and

1.44 (7.5% RSD) for R6G. The slightly elevated efficiency coefficient of R6G may have been caused by partial separation of a minor variant peak. It should also be noted that the faster electroosmotic mobility obtained with this BGE yields higher theoretical plate counts at a given field strength, as indicated by eq 2.1. For this experiment the R6G efficiency coefficient of 1.44 corresponded to 61,600 theoretical plates (2.8 million plates per meter). Separation efficiency for both dyes on all devices studied was greater than 44,000 theoretical plates (2 million plates per meter).

2.3.3 Characterization of stability for CVD deposited aminopropyl silanes

The stability of the surface coatings for CE-MS applications is important for two reasons. In extreme cases of instability, chemical bleeding can lead to an elevated MS background signal or even fouling of the MS inlet. In all cases, coating instability will affect the quality of the separation in the form of excessive band broadening and migration time shifts, which have been reported previously for APS coatings administered in the liquid phase.[48-49] A surface coating with high stability that successfully inhibits analyte adsorption can be used in consecutive runs without the need to rinse or recoat the separation channel. The instability of many surface coatings reported in the literature makes them unsuitable for continuous use without reconditioning the surface between runs.[9, 16-17, 50] In this work coating stability was measured under two different storage conditions to simulate how devices might be used for CE-ESI-MS experiments. Devices were stored in a background electrolyte chosen for optimized ESI sensitivity (50% acetonitrile, 0.1% formic acid, pH 2.8) at room temperature to test the hydrolytic stability of the coatings. Devices were also stored dry, in sealed vacuum bags and kept refrigerated at 4 °C to simulate storage after coating but prior to use. Previous reports characterizing CVD deposited APS on silicon dioxide surfaces suggest that APDIPES may be

more stable than APTES as the bulky side groups of APDIPES can hinder hydrolysis of the silane bond.[38] Four total devices were characterized for this study; one device coated with each APS reagent in each of the two storage conditions. The devices were analyzed by the same CE-LIF method described previously to quantify the electroosmotic mobility and band broadening. The devices were analyzed the day of coating to establish initial performance and again on days 2, 6, and 7 of storage so that changes in performance could be tracked over time. Figure 2.4A shows the change in EOF observed over 1 week of storage for all four devices. The anodic EOF slowed slightly over the 1 week storage period for all cases, with the greatest change in EOF observed for APDIPES stored under vacuum (6.5% decrease in EOF). EOF measurements were reproducible with measurement error less than 1% RSD. Figure 2.4B shows the observed R6G efficiency coefficient versus storage time. All of the devices had an initial Δ value of approximately 1.2, with the greatest increase in band broadening observed on day 6 of the vacuum stored APTES device ($\Delta = 1.53$). Efficiency coefficient measurements had uncertainties of $\leq 5\%$ RSD. These results show that both surface modification reagents can be expected to yield consistently good performance over a 1 week time period when used with acidic BGE. In practice in our lab CVD-coated devices have been used reproducibly over the course of days to weeks for CE-ESI-MS analyses.[51] Future work will be required to measure coating stability over longer periods of time.

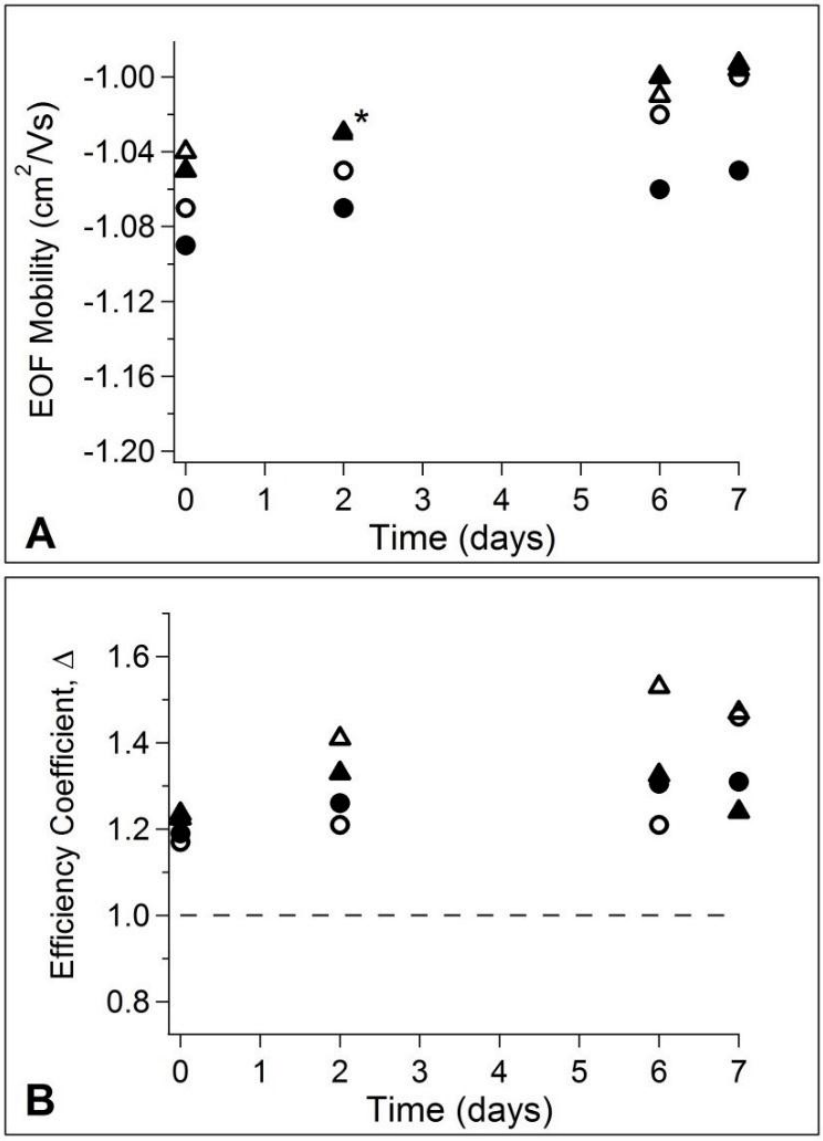

Figure 2.4 Performance of microfluidic devices coated with APTES and APDIPES. APTES coatings are displayed as triangles, APDIPES as circles. Open symbols indicate vacuum storage at 4 °C whereas closed symbols indicate wet storage at room temperature. A) Electroosmotic mobility versus time. B) Efficiency coefficient versus time. Overlapping data for APTES runs are indicated with an asterisk.

2.3.4 CE-ESI-MS of peptide standards

Because APTES and APDIPES were found to yield similar performance only APDIPES was used to demonstrate the utility of the CVD coating method for CE-ESI-MS. The initial performance of CE-ESI devices was characterized using peptide standards. The goals of this

analysis were to confirm that peptides did not interact with the APDIPES surface, yielding efficient separations, and that the coatings were compatible with ESI-MS. The CE-ESI devices had a longer separation channel (23 cm) than the CE-LIF devices (3 cm). These experiments therefore also served to confirm that the CVD method could produce a uniform coating inside longer microfluidic channels. Figure 2.5 shows a representative electropherogram for the CE-ESI-MS separation of four model peptides on an APDIPES coated CE-ESI device. Fluorescein was also added to this sample as an EOF marker.

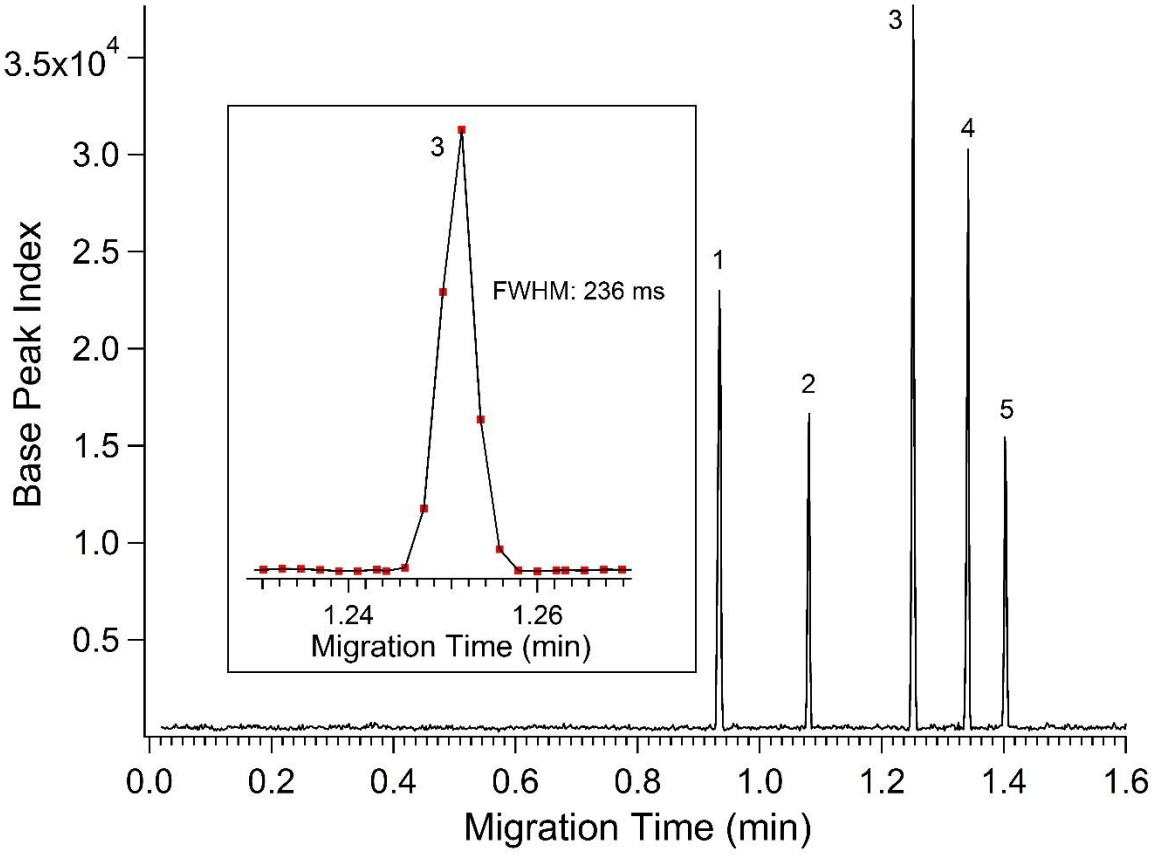

Figure 2.5 Base peak electropherogram showing; fluorescein (1), methionine enkephalin (2), angiotensin II (3), bradykinin (4) and thymopentin (5) separated using a CE-ESI microfluidic device coated with APDIPES using a field strength of 410 V/cm and 50% acetonitrile, 0.1% formic acid (pH 2.8) BGE. Mass spectra were acquired with a Synapt G2 mass spectrometer at a rate of 8 summed scans per second.

The inset of Figure 2.5 shows a single peptide peak (angiotensin II) in greater detail. These separations produced symmetrical, temporally narrow peaks, with a median base peak width (4σ) of 384 ± 63 ms (n = 3). The run-to-run migration time reproducibility was stable with less than 0.3% RSD for all peptides. No background ions associated with the APDIPES coating were detected, confirming the stability of the coating and MS compatibility. As with all of the data presented here the channels were not flushed or equilibrated between runs permitting rapid, serial injections. The average separation efficiency for the peptides used in this set of experiments was 680,000 theoretical plates. This represents a substantial improvement in performance from our previous results using liquid phase coating methods which resulted in an average separation efficiency of 200,000 theoretical plates for CE-ESI-MS of peptide standards.[5] The average Δ value for CE-MS using the CVD coating method was 1.6 for the peptide standards, indicating some further improvement may be possible. The peptide peaks were sampled approximately five times per peak on average using the 8 Hz MS acquisition rate. This under-sampling could underestimate peak height and inflate the measured peak widths slightly. These results indicate that the CVD silanization method is fully compatible with ESI-MS and is capable of coating long channel networks for exceptional separation performance.

2.3.5 CE-ESI-MS of enolase tryptic digest

After characterizing the performance of CVD deposited aminopropyl silane coatings we simulated a peptide mapping experiment by performing CE-ESI-MS of an enolase tryptic digest. This sample contains a complex mixture of peptides and gives a better indication of separation peak capacity than the peptide standards. An electropherogram of this separation is shown in Figure 2.6. For the overall CE-ESI-MS separation we observed a median base peak width of 375 ms within the 24-second migration time window (a peak capacity of 64). The insets in Figure 2.6

show the mass spectra obtained for the indicated peptide peaks. The spectrum from the earlier peak is dominated by a doubly charged tryptic peptide with a molecular weight of 1,156.6 Da. The spectrum from the later peak is dominated by a charge state envelope from an unidentified sample component with a molecular weight of 15.7 kDa. We have observed this unidentified sample component in a number of different samples obtained from Waters Corporation, including the intact protein sample described below. While we have not identified this component, its presence highlights the ability of CE-ESI-MS to efficiently separate a wide range of peptides and proteins concurrently. We believe this property makes CE-ESI-MS well-suited for peptide mapping experiments.

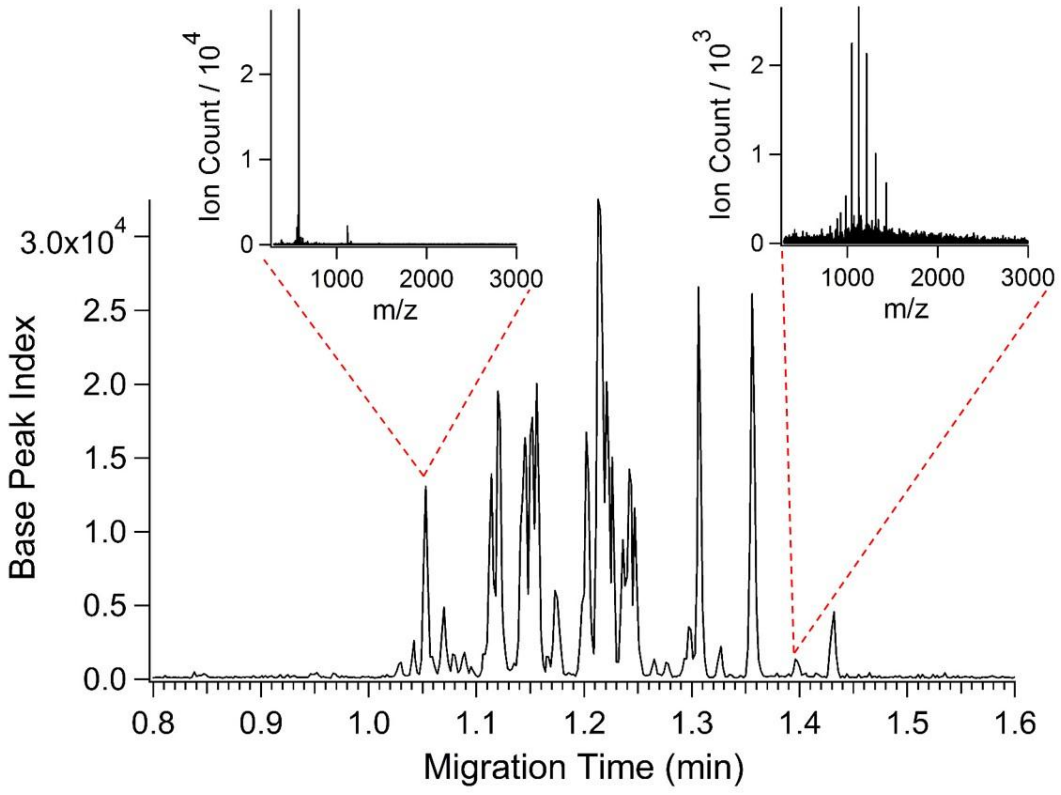

Figure 2.6 Base peak electropherogram for the analysis of a 5 μM tryptic digest of the enzyme enolase. All other experimental conditions were the same as in Figure 2.5. MS spectra insets show a doubly charged peptide with a molecular weight of 1,156.6 Da eluting at 1.05 min as well as a protein envelope eluting at 1.4 min associated with a 15.7 kDa molecular weight species.

The data from the CE-ESI-MS analysis of enolase tryptic digest was further processed using BiopharmaLynx to simulate a peptide mapping experiment. By automated matching of observed masses to the amino acid sequence of yeast enolase, 85% sequence coverage was achieved with 42 identified peptides. Of the 52 possible tryptic fragments 30 were identified (allowing for no missed cleavages or modifications), including all 25 of the possible tryptic fragments larger than 700 Da. Expected tryptic fragments with molecular weights less than 450 Da were not detected. It is possible that more of these low mass fragments could have been identified if the instrument had been set to scan below 300 m/z. It is also possible that some of these smaller components might be lost during sample preparation by the supplier.[52]

2.3.6 CE-ESI-MS of intact proteins

In addition to peptide separations, the APDIPES-coated CE-ESI device was used to analyze a commercial intact protein standard mixture. A total ion electropherogram from one of these separations is shown in Figure 2.7. The mass spectra from the four most intense peaks are also shown. All six of the proteins present in this sample were identified in the four most intense peaks. The observed masses and assignments are listed in Table 2.3. Three less abundant components observed (peaks 2, 3, and 4) did not correspond to any known sample components. Minor variants were observed for enolase and myoglobin. The observed mass spectrum for peak 7, assigned as phosphorylase b, could not be deconvoluted. This assignment was made based on the process of elimination and previous work. The efficiency values calculated for the peaks observed in this separation ranged from 100,000 to 400,000 theoretical plates (an average of 1.5 million plates per meter). Peak shapes for fully resolved components were Gaussian and symmetrical, suggesting that the highly charged protein molecules were effectively repelled from the positively charged APS surface. The run-to-run migration time reproducibility was stable

with less than 0.7% RSD (n = 3) for all proteins as determined from their extracted ion electropherograms.

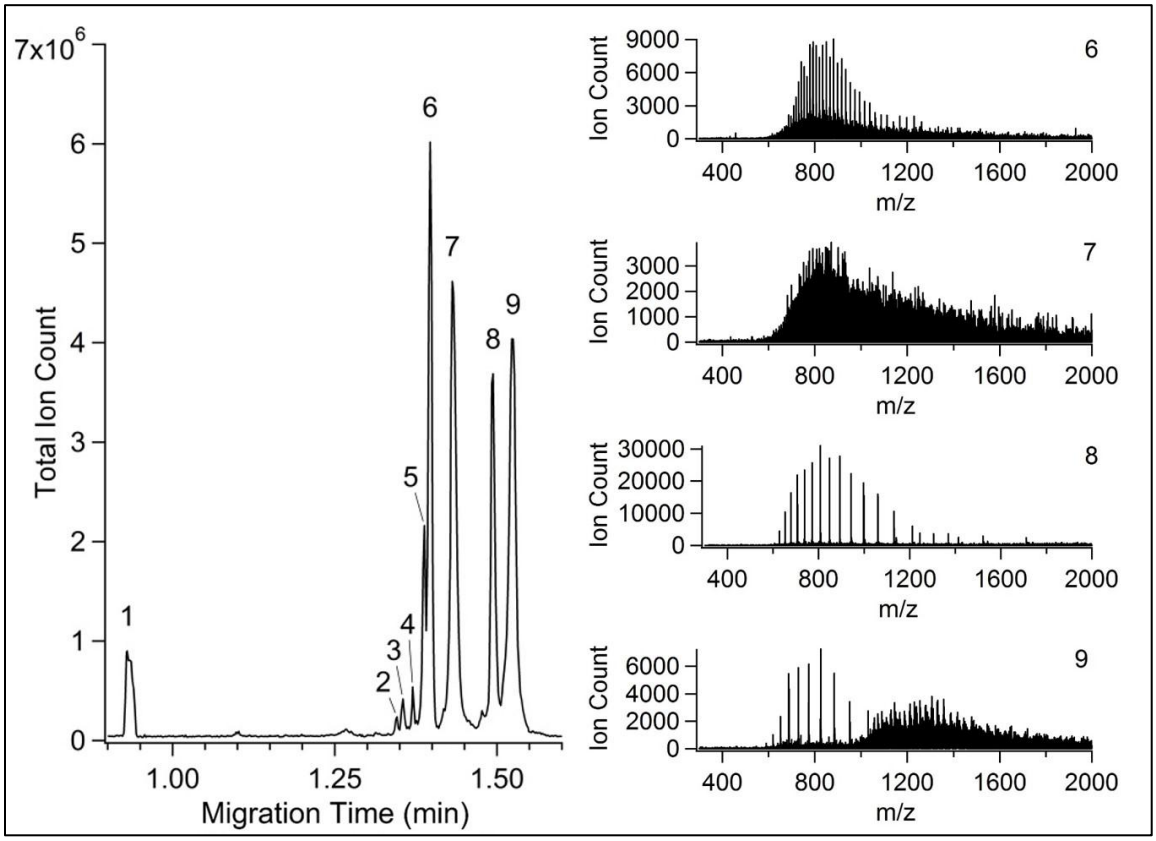

Figure 2.7 TIC electropherogram of an intact protein standard mixture analyzed by CE-MS using a CVD APS coated microchip. Insets show mass spectra for the most intense protein bands including the co-elution of cytochrome c and the larger protein BSA in peak 9.

Table 2.3 Peaks observed by CE-ESI-MS of the intact protein mixture.*

Peak #	Migration Time (min)	FWHM (s)	MW observed (kDa)	Assignment
1	0.93	N/A	N/A	neutral contaminant
2	1.35	0.222	26.7	?
3	1.36	0.299	61.2	?
4	1.37	0.288	15.7	?
5	1.39	0.327	46.8	enolase
6	1.40	0.356	46.7	enolase
7	1.43	0.581	?	phosphorylase b
8	1.49	0.429	17.0 and 13.7	myoglobin and ribonuclease A
9	1.52	0.721	12.4 and 66.4	cytochrome c and BSA

*50% acetonitrile, 0.1% formic acid BGE

While we strongly advocate quantifying CE separation performance using the efficiency coefficient metric, the molecular complexity of intact proteins presents an added complication to such an approach. For such molecules, a CE band may include a population of species possessing slight differences in electrophoretic mobility (due to heterogeneity in the folding structure, or the presence of minor chemical variants). So, the variance of a protein peak may be indicative of the molecules within the band and not the quality of the surface coating. Future work will be directed at evaluating intact protein separations more thoroughly. While the efficiency of the intact protein separations reported here compares favorably to other literature reports,[15-17, 53-57] the resolution could be further improved by lowering the electroosmotic flow rate or by using longer separation channels and a higher separation voltage.

2.4 Conclusions

Chemical vapor deposition of aminopropyl silanes is an excellent method for coating microfluidic CE-ESI devices. The method is simple, fast, and well-suited to bulk processing of multiple devices. Stable surface coatings were produced with excellent device-to-device reproducibility. The coated devices exhibited strong anodic EOF and exceptional electrophoretic separation efficiency for a range of neutral and cationic analytes. Coating stability was sufficient for storage over at least a 1-week period and coatings have exhibited stable performance in acidic BGE for days to weeks without reconditioning. The CE-LIF method used to evaluate the performance of the coating is capable of accurately measuring electroosmotic mobility and band broadening within the separation column. The efficiency coefficient (Δ) is introduced to clearly indicate the efficiency of a separation relative to the theoretical optimum. This approach facilitates direct comparison of performance between devices and across instrument platforms making it a useful tool for method optimization. Use of this metric would aid in the comparison

of various CE experiments. CE-ESI-MS separations indicate that this coating method is fully compatible with long separation channels (up to at least 23 cm) and ESI-MS. To our knowledge the CE-ESI-MS separations of peptides and intact proteins described here are the most efficient ever reported. Future work will explore the limits of coating longer separation channels while maintaining separation quality. While the work reported here utilized microfluidic devices, the approach should also be appropriate for coating fused silica capillary columns. These coatings could also provide an ideal base layer for further chemical modification of surfaces. The subsequent chapter describes progress in utilizing APDIPES as a base layer for generating high efficiency surface coatings with a range of EOF magnitudes for enhanced resolution.

2.5 References

1. Ramautar, R., Heemskerk, A. A. M., Hensbergen, P. J., Deelder, A. M., Busnel, J.-M., Mayboroda, O. A., *J. Proteomics* **2012**, *75*.

2. Bonvin, G., Veuthey, J. L., Rudaz, S., Schappler, J., *Electrophoresis* **2012**, *33*. 552-562.

3. Figeys, D., vanOostveen, I., Ducret, A., Aebersold, R., *Anal. Chem.* **1996**, *68*. 1822-1828.

4. Janini, G. M., Conrads, T. P., Wilkens, K. L., Issaq, H. J., Veenstra, T. D., *Anal. Chem.* **2003**, *75*. 1615-1619.

5. Mellors, J. S., Gorbounov, V., Ramsey, R. S., Ramsey, J. M., *Anal. Chem.* **2008**, *80*. 6881-6887.

6. Moini, M., *Anal. Chem.* **2001**, *73*. 3497-3501.

7. Samskog, J., Wetterhall, M., Jacobsson, S., Markides, K., *J. Mass Spectrom.* **2000**, *35*. 919-924.

8. Pioch, M., Bunz, S.-C., Neusuess, C., *Electrophoresis* **2012**, *33*.

9. Huhn, C., Ramautar, R., Wuhrer, M., Somsen, G. W., *Anal. Bioanal. Chem.* **2010**, *396*. 297-314.

10. Elhamili, A., Wetterhall, M., Arvidsson, B., Sebastiano, R., Righetti, P. G., Bergquist, J., *Electrophoresis* **2008**, *29*. 1619-1625.

11. Faserl, K., Sarg, B., Kremser, L., Lindner, H., *Anal. Chem.* **2011**, *83*. 7297-7305.

12. Feldmann, A., Claussnitzer, U., Otto, M., *J. Chromatogr., B* **2004**, *803*. 149-157.

13. Ghosal, S., *Anal. Chem.* **2002**, *74*. 4198-4203.

14. Hardenborg, E., Zuberovic, A., Ullsten, S., Soderberg, L., Heldin, E., Markides, K. E., *J. Chromatogr., A* **2003**, *1003*. 217-221.

15. Haselberg, R., de Jong, G. J., Somsen, G. W., *Electrophoresis* **2011**, *32*. 66-82.

16. Haselberg, R., Brinks, V., Hawe, A., de Jong, G. J., Somsen, G. W., *Anal. and Bioanal. Chem.* **2011**, *400*. 295-303.

17. Haselberg, R., de Jong, G. J., Somsen, G. W., *J. Sep. Sci.* **2009**, *32*. 2408-2415.

18. He, M., Zeng, Y., Jemere, A. B., Harrison, D. J., *J. Chromatogr., A* **2012**, *1241*. 112-116.

19. Monton, M. R. N., Tomita, M., Soga, T., Ishihama, Y., *Anal. Chem.* **2007**, *79*. 7838-7844.

20. Ramautar, R., Mayboroda, O. A., Derks, R. J. E., van Nieuwkoop, C., van Dissel, J. T., Sornsen, G. W., Deelder, A. M., de Jong, G. J., *Electrophoresis* **2008**, *29*. 2714-2722.

21. Ullsten, S., Zuberovic, A., Wetterhall, M., Hardenborg, E., Markides, K. E., Bergquist, J., *Electrophoresis* **2004**, *25*. 2090-2099.

22. Jorgenson, J. W., Lukacs, K. D., *Anal. Chem.* **1981**, *53*. 1298-1302.

23. Jorgenson, J. W., Lukacs, K. D., *J. Chromatogr.* **1981**, *218*. 209-216.

24. Jorgenson, J. W., Lukacs, K. D., *Clin. Chem.* **1981**, *27*. 1551-1553.

25. Oda, R. P., Landers, J. P., in *Hand Book of Capillary Electrophoresis*, ed. J. P. Landers. CRC Press: Boca Raton, Second edn., 1997, pp 2-20.

26. Petersen, N. J., Nikolajsen, R. P. H., Mogensen, K. B., Kutter, J. P., *Electrophoresis* **2004**, *25*. 253-269.

27. Datta, S., Ghosal, S., *Phys. Fluids* **2008**, *20*.

28. Squires, T. M., Quake, S. R., *Rev. Mod. Phys.* **2005**, *77*. 977-1026.

29. Jorgenson, J. W., Lukacs, K. D., *Science* **1983**, *222*. 266-272.

30. Chambers, A. G., Mellors, J. S., Henley, W. H., Ramsey, J. M., *Anal. Chem.* **2011**, *83*. 842-849.

31. Mellors, J. S., Jorabchi, K., Smith, L. M., Ramsey, J. M., *Anal. Chem.* **2010**, *82*. 967-973.

32. Pattky, M., Huhn, C., *Anal. Bioanal. Chem.* **2013**, *405*. 225-237.

33. Chen, Z., Ghosal, S., *Bull. Math. Biol.* **2012**, *74*. 346-355.

34. Datta, S., Ghosal, S., Patankar, N. A., *Electrophoresis* **2006**, *27*. 611-619.

35. Ghosal, S., *Electrophoresis* **2004**, *25*. 214-228.

36. Ghosal, S., *J. Fluid Mech.* **2002**, *459*. 103-128.

37. Herr, A. E., Molho, J. I., Santiago, J. G., Mungal, M. G., Kenny, T. W., Garguilo, M. G., *Anal. Chem.* **2000**, *72*. 1053-1057.

38. Zhang, F., Sautter, K., Larsen, A. M., Findley, D. A., Davis, R. C., Samha, H., Linford, M. R., *Langmuir* **2010**, *26*. 14648-14654.

39. Pang, I., Kim, S., Lee, J., *Surf. Coat. Technol.* **2007**, *201*. 9426-9431.

40. Shirahata, N., Hozumi, A., *J. Nanosci. Nanotechnol.* **2006**, *6*. 1695-1700.

41. Popat, K. C., Robert, R. W., Desai, T. A., *Surf. Coat. Technol.* **2002**, *154*. 253-261.

42. Culbertson, C. T., Jacobson, S. C., Ramsey, J. M., *Anal. Chem.* **1998**, *70*. 3781-3789.

43. Jacobson, S. C., Hergenroder, R., Koutny, L. B., Warmack, R. J., Ramsey, J. M., *Anal. Chem.* **1994**, *66*. 1107-1113.

44. Jacobson, S. C., Hergenroder, R., Koutny, L. B., Ramsey, J. M., *Anal. Chem.* **1994**, *66*. 1114-1118.

45. Thorsteinsdottir, M., Isaksson, R., Westerlund, D., *Electrophoresis* **1995**, *16*. 557-563.

46. Anderson, A. S., Dattelbaum, A. M., Montano, G. A., Price, D. N., Schmidt, J. G., Martinez, J. S., Grace, W. K., Grace, K. M., Swanson, B. I., *Langmuir* **2008**, *24*. 2240-2247.

47. Zhu, M. J., Lerum, M. Z., Chen, W., *Langmuir* **2012**, *28*. 416-423.

48. Waterval, J. C. M., Hommels, G., Bestebreurtje, P., Versluis, C., Heck, A. J. R., Bult, A., Lingeman, H., Underberg, W. J. M., *Electrophoresis* **2001**, *22*. 2709-2716.

49. Cao, P., Moini, M., *J. Am. Soc. Mass Spectrom.* **1998**, *9*. 1081-1088.

50. MacDonald, A. M., Bahnasy, M. F., Lucy, C. A., *J. Chromatogr., A* **2011**, *1218*. 178-184.

51. Mellors, J. S., Black, W. A., Chambers, A. G., Starkey, J. A., Lacher, N. A., Ramsey, J. M., *Analytical Chemistry* **2013**, *85*. 4100-4106.

52. Whitmore, C. D., Gennaro, L. A., *Electrophoresis* **2012**, *33*. 1550-1556.

53. Haselberg, R., de Jong, G. J., Somsen, G. W., *Anal. Chim. Acta* **2010**, *678*. 128-134.

54. Haselberg, R., Ratnayake, C. K., de Jong, G. J., Somsen, G. W., *J. Chromatogr., A* **2010**, *1217*. 7605-7611.

55. Jurcic, K., Yeung, K. K. C., *Electrophoresis* **2009**, *30*. 1817-1827.

56. Elhamili, A., Wetterhall, M., Sjodin, M., Sebastiano, R., Bergquist, J., *Electrophoresis* **2010**, *31*. 1151-1156.

57. Sebastiano, R., Mendieta, M. E., Contiello, N., Citterio, A., Righetti, P. G., *Electrophoresis* **2009**, *30*. 2313-2320.

CHAPTER 3: AMINOPROPYL SILANE-POLYETHYLENE GLYCOL SURFACE COATINGS FOR MODULATING THE EOF OF HIGHLY EFFICIENT CE-ESI-MS

3.1 Introduction

CE has tremendous potential for the separation of biological molecules and is capable of producing highly efficient separations with short analysis times.[1-8] To maximize the utility of CE for many biological applications it must be compatible with mass spectrometry (MS) due to the inherent complexity of biological samples and the information-rich nature of MS. For bioanalytical applications surface coatings play a vital role in analyte-wall interaction inhibition as well as dictating the magnitude and direction of the electroosmotic flow (EOF).[9-11] The inhibition of analyte-wall interactions is paramount for realizing the potential time and efficiency benefits of CE and EOF control is necessary for resolving complex mixtures.[8] Efficient CE requires that surface coatings be highly uniform because nonuniform coatings lead to excessive band broadening.[8, 12] For electrospray ionization (ESI)-MS surface coatings must also be static. Methods that use dynamic coatings as opposed to static coatings or rely on buffer additives such as salts lead to elevated MS background signal and ionization suppression.[9] For similar reasons it is preferable that static coatings be covalently attached to the surface.[13-15] Many surface coating methods exist but few approach the theoretical separative performance maximum of CE.[8] What is needed is a surface coating method that produces highly efficient separations without the use of buffer additives enabling stable and sensitive ESI-MS. Additionally, a range of EOF magnitudes that are applicable to biological analytes is desirable.

In the literature, it is common to find CE surface coatings that either yield a strong EOF relative to the electrophoretic mobility (μ_{ep}) of biological analytes or a near-zero EOF.[9] Highly efficient, ESI-MS compatible surface coatings that offer intermediate values of EOF are missing from the available coating technology. The benefit of having many EOF magnitudes available is apparent when considering the resolution equation for CE:

$$R_s = 0.177\left(\mu_{ep,1} - \mu_{ep,2}\right)\left[\frac{V}{D(\bar{\mu}_{ep} + \mu_{eo})}\right]^{1/2} \quad (3.1)$$

From eq 1 it is evident that resolution in CE is theoretically maximized when the EOF (μ_{eo}) is equal in magnitude and opposite in direction to the average analyte electrophoretic mobility ($\bar{\mu}_{ep}$) regardless of the voltage applied (V) or the analyte diffusivity (D). Though this condition results in maximum resolution, by considering eq 2, it is apparent that this condition also results in average migration times ($\bar{t}$) that approach infinity regardless of the separation channel length (l) or electric field strength (E).

$$\bar{t} = \frac{l}{E(\bar{\mu}_{ep} \mp \mu_{eo})} \quad (3.2)$$

From eq 1 and eq 2 we see that separations performed at the maximum resolution condition are impossible due to the effect on analysis time. These equations show that controlling μ_{eo} is crucial for designing conditions that meet both the resolution and analysis time requirements for a given separation. Separation results using coatings with a range of EOF magnitudes have been published previously.[6, 11, 15-22] Based on reported efficiency values in the literature as well as our experience, they have resulted in separation performance that is far from optimal when compared to the theoretical limit for CE.[8] For a surface coating well suited to its intended application, the EOF should balance the resolution and analysis time requirements based on $\bar{\mu}_{ep}$ while

maintaining high separation efficiency. For biological analytes, MS compatibility of the coating and background electrolyte (BGE) is imperative.

Our lab has recently published work describing covalent, cationic surface coatings achieved by chemical vapor deposition (CVD) of aminopropyl silane (APS) reagents.[8] The CVD method produced a uniform surface of primary amines inside microfluidic channels, resulting in an anodic EOF. The magnitude of this EOF was 4x-5x greater than $-\bar{\mu}_{ep}$ for the intended analytes resulting in separations that were heavily dominated by μ_{eo}. These coatings were used in conjunction with CE-ESI microchips coupled to MS to separate mixtures of peptides and proteins. The separation efficiency was found to be exceptional, resulting in near diffusion-limited performance.[8] However, it would be desirable to have coatings that maintain this high level of efficiency while offering a range of EOF magnitudes for improved resolution according to eq 1. The APS coatings are an excellent base layer for subsequent covalent modification due to the uniform layer of reactive primary amines. Polyethylene glycol (PEG)-based surface coatings are attractive for CE due to their hydrophilic nature, which has been shown to reduce adsorption of biological species.[23-24] A series of NHS-PEG reagents with varying chain lengths are commercially available for improving protein solubility and are designed to target the primary amines located on protein surfaces. Therefore NHS-PEG is a well-suited reagent for the modification of our APS CVD coatings and offers a series of reagents for the generation of a range of EOF.[25] Wang and coworkers published a PEG-based coating method that used a (3-aminopropyl)triethoxysilane (APTES) base layer, administered in the liquid phase and an *n*-hydroxy succinimide ester of PEG (NHS-PEG) to modify this layer for CE.[25] Results from the Wang report showed that PEGylation reduced analyte adsorption though the separative performance was poor and the method was incompatible with MS. Other iterations of PEG-based

surface coatings for CE have been published.[15, 26] Methods for PEG-based coatings have been developed which lead to good separation efficiencies[27] or are MS-compatible[14] but not both.

In this work we describe a coating method for CE-ESI-MS of biological analytes that produces efficient separations while offering multiple EOF magnitudes. Devices coated with (3-aminopropyl)di-isopropylethoxysilane (APDIPES) via CVD were subsequently treated with NHS-PEG of varying chain lengths to produce a broad range of EOF magnitudes. To determine the relationship between EOF and PEG chain length, CE separations were performed using laser induced fluorescence (LIF) experiments. Additionally, microfluidic chips with integrated ESI emitters[28] were coated and used to perform CE-ESI-MS of peptide and protein mixtures. A peptide mixture was separated using an APDIPES-PEG surface coating with intermediate EOF. A mixture of intact proteins was separated using an APDIPES-PEG surface coating with a near-zero EOF.

3.2 Experimental

3.2.1 Reagents and materials.

MS-grade organic solvents (acetonitrile, 2-propanol), formic acid (99.9% purity) and potassium hydroxide were obtained from Fisher Scientific (Fairlawn, NJ). Distilled water was deionized with a Nanopure Diamond water purifier (Barnstead International, Dubuque, IA). Fluorescein, rhodamine 6G, and trichloro(1H,1H,2H,2H-perfluorooctyl)silane were obtained from Sigma-Aldrich (St. Louis, MO). Methyl-terminated polyethylene glycol *n*-hydroxy succinimide esters (NHS-PEG) with 4, 12, and 24 polymer units, corresponding to molecular weights of 333 Da, 686 Da and 1,214 Da respectively, were purchased through Fisher Scientific. NHS-PEG reagent with 110 polymer units (MW = 5 kDa) was purchased from Fluka. NHS-PEG reagents with 223 and 450 polymer units (MW = 10 kDa and 20 kDa, respectively) were

purchased from JenKem Technology (Beijing, China). Additional 20 kDa NHS-PEG reagent was purchased from Nanocs (Boston, MA). Silane reagent, 3-(aminopropyl)di-isopropyl-ethoxysilane (APDIPES), was obtained from Gelest (Morrisville, PA). Peptide analytes bradykinin, methionine-enkephalin, thymopentin and angiotensin II were obtained from American Peptide Company (Sunnyvale, CA). MassPrep enolase tryptic digest was provided by Waters Corporation (Milford, MA). Intact proteins carbonic anhydrase I (human), hemoglobin (human), serum albumin (human), and cytochrome c (equine) were acquired from Sigma Aldrich (St. Louis, MO). Lysozyme (egg white) was acquired through Fisher Scientific.

3.2.2 Fabrication of microfluidic devices

Two microfluidic device designs were used for this work. Capillary electrophoresis microchips used with LIF detection were fabricated from 0.9 mm thick B270 glass purchased from Telic Company (Valencia, CA). CE-ESI microchips (Figure 3.1) were fabricated using 0.5 mm thick B270 glass obtained from Caliper Life Sciences (Hopkinton, MA). Previously described photolithography and wet chemical etching techniques were used to etch all microchannels to a depth of 10 μm and a full width of 70 μm.[28-29] To form integrated ESI emitters the corners of CE-ESI devices were diced to 90° using a precision dicer (Dicing Technology Incorporated, Longwood, FL). The emitters on these devices were then polished to remove dicing imperfections using a lapping wheel with 3 μm cerium oxide abrasive lapping paper from Ultra Tec (Santa Ana, CA). Glass cylinders, 8 mm in diameter, were attached to all devices for use as solvent reservoirs using a chemically resistant epoxy (Loctite E-120HP, Henkel Corporation, Germany).

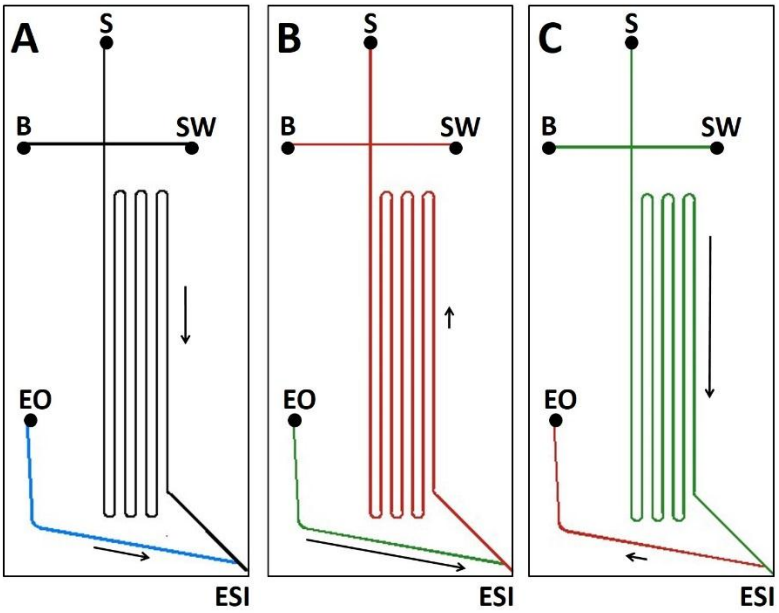

Figure 3.1 Microfluidic chip design and surface coatings used for CE-ESI. A) Separation channel coated with PEG_{24} (black) and native glass EO pump channel (blue) used for the separation of tryptic peptides. B) Separation channel coated with PEG_{450} (red) and EO pump channel coated with APDIPES (green) used for separation of intact proteins. C) Separation channel coated with APDIPES (green) and EO pump channel coated with PEG_{450} (red) used for comparison to devices with PEGylated separation channels. Arrows indicate EOF direction and relative magnitude for each microchannel.

3.2.3 Surface coating methods

Microfluidic devices were coated with APDIPES using a chemical vapor deposition process[8] followed by PEGylation with one of six NHS-PEG reagents. The PEGylation procedure results in a covalent bond between the PEG chain and the primary amines of the surface coating. NHS-PEG solutions were prepared in 100 mM phosphate buffer (pH 7.5) at concentrations between 1 and 10 mg/mL. Microfluidic channels were PEGylated by flowing the NHS-PEG reaction mixture through the channels for a period of 1 hour. Flow was controlled by applying suction at the ESI emitter of CE-ESI devices (Figure 3.1) and at the waste port of CE-LIF devices. The PEGylation of CE-ESI devices with the longest chain PEG reagent was performed using suction at the ESI tip as well as a head pressure of 50 psi applied to each of the three

reservoirs making up the injection cross. PEGylated channels were subsequently rinsed with DI water for 10 min followed by BGE for 10 min. After rinsing the device, the external surface of the ESI emitter was coated with trichloro-(1H,1H,2H,2H-perfluorooctyl)-silane to increase the surface hydrophobicity and facilitate ESI. A micropipet was used to apply 3 μL of silane to the emitter surfaces. This volume was allowed to sit undisturbed for 30 s and was then removed using suction. Any excess reagent was wiped off using a disposable cloth. The microchannels of the device were then dried using suction and the tip coating was cured at room temperature for at least 10 min.

The CE-ESI chip design with three coating schemes is illustrated in Figure 3.1. The design includes an injection cross, a 23 cm serpentine separation channel, an electroosmotic pump, and an ESI orifice (ESI). The turns on all CE-ESI devices were asymmetrically tapered to minimize band broadening.[28, 30-31] Devices featured four reservoirs as indicated in Figure 3.1; background electrolyte (B), sample (S), sample waste (SW) and electroosmotic pump (EO). The device in Figure 3.1A was used with PEG_{24} coatings in which the separation channel is PEGylated and the EO pump channel has been stripped to bare glass using a 40 mg/mL potassium hydroxide solution in 80% 2-propanol. Figure 3.1B shows a CE-ESI device used with PEG_{450} coatings and an APDIPES coated EO pump channel. The low EOF resulting from the PEG_{450} coating requires a reversal of voltage polarity to operate the device. Figure 3.1C describes a device with an APDIPES-coated separation channel and a PEG_{450}-coated side channel that was used for direct comparison to device B.

3.2.4 Surface characterization via CE-LIF

All microfluidic devices were operated by applying voltages to the solvent reservoirs. Polyethylene caps (Grace Davison Discovery Sciences, Bannockburn, IL) were placed on each

reservoir to prevent solvent evaporation. Platinum wire electrodes (Alpha Aesar, Ward Hill, MA) were inserted into each reservoir through small holes in the reservoir caps. Simple microfluidic chips featuring an injection cross and a 3 cm separation channel were used to perform initial characterization of the PEGylated surfaces using CE-LIF as previously described.[8] For this work a total of 18 microfluidic devices were used. CE-LIF was performed using a Nikon Eclipse Ti-U inverted microscope (Rochester, NY) equipped with a dual filter turret. The 488 nm beam from a continuous wave, tunable argon ion laser by Melles Griot Laser Group (Carlsbad, CA) was directed into the back of the microscope at an intensity of 2 mW and diverted towards the stage using a Nikon filter cube containing a Semrock dichroic mirror. Fluorescence was collected in an epifluorescence setup through a 488 nm Semrock BrightLine long pass filter and detected using a photomultiplier tube from Hamamatsu (Bridgewater, NJ, model H6780). The microscope was equipped with a Sony Exwave HAD 3 CCD color video camera, Model DXC-390 (Sony Corp, Japan) and a Nikon Intensilight mercury arc lamp for fluid observation. Devices were mounted on the microscope using a custom polycarbonate stage (to minimize the chance of electrical arcing). Caution should be used when working with high voltage power supplies including appropriate grounding and personal protective equipment. The electrodes were powered by a custom-built Bertan Model 2866, fast-switching, 6-channel power supply capable of supplying 0 to +10 kV to each reservoir independently. Depending on the surface coating and resultant EOF, two voltage profiles, found in Table 3.1, were used. For longer chain PEG surfaces the reduced EOF magnitude was less than the electrophoretic mobility of the analytes, requiring a reversal of voltage polarity.

Table 3.1 Applied Voltage Profiles for CE-LIF Analyses.

	Voltages Applied (kV)			
Coating	**B**	**S**	**SW**	**W**
APDIPES	0	0	+1.4	+2.0
PEG_4 - PEG_{110}	0	0	+1.4	+2.0
PEG_{223} - PEG_{450}	+1.7	+1.4	+0.7	0

3.2.5 Peptide and protein analyses via CE-ESI-MS

For MS analysis, CE-ESI devices were mounted on a custom built polycarbonate stage with the ESI corner approximately 5 mm from the sample cone inlet of a Synapt G2 quadrupole-ion mobility-time of flight mass spectrometer (Waters Corporation, Milford, MA). A $1/16^{th}$ inch thick, 4 cm by 5 cm, single-sided copper clad circuit board (M.G. Chemicals, Burlington, Ontario, Canada) was used to shield the electrospray orifice from the high voltages applied to the microfluidic reservoirs. A thin slit was cut into the rectangular board such that the ESI corner could protrude 3-5 mm through the slit. A relatively low, positive potential (500 V) was applied to the shield electrode during CE-ESI operation. Voltage profiles used for operation of all three devices are found in Table 3.2.

Table 3.2 Applied Voltage Profiles for CE-ESI-MS Analyses.

	Voltage (kV)				E-field ($V^{-1}cm^{-1}$)
Coating	**B**	**S**	**SW**	**EO**	**-**
APDIPES	-6	-6	-5	+5	375
PEG_{24}	-6	-6	-5	+5	375
PEG_{24}	-15	-15	-14	+6.5	745
PEG_{450}	+18	+18	+16	+2.75	500

CE-ESI devices coated with PEG_{24} were operated using a home-built power supply containing five individual power supply modules from UltraVolt Inc. (Ronkonkoma, NY). Three of the modules (10A12-N4) could supply 0 to -10 kV while the other two modules (10A12-P4) could supply 0 to +10 kV. CE-ESI devices coated with PEG_{450} were operated using an analogous

home-built supply in which two of the modules could supply 0 to +10 kV and three of the modules (20A24-P15) could supply 0 to +20 kV. The power supplies were controlled via a SCB-68 breakout box connected to a PC via a PCI 6713 DAQ card (National Instruments, Austin TX). A LabVIEW program was used to control voltage outputs. The MS was operated in "Sensitivity mode" at an acquisition rate of 90 ms per summed scan with an inter-scan delay of 24 ms. Data were acquired from 300 to 3000 m/z. MassLynx software on the MS control computer was used for data acquisition, triggered by the LabVIEW program used for electrokinetic control of the microfluidic device. Electropherograms collected in MassLynx were exported to IGOR Pro for peak fitting analysis. Proteins were identified using the maximum entropy software built in to MassLynx (MaxEnt 1).

3.3 Results and discussion

3.3.1 Surface coating characterization

The effect of PEG chain length on the EOF was determined using LIF detection of the neutral marker fluorescein. The EOF in a single BGE (50% acetonitrile, 0.1% formic acid), chosen because it is well suited for CE-ESI-MS of peptides and proteins, was measured. A plot of the observed EOF versus PEG chain length with APDIPES as a base layer is shown in Figure 3.2. The fitted line includes data from the unmodified APDIPES surface and five of the six PEG reagents studied, excluding PEG_4. This plot shows that the reduction in EOF increased as the PEG chain length increased for five of the six reagents studied. The PEG_{450} surface resulted in the greatest reduction in EOF (97.0%) with a magnitude of 3.2 (± 0.9) $x10^{-5}$ $cm^2V^{-1}s^{-1}$. The PEG_{12} surface resulted in the least reduction in EOF (41.0%) with a magnitude of 6.25 (± 0.06) $x10^{-4}$ $cm^2V^{-1}s^{-1}$. The effect of PEG reagent on EOF was found to be highly reproducible for all reagents studied as is evident from the small error bars in Figure 3.2. The PEG reagents used to

generate this data were acquired from three separate vendors highlighting the reproducibility of the polymer effect on EOF.

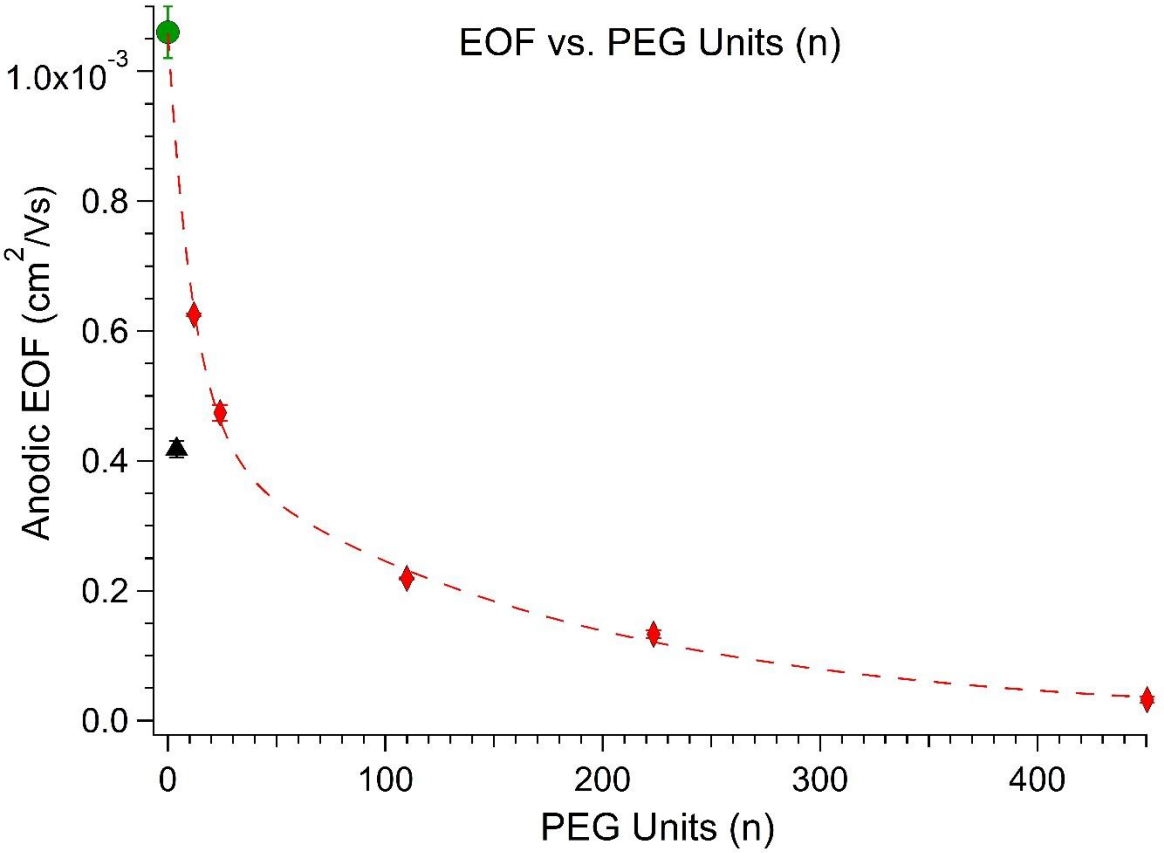

Figure 3.2 A study of EOF versus PEG chain length for PEG reagents ranging from 4 to 450 polymer units. PEG_{12} – PEG_{450} coatings are represented by red diamonds. The green circle represents data from devices coated with APDIPES only. The PEG_4 coating is represented by a black triangle (excluded from fit). EOF was reduced to a minimum of 3.2 $x10^{-5}$ $cm^2V^{-1}s^{-1}$. The red dashed line is a double exponential fit to all points excluding the PEG_4 surfaces (see text for discussion on exclusion). Error bars are ± one standard deviation (n = 3). Error bars for most PEG coatings are within the markers.

Interestingly, the shortest PEG chain investigated (PEG_4) yielded an EOF (4.2 (± 0.3) $x10^{-4}$ $cm^2V^{-1}s^{-1}$, 60% reduction) that was lower than expected based on the trend set by the other PEG derivatives. To understand the anomalous PEG_4 result, the mode by which PEGylation affects the EOF is considered. There are two possibilities for how the PEG reagents modify the

EOF: 1) reduction of the surface ζ-potential by conversion of cationic primary amines to uncharged amides, and 2) imparting viscous drag at the channel walls due to the PEG chains extending into the electrical double layer. For the NHS-PEG reagents studied, these two effects on EOF are considered to be working in concert. It appears that for PEG chain lengths ranging from 12 units to 450 units, the dominant effect in terms of EOF reduction is due to viscous drag in the electrical double layer. The EOF versus PEG chain length curve generated from these coatings is exponential in nature which is in good agreement with electrical double layer theory and previous observations of the effect of polymer chain length on EOF.[27] The anomalously low EOF observed with the PEG_4 polymer chain suggests that reduction of the ζ-potential occurs to a greater extent with this reagent than with the others. This behavior could be explained by differences in coating density achieved with the different PEG reagents. In other words, steric hindrance prevents the larger NHS-PEG reagents from reacting with most of the potential surface bonding sites; but the long polymer chains that do bond to the surface reduce the EOF by viscous drag. The smaller, PEG_4 reagent can react with a larger percentage of bonding sites, turning positively charged amine groups into uncharged amide linkages and significantly reducing the ζ-potential of the microchannel surface.

3.3.2 APTES PEGylation and non-functionalized PEG

CVD coatings of APTES were investigated as a base layer for PEGylation with NHS-PEG. The same NHS-PEG reagents and procedure for APDIPES PEGylation were applied to APTES in triplicate. A plot of the observed EOF versus NHS-PEG chain length on APTES can be found in the Figure 3.3. NHS-PEG did not produce the same exponential trend observed using APDIPES. Five of the six NHS-PEG reagents resulted in similar EOF reduction (~43%). NHS-PEG_{110} produced the greatest EOF reduction on APTES (70%). In addition to a narrower range

of EOF, the amount of EOF reduction was less reproducible on APTES than when using APDIPES. These results may be attributable to hydrophobicity differences for each APS reagent or possibly the variability of surface structures that can be formed by APTES as compared to APDIPES. APTES is known to form multiple structures when bonded to silica, including cyclical rings, due to its tri-functional nature.[32] It is possible that these properties affect the NHS-PEGylation reaction though this effect needs to be studied further. These results emphasize the benefits of using APDIPES as a base layer as opposed to APTES for producing a range of EOF values.

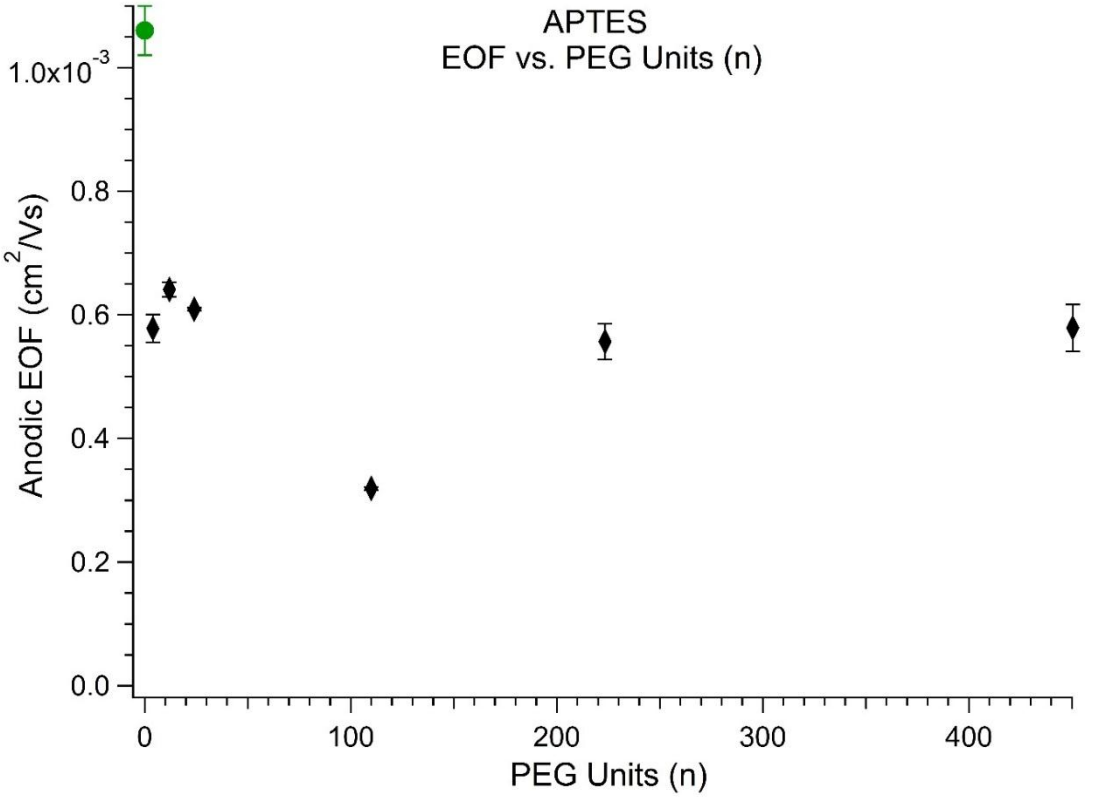

Figure 3.3 A plot of EOF versus PEG chain length using APTES as the base layer. The EOF of the APTES surface is represented by the green circle. NHS-PEG reagents are represented with black diamonds. Error bars are ± one standard deviation (n = 3). As compared to the plot generated when APDIPES was used as the base layer this plot shows a narrower range of EOF magnitudes, less reproducibility for all PEG reagents studied, and a minimum EOF that is an order of magnitude greater than that achieved with APDIPES-PEG_{450}.

To investigate the potential effects of adsorption versus covalent attachment of PEG, PEG reagents without NHS functionalization were applied to APDIPES surfaces. PEG chains of 450 polymer units and 4 polymer units were each applied to APDIPES surfaces in triplicate. The non-functionalized PEG_{450} resulted in an average EOF reduction of only 67% compared to the 97% reduction observed with NHS-PEG_{450}. The non-functionalized PEG_4 resulted in an average EOF reduction of only 15% compared to the 60% reduction observed with NHS-PEG_4. Additionally, the non-functionalized PEG surfaces were found to produce less efficient separations and less stable EOF than the NHS-PEG surfaces (data not shown). These effects have been observed previously with adsorbed PEG coatings.[13] These findings highlight the benefits of using the NHS-PEG reagents, which have specificity for primary amines and form covalent bonds.

3.3.3 CE-ESI-MS of enolase tryptic digest

A PEG_{24} coated CE-ESI device was used to analyze tryptic peptides of the enzyme enolase and operated using the voltage profiles found in Table 3.2. The digest sample is a mixture of peptides ranging in mass from below 300 Da to over 3 kDa. In Figure 3.3, representative base peak index electropherograms acquired on a PEGylated device (A, B) and an APDIPES coated device (C) are shown. The PEG_{24} surface coating reduced the EOF of the APDIPES surface from 1.06 $x10^{-3}$ $cm^2 V^{-1} s^{-1}$ to 4.7 $x10^{-4}$ $cm^2V^{-1}s^{-1}$ (44%). Figure 3.3A and C show separations on the PEG_{24} surface and the APDIPES surface respectively at the same field strength (375 V/cm). Note that the migration times in A are nearly 2x as long as B and C. The reduced EOF due to PEGylation of the separation channel resulted in improved peak capacity and resolution for the separation of enolase tryptic peptides. The separation using an unmodified APDIPES surface operated at 375 V/cm (Figure 3.3C) yielded a separation window of 25 s with

a median peak width at base (4σ) of 0.35 s, resulting in a peak capacity of 71. The PEG_{24} surface operated at 375 V/cm (Figure 3.3A) produced a 140 s separation window with a median peak width at base of 1.10 s, resulting in a peak capacity of 128. These results show that the PEG_{24} coating successfully reduced the EOF without significantly reducing the separation efficiency observed on the APDIPES coating.

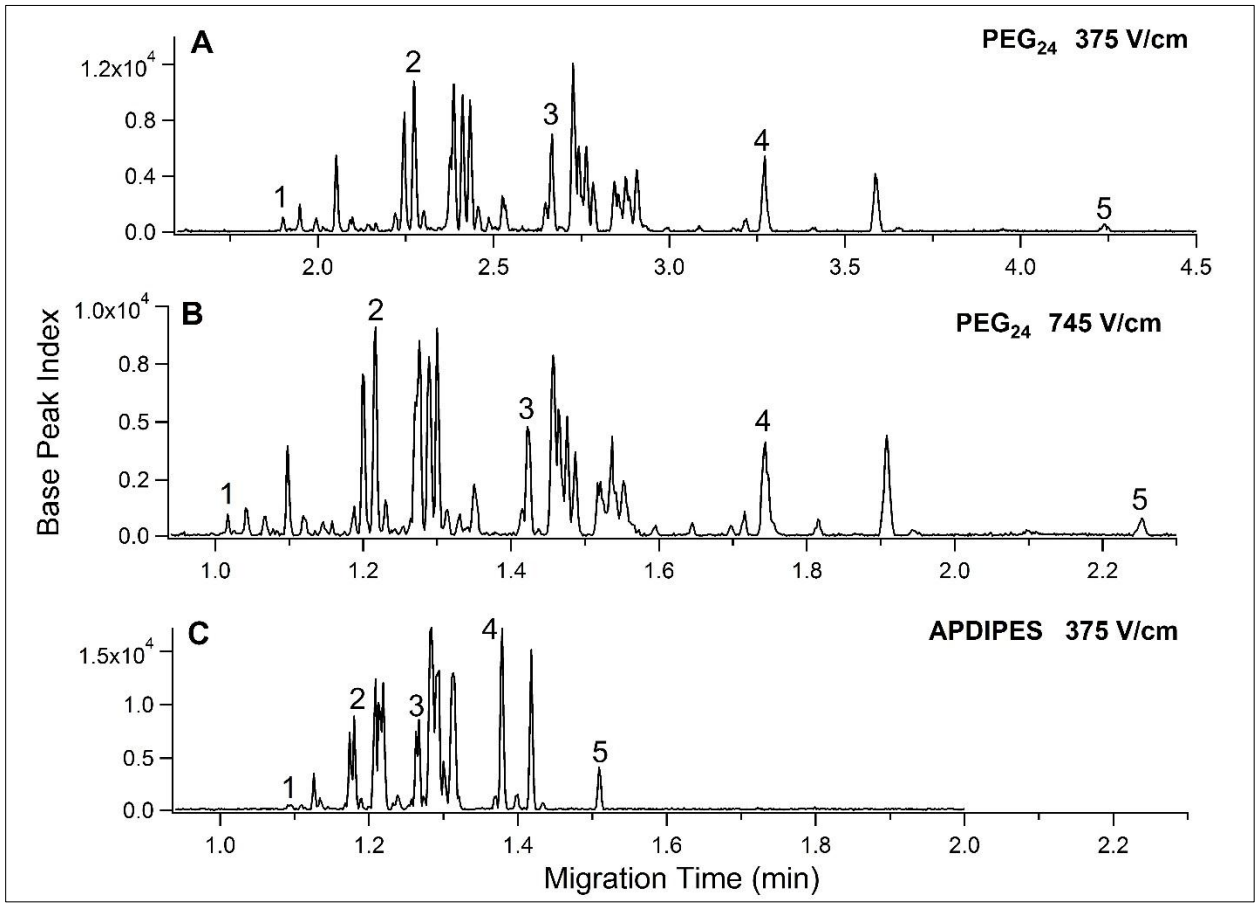

Figure 3.4 Comparison of 5 μM enolase tryptic digest separations performed on different surface coatings using 50% acetonitrile, 0.1% formic acid BGE. A) PEG_{24} coated device operated at 375 $V^{-1}cm^{-1}$. B) PEG_{24} coated device operated at 745 $V^{-1}cm^{-1}$. APDIPES coated device operated at 375 $V^{-1}cm^{-1}$. C) APDIPES coated device operated at 375 $V^{-1}cm^{-1}$. Peak numbers correspond to the same peptides in each electropherogram to facilitate comparisons.

To more directly compare the absolute efficiency of the APDIPES and PEG_{24} coatings, the metric Δ (ratio of the apparent diffusion coefficient to molecular diffusion coefficient) was

used. This metric has been used previously to assess the separation performance of APDIPES coatings by comparing the apparent broadening rate exhibited by peptide standards to the diffusion coefficients for these same molecules.[8] As defined, a Δ value of 1 indicates diffusion-limited CE performance. In our previous report on APDIPES coatings a Δ value of 1.6 was achieved[8] while the separation of peptide standards using the PEG_{24} coated devices resulted in an average Δ value of 1.8. These results show that the PEG_{24} coating maintains a similar amount of non-diffusional band broadening as the APDIPES coating. In addition to improving the peak capacity over an APDIPES surface coating, the PEG_{24} coating resulted in highly reproducible migration times without the need for reconditioning between runs. The calculated μ_{ep} reproducibility was 1.09% RSD for APDIPES and 1.8% RSD for PEG_{24} (n = 3).

The high speed, high efficiency separations performed using the APDIPES surface coating yield temporally narrow peaks which push the limits of the data acquisition rate of the mass spectrometer. Use of APDIPES coated devices at separation field strengths above 500 V/cm would therefore require a faster MS data acquisition rate to avoid severe undersampling. The decreased EOF associated with the PEG_{24} surface coating results in wider peaks enabling devices coated with PEG_{24} coatings to be operated at higher field strengths while maintaining adequate MS data sampling. Figure 3.3B shows the results from operating the PEG_{24} coated device at a higher field strength (745 V/cm). This separation resulted in a 74 s separation window and median peak width at base of 0.60 s resulting in 12 MS data points per peak at an acquisition rate of 20 Hz. This separation produced a peak capacity of 124, which is consistent with the peak capacity generated at 345 V/cm (n_c = 128). We found that increasing the electric field strength on the PEG_{24} surface resulted in a dead time comparable to that observed on the APDIPES coated device without sacrificing the elevated peak capacity. Increasing the field

strength to 745 V/cm resulted in an increase in the average Δ value for peptide standards from 1.8 at 375 V/cm to 3.1 at 745 V/cm, indicating that the high field strength separation resulted in increased non-diffusional band broadening. The higher voltage applied offset the increased non-diffusional band broadening such that the same absolute efficiency and peak capacity were obtained. Further optimization of the PEG coating method could potentially improve the efficiency of the high field strength separation by as much as 3x and the peak capacity by as much as 1.7x.

The effect of improved peak capacity observed with the PEG_{24} surface coating is evident when comparing peak 2 in Figures 3B and C. The resolution between peak 2 and its neighbor is 1.04 on the APDIPES surface but increases to 1.92 on the PEG_{24} surface, a 1.8x improvement. This improvement is in good agreement with the expected theoretical improvement in resolution based on $\bar{\mu}_{ep}$ (-2.5 x10^{-3} $cm^2V^{-1}s^{-1}$), μ_{eo} (4.7 x10^{-3} $cm^2V^{-1}s^{-1}$), and eq 3.1 (1.9x improvement). One potential drawback to the PEG_{24} surface coating is that it results in greater electrokinetic bias due to the gated injection scheme. By utilizing an alternative injection scheme, such as a pinched injection, it may be possible to eliminate or minimize the effect of electrokinetic bias on these results.[31, 33]

3.3.4 CE-ESI-MS of intact proteins

A mixture containing five intact proteins (carbonic anhydrase I, hemoglobin, human serum albumin, cytochrome c, lysozyme) was separated to compare the performance of coatings with high EOF and near-zero EOF. Our previous microchip CE-ESI devices all operated with a strong anodic EOF in the separation channel and either a reduced anodic or cathodic EOF in the electroosmotic pump channel (Figure 3.1A and C). PEG_{450} coated devices have a near-zero anodic EOF in the separation channel (3.2 (± 0.9) x10^{-5} $cm^2V^{-1}s^{-1}$) and a strong anodic EOF in

the electroosmotic pump channel (1.06 x10^{-3} $cm^2V^{-1}s^{-1}$, Figure 3.1B). PEG_{450} surface coatings necessitate a reversal of the voltage polarity so that mobile, cationic analytes migrate toward the ESI interface. The voltage profile listed in Table 3.1 was used for these experiments.

Representative electropherograms collected on microfluidic devices coated with APDIPES and PEG_{450} are shown in Figure 3.4A and B respectively.

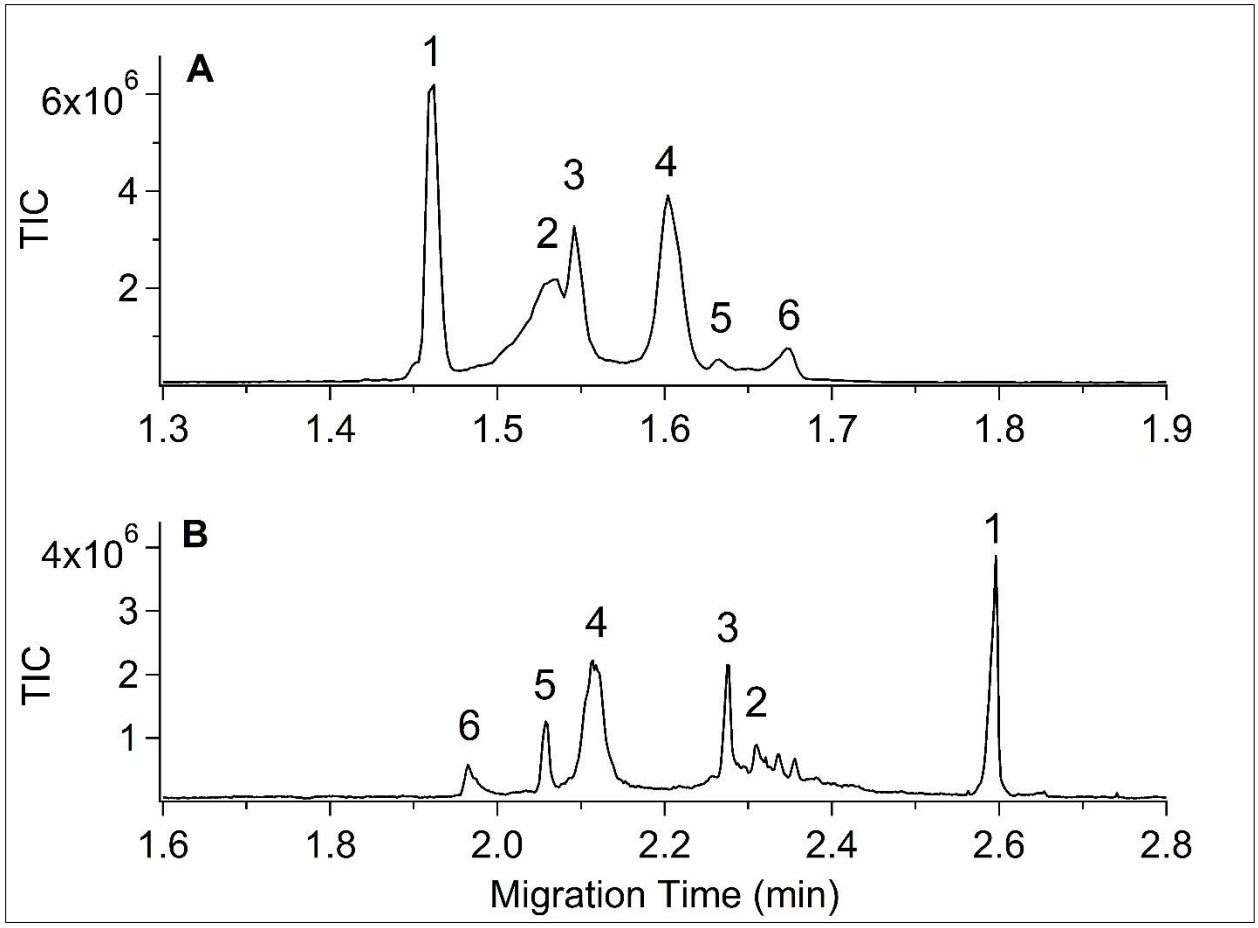

Figure 3.5 Total ion count electropherograms comparing separations of a 5 μM mixture of intact proteins on a CE-ESI microfluidic device coated with A) APDIPES, E = 375 $V^{-1}cm^{-1}$ and B) PEG_{450}, E = 500 $V^{-1}cm^{-1}$.

Two subunits of the protein hemoglobin were identifiable in each electropherogram and are labeled as peak 2 (β-hemoglobin, 15.9 kDa) and peak 3 (α-hemoglobin, 15.1 kDa). The median peak width at base (4σ) across all proteins in the mixture was comparable for both the

APDIPES device (1.09 s) and the PEG_{450} device (1.15 s). As expected, the low EOF of the PEGylated device enhanced the resolution of the separation by magnifying differences in apparent analyte mobility in accordance with eq 3.1. The electrophoretic mobilities for this intact protein mixture calculated from separations using APDIPES ranged from 2.53 $x10^{-4}$ $cm^2V^{-1}s^{-1}$ to 3.42 $x10^{-4}$ $cm^2V^{-1}s^{-1}$ with an average value of 3.02 $x10^{-4}$ $cm^2V^{-1}s^{-1}$. Based on eq 1, separations using the PEG_{450} surface (μ_{eo} = 3.2 $x10^{-5}$ $cm^2V^{-1}s^{-1}$) should result in nearly 2x greater resolution than with the APDIPES surface. From the data in Figure 3.4, we can quantify a significant improvement in resolution between the two neighboring peaks, cytochrome c (peak 5) and human serum albumin (peak 4). The device coated with PEG_{450} yielded a resolution of 2.89 versus 1.51 for the APDIPES coated device (1.9x improvement). The improvement in resolution is more clearly evident in the separation of the hemoglobin subunits (peaks 2 and 3). Figure 3.4B shows the resolution of the α and β subunits of hemoglobin, and partial separation of additional hemoglobin subunit variants. These peaks were not resolved using the APDIPES coated device.

Further comparison of the separation performance for the different surface coatings in terms of separation efficiency and peak capacity is non-trivial. Due to the intrinsic heterogeneity of intact proteins, it can be difficult to make reliable peak width measurements. Subspecies of protein variants and other differences across a class of protein molecules which make up the proteoform can convolute the electropherogram.[34] Due to this heterogeneity it is not clear whether protein peaks are broadened due to analyte band dispersion or whether the apparent peak width is a result of multiple, partially resolved protein species. It is more informative to compare the separative performance of the PEG_{450} surface coating to the APDIPES coating using peptides rather than intact proteins. The four peptide standard previously used to quantify separation performance was separated on the PEG_{450} surface coating. Separation performance of the PEG_{450}

surface coating resulted in an average Δ value of 2.3. This value is higher than the Δ values determined for the APDIPES (1.6) and PEG_{24} (1.8) surface coatings in this report but it is still a highly efficient separation. Further optimization of the PEG coating method could potentially yield even better separation performance.

The issue of potential protein adsorption to the surface coatings is important for CE and is not directly addressed by the peptide Δ values reported. To assess the potential adsorption of proteins, the electrophoretic mobilities of each protein using both APDIPES and PEG_{450} surface coatings were determined. In the absence of adsorption, the value of μ_{ep} for a given analyte should remain constant in a given BGE regardless of the surface chemistry. All protein μ_{ep} values measured (Table 3.3) on the two different surfaces agreed within 2%. Migration time reproducibility was also determined for all components in the intact protein mixture for both surface coatings. Migration times for the intact proteins were assessed over three replicate runs without surface reconditioning and were found to be stable for both the APDIPES (0.3% RSD) and PEG_{450} (0.3% RSD) coatings.

Table 3.3 Intact Protein Masses and μ_{ep} Values

Peak	[1]Mass (kDa)	APDIPES	PEG_{450}
-	-	[2]μ_{ep}	[2]μ_{ep}
1. carbonic anhydrase I	28.8	2.53	2.53
2. β-hemoglobin	15.9	2.86	2.89
3. α-hemoglobin	15.1	2.92	2.94
4. human serum albumin	66.6	3.16	3.20
5. cytochrome c	12.4	3.27	3.30
6. lysozyme	14.3	3.42	3.47

[1]Masses from MaxEnt 1 deconvolution
[2](x 10^{-4} cm^2 V^{-1} s^{-1})

The highly reproducible migration times along with the strong agreement between the observed μ_{ep} values indicate little to no difference in analyte-wall interactions between the proteins and

each of the surface coatings employed. The PEG_{450} surface coating improved the resolution of the intact protein mixture over the APDIPES coating while inhibiting surface adsorption leading to efficient separation in < 3 min.

3.4 Conclusions

A coating method for CE-ESI-MS of peptides and proteins that offers a range of EOF magnitudes based on the length of the PEG polymer chain was described. The CVD method creates a uniform layer of primary amines within microfluidic channels for subsequent covalent attachment of NHS-PEG reagents. The EOF of the resulting microfluidic channel was found to be reproducibly dependent on the polymer chain length of the NHS-PEG reagent used. The coatings improved resolution for CE-ESI-MS separations of complex biological mixtures by better optimizing the EOF in relation to the average electrophoretic mobility of the analytes. The magnitude of EOF reduction trended with the PEG chain length for five of the six reagents studied. From the observations of PEG chain length and EOF reported here it is suggested that for longer PEG chains the EOF reduction occurs primarily because of viscous drag in the electrical double layer. The shortest PEG chain is thought to exhibit enhanced EOF reduction (relative to its PEG chain length) due to reactions with a larger percentage of surface amines than the longer chain PEG reagents. All reagents reproducibly reduced the EOF of the APDIPES coated surface allowing selection of a desired EOF based on the resolution and analysis time requirements dictated by the sample.

A surface coating resulting in an intermediate EOF (PEG_{24}) was used to analyze a tryptic digest of the enzyme enolase. The 44% reduction in EOF as compared to the APDIPES surface resulted in a 75% increase in the peak capacity. In less than 2.5 min a peak capacity of 124 was generated. The PEG reagent with the longest polymer chain (PEG_{450}) resulted in a 97% reduction

in the EOF as compared to the APDIPES surface. The PEG_{450} coated devices resulted in fast, highly efficient separations of intact proteins with improved resolution as compared to APDIPES. Efforts to optimize the performance of all PEG coatings are ongoing. Future work will explore the effects of changes to the reaction conditions (temperature, pH, concentration, organic modifier) and the subsequent effect on EOF and separation performance.

3.5 References

1. Jorgenson, J. W., Lukacs, K. D., *Anal. Chem.* **1981**, *53*. 1298-1302.

2. Jorgenson, J. W., Lukacs, K. D., *Science* **1983**, *222*. 266-272.

3. Ban, E., Park, S. H., Kang, M.-J., Lee, H.-J., Song, E. J., Yoo, Y. S., *Electrophoresis* **2012**, *33*.

4. Ramautar, R., Heemskerk, A. A. M., Hensbergen, P. J., Deelder, A. M., Busnel, J.-M., Mayboroda, O. A., *J. Proteomics* **2012**, *75*.

5. Ramautar, R., Mayboroda, O. A., Derks, R. J. E., van Nieuwkoop, C., van Dissel, J. T., Sornsen, G. W., Deelder, A. M., de Jong, G. J., *Electrophoresis* **2008**, *29*. 2714-2722.

6. Haselberg, R., de Jong, G. J., Somsen, G. W., *Electrophoresis* **2013**, *34*. 99-112.

7. Haselberg, R., de Jong, G. J., Somsen, G. W., *Anal. Chem.* **2013**, *85*. 2289-2296.

8. Batz, N. G., Mellors, J. S., Alarie, J. P., Ramsey, J. M., *Anal. Chem.* **2014**, *86*. 3493-3500.

9. Huhn, C., Ramautar, R., Wuhrer, M., Somsen, G. W., *Anal. Bioanal. Chem.* **2010**, *396*. 297-314.

10. Kleparnik, K., *Electrophoresis* **2013**, *34*. 70-85.

11. Faserl, K., Sarg, B., Kremser, L., Lindner, H., *Anal. Chem.* **2011**, *83*. 7297-7305.

12. Ghosal, S., *Anal. Chem.* **2002**, *74*. 4198-4203.

13. Fermas, S., Daniel, R., Gonnet, F., *Anal. Biochem.* **2008**, *372*. 258-260.

14. Razunguzwa, T. T., Warrier, M., Timperman, A. T., *Anal. Chem.* **2006**, *78*. 4326-4333.

15. Schulze, M., Belder, D., *Electrophoresis* **2012**, *33*. 370-378.

16. Pattky, M., Huhn, C., *Anal. Bioanal. Chem.* **2013**, *405*. 225-237.

17. Sola, L., Chiari, M., *J. Chromatogr., A* **2012**, *1270*. 324-329.

18. Ullsten, S., Zuberovic, A., Wetterhall, M., Hardenborg, E., Markides, K. E., Bergquist, J., *Electrophoresis* **2004**, *25*. 2090-2099.

19. He, M., Zeng, Y., Jemere, A. B., Harrison, D. J., *J. Chromatogr., A* **2012**, *1241*. 112-116.

20. MacDonald, A. M., Bahnasy, M. F., Lucy, C. A., *J. Chromatogr., A* **2011**, *1218*. 178-184.

21. Haselberg, R., de Jong, G. J., Somsen, G. W., *Electrophoresis* **2011**, *32*. 66-82.

22. Feldmann, A., Claussnitzer, U., Otto, M., *J. Chromatogr., B* **2004**, *803*. 149-157.

23. Sharma, S., Johnson, R. W., Desai, T. A., *Biosens. Bioelectron.* **2004**, *20*. 227-239.

24. Anderson, A. S., Dattelbaum, A. M., Montano, G. A., Price, D. N., Schmidt, J. G., Martinez, J. S., Grace, W. K., Grace, K. M., Swanson, B. I., *Langmuir* **2008**, *24*. 2240-2247.

25. Wang, A. J., Feng, J. J., Fan, J., *J. Chromatogr., A* **2008**, *1192*. 173-179.

26. Sun, X. F., Li, D., Lee, M. L., *Anal. Chem.* **2009**, *81*. 6278-6284.

27. Huang, M. X., Vorkink, W. P., Lee, M. L., *J. of Microcol. Sep.* **1992**, *4*. 135-143.

28. Mellors, J. S., Gorbounov, V., Ramsey, R. S., Ramsey, J. M., *Anal. Chem.* **2008**, *80*. 6881-6887.

29. Jacobson, S. C., Hergenroder, R., Koutny, L. B., Ramsey, J. M., *Anal. Chem.* **1994**, *66*. 1114-1118.

30. Culbertson, C. T., Jacobson, S. C., Ramsey, J. M., *Anal. Chem.* **1998**, *70*. 3781-3789.

31. Jacobson, S. C., Hergenroder, R., Koutny, L. B., Warmack, R. J., Ramsey, J. M., *Anal. Chem.* **1994**, *66*. 1107-1113.

32. Etienne, M., Walcarius, A., *Talanta* **2003**, *59*. 1173-1188.

33. Solignac, D., Gijs, M. A. M., *Anal. Chem.* **2003**, *75*. 1652-1657.

34. Smith, L. M., Kelleher, N. L., Consortium Top Down, P., *Nature Methods* **2013**, *10*. 186-187.

CHAPTER 4: HIGH SPEED MICROCHIP CAPILLARY ELECTORPHORESIS-ELECTROSPRAY IONIZATION-MASS SPECTROMETRY WITH FAST SCANNING MS DETECTION

4.1 Introduction

Microfluidic devices are especially well suited for maximizing the separative performance of capillary electrophoresis (CE).[1-6] Microchips can be used to reproducibly manipulate nanoliter to picoliter fluid volumes by integrating multiple functions into one device promoting high separation speed and efficiency.[7-8] Capillary electrophoresis with analysis times of less than 1 s has been demonstrated using microchips coupled with laser induced fluorescence detection.[7] If the potential of high speed CE (HSCE) is to be realized for biological analytes, devices must be coupled to mass spectrometry (MS). Coupling highly efficient CE with ESI-MS is a powerful technique due to the separative power of CE and the informative power of MS.[9-11] Microfluidic devices with integrated electrospray ionization emitters (ESI) have been used to generate highly efficient separations coupled with MS detection.[3-4] Microchip CE-ESI-MS separations have been achieved with analysis times of 0.5 – 2 min.[3-4, 12-13] Separations on this time scale are considered high speed for CE-ESI performed in conventional capillaries whereas this performance is routine for microchip CE-ESI. CE-ESI microchips have been operated on even faster time scales when coupled to liquid chromatography (LC) for two-dimensional (2D) analyses. Previous work has demonstrated microchip CE-ESI-MS with analysis times from 10 – 20 s.[13-14] The speed of microchip CE-ESI-MS has been limited not by separation performance but rather by the data acquisition rates of commercial mass spectrometers. Increasing the speed at which microchip CE-ESI can be performed would be beneficial to LC-CE-ESI-MS analyses

but requires increased MS data acquisition rates. Recent advances in commercially available MS instruments have increased acquisition rates to ≥ 100 Hz making HSCE coupled with MS detection feasible.[15] With increased MS acquisition rates the high speed, high efficiency performance of microfluidic devices can be applied to biological analytes and could be used to increase the separative performance of LC-CE-ESI-MS.

Maximizing the speed of microchip CE coupled to ESI-MS poses multiple practical challenges. To generate high separation speeds large voltages are commonly applied while using CE conditions that promote high EOF. Using low ionic strength background electrolytes (BGEs) maximizes the size of the electric double layer in CE leading to high EOF. For the separation of biological molecules such BGE conditions result in deleterious analyte-wall interactions. These interactions can be mitigated through the use of surface coatings however, a coating must be highly uniform to function well at high separation speeds. Pressure driven flow can arise from micro-heterogeneities in surface charge leading to increased non-diffusional band broadening through Taylor dispersion. This effect is exacerbated when the voltage applied is increased leading to worse separative performance.[16-17] Any other effects that give rise to pressure driven flow in the CE system, such as those arising from the ESI interface, will result in non-diffusional band broadening that is also made worse at high voltage. These considerations highlight the practical difficulties associated with achieving separations at high speed that are also highly efficient.

In this work the capabilities of HSCE-ESI microchips with integrated nanoelectrospray emitters were demonstrated for biological analytes. Glass microfluidic devices coated with (3-aminopropyl)di-isopropylethoxysilane (APDIPES) via chemical vapor deposition (CVD) were used for the separation of peptide and intact protein mixtures. This coating method produces

static, covalent coatings which are well suited for HSCE-ESI-MS due to their high EOF and excellent migration time reproducibility (< 1% RSD). APDIPES coatings have been used previously to generate highly efficient CE-ESI-MS separations of peptides and intact proteins in < 2 min with average peak widths of < 0.4 s.[4] To adequately sample the temporally narrow peaks generated by HSCE-ESI devices coated with APDIPES a Synapt G2 mass spectrometer was operated with new firmware to enable increased data acquisition rates. Data acquisition rates up to 222 Hz were demonstrated. A microfluidic device with a 3 cm separation channel was used to separate simple mixtures of peptides and intact proteins in ≤ 10 s. A tryptic digest was analyzed via HSCE-ESI-MS/MS with CE separation times of 10 s. Finally, a device with a 1 cm separation channel was used to demonstrate a separation of peptides in < 1 s.

4.2 Experimental

4.2.1 Reagents and materials

MS-grade acetonitrile and 2-propanol, formic acid (99.9%), lysozyme (egg white), and potassium hydroxide were obtained from Fisher Chemical (Fairlawn, NJ). Water was purified with a Nanopure Diamond water purifier (Barnstead International, Dubuque, IA). Intact β-lactoglobulin was obtained from Sigma-Aldrich (St. Louis, MO). (3-aminopropyl)di-isopropylethoxysilane (APDIPES) was obtained from Gelest (Morrisville, PA). Peptide analytes bradykinin, methionine-enkephalin, thymopentin and angiotensin II were obtained from American Peptide Company (Sunnyvale, CA). MassPrep™ bovine serum albumin (BSA) tryptic digest was provided by Waters Corporation (Milford, MA). Methyl-terminated polyethylene glycol *n*-hydroxy succinimide ester (NHS-PEG) with 450 polymer units was obtained from JenKem Technology (Beijing, China). Coated substrates made from 0.5 mm thick B270 glass were purchased from Caliper, A Perkin Elmer Company (Hopkinton, MA).

4.2.2 Fabrication of microfluidic devices

Microfluidic chips for high speed CE-ESI were fabricated in house using previously described photolithography and wet chemical etching techniques with the mask designs in Figure 4.1. The ESI emitters of each device were polished to remove dicing imperfections using a lapping wheel with 3 μm lapping paper from Ultra Tec (Santa Ana, CA). Glass cylinders, 8 mm in diameter, were attached to all devices for use as solvent reservoirs with chemically resistant epoxy (Loctite E-120HP, Henkel Corporation, Germany). The HSCE-ESI designs include four functional elements: an injection cross, a separation channel (3 cm and 1 cm in length), an electroosmotic pump, and an ESI orifice. The reservoir labels indicate sample (S), background electrolyte (BGE), sample waste (SW), and electroosmotic pump (EO) reservoir locations.

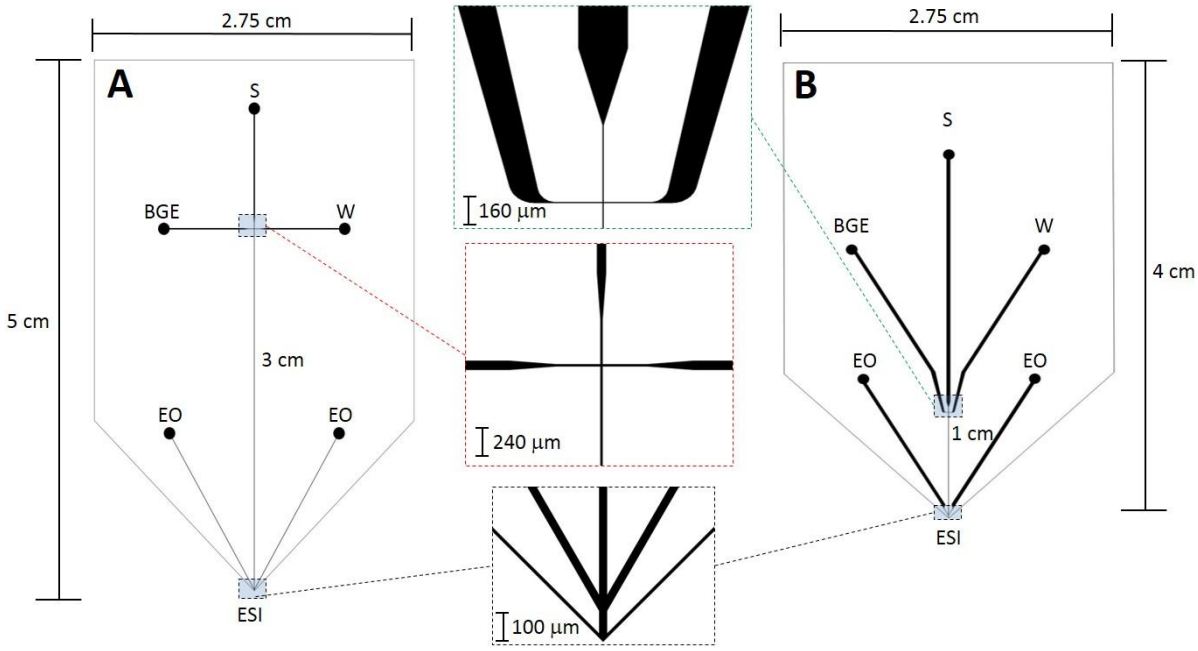

Figure 4.1 Microfluidic chip designs used for HSCE-ESI. Both designs consist of three elements; a separation channel, an injection cross with tapered channels, and electroosmotic (EO) pump channels for integrated ESI. All channels were etched to 10 μm deep. A 1-cm long

separation channel is incorporated in design A, design B has a 3-cm long separation channel; separation channels for each design were 30 μm wide after etching.

Microchannel dimensions were 10 μm deep and 30 μm wide for the separation channels in each design and the EO pump channels of the 3 cm design. The channels connected to the gate of the 3 cm device (A) were tapered from a width of 80 μm to 30 μm. The 1 cm device design (B) has tapered channels at the gate and at the EO pump channels. The channels taper from 300 μm to 30 μm.

4.2.3 Surface coating methods

Devices were coated with (3-aminopropyl)di-isopropylethoxysilane (APDIPES) in the gas phase at low pressure using a commercially available LabKote CVD system (Yield Engineering Systems, Livermore, CA) as described in Chapter 2.[4] This coating method results in a layer of covalently attached amines within the microchannels resulting in a high, anodic EOF. The microchips used in this work rely on differential EOF between the separation channel and the EO pump channel to facilitate electrospray. This is achieved by suppressing the anodic EOF of the APDIPES coated EO pump channels by reacting them with n-hydroxy succinimide polyethylene glycol ester (NHS-PEG) containing a polymer chain of 450 units as described in Chapter 3. Briefly, a 10 mg/mL solution of NHS-PEG reagent in pH 7.5 phosphate buffer (100 mM) was flushed through the EO pump channels for a period of 1 h followed by rinsing with water for 15 min. The separation channel was filled with 50% acetonitrile, 0.1% formic acid solution during PEGylation.

4.2.4 Operation of microfluidic devices

All microfluidic devices used in this work were operated by application of voltages to the solvent reservoirs. Polyethylene caps (Grace Davison Discovery Sciences, Bannockburn, IL) were placed on each reservoir to minimize solvent evaporation. Platinum wire electrodes (Alpha

Aesar, Ward Hill, MA) were inserted through small holes in the reservoir caps into each reservoir. The electrodes were powered by a custom-built Bertan Model 2866, fast-switching, 6-channel power supply capable of supplying 0 to +10 kV to each reservoir independently. The power supplies were controlled via a SCB-68 breakout box connected to a PC via a PCI 6713 DAQ card. A LabVIEW (National Instruments, Austin, TX) program was used to control voltage outputs. Devices were operated according to the voltage profiles in Table 4.1.

Table 4.1. Voltage Profiles for HSCE Analyses

		Injection Voltages (kV)				Separation Voltages (kV)			
Length	**[a]Field Strength**	**BGE**	**S**	**W**	**EO**	**BGE**	**S**	**W**	**EO**
3 cm	1,500	+0.5	0	+0.5	+5.5	0	0	+1.0	+5.5
3 cm	500	+2.25	+2.0	+2.25	+4.0	+2.0	+2.0	+2.5	+4.0
1 cm	2,400	+0.5	0	+0.5	+3.5	0	0	+1.0	+3.5

[a]Volts per cm

4.2.5 High speed mass spectrometry data collection

For this work a Synapt G2 mass spectrometer (Waters Corporation, Milford, MA) was used for analysis. The instrument is an ion mobility spectroscopy-quadrupole-time of flight-(IMS-qTOF)-MS. For this work the high speed data acquisition capabilities of the MS normally used to collect IMS data were used in combination with new firmware settings to acquire HSCE-ESI-MS data with increased MS data acquisition rates. When operating the instrument in this high speed acquisition mode the instrument control voltages which dictate the release of ion packets into both the TOF analyzer as well as the IMS drift cell were synchronized. This synchronization, in addition to the new firmware, allows the user to collect data in the IMS drift cell data bins for longer periods of time such that HSCE separations, which occur on the seconds time scale, can be collected. The data acquisition rate is ultimately determined by the MS scan time that is programmed into the firmware by the user. The MS scan time can be programmed to

collect HSCE-ESI-MS data across only the CE separation window, excluding the CE dead-time. This “dead time exclusion” method was used to achieve the minimum MS scan time and the maximum MS data acquisition rate possible without the loss of CE peaks

4.2.6 Data analysis for high speed MS and MS/MS

Data analysis for an intact protein mixture separated using a HSCE-ESI microchip was performed using the software package MaxEnt 1 (Water Corporation). MS data were summed under the full width of each protein peak to generate a total ion count summed mass spectrum using MassLynx (Waters Corporation). MaxEnt 1 was programmed to deconvolute each summed spectrum with a maximum of 15 iterations. A mass range of 5 kDa to 100 kDa was used with a programmed width at half-height of 0.8 Da. The output resolution was set to 1.0 Da/channel.

For data independent MS/MS, data were analyzed using Protein Lynx Global Server (Waters Corporation). The workflow parameters were set to search against the SwissProt 1.0 database and the maximum protein mass for the search was 250 kDa. The software was set to look for tryptic peptides with the possibility of one missed cleavage. Cysteine carbamidomethylation and methionine oxidation were the only structure modifications accepted. The software thresholds accepted a minimum of 3 fragments per peptide and 7 fragments per protein. The same workflow parameters were used for single scan as well as averaged MS/MS data.

With the MS instrument operating in normal data acquisition mode data independent tandem MS is performed using MS^e. To perform data independent MS/MS experiments using the new high speed MS data acquisition method the standard MS^e protocol was altered. Tandem MS was performed using two HSCE-ESI injections performed sequentially: one injection was used for analysis at low collision energy and one was used for analysis at high collision energy. The

data from each analysis was automatically summed into a single data file such that the data analysis software (PLGS) could use the same MS^e analysis algorithms, already in place, to analyze the data. This approach allows for the HSCE-ESI-MS/MS data to be collected with high MS data acquisition rates. The total analysis time for a HSCE-ESI-MS/MS experiment was the sum of two HSCE separation times because two CE injections were required for a single MS/MS experiment.

4.3 Results and discussion

4.3.1 Data acquisition for HSCE-ESI-MS

HSCE-ESI-MS was performed using microfluidic devices with integrated ESI emitters. To properly sample the temporally narrow peaks generated by these devices a new high speed acquisition mode for the MS was used. The instrument utilizes a time-of-flight (TOF) mass analyzer which is capable of acquiring data at spectral rates up to 2000 Hz according to instrument specifications. In practice, an interscan delay (ISD) associated with writing stored data to memory limits the instrument to a maximum data acquisition rate of 20 Hz. In addition to the TOF analyzer the instrument is equipped to perform ion mobility spectroscopy (IMS). IMS separations occur on the millisecond time scale which is too fast for data collection at 20 Hz. To account for this, the IMS uses on board memory which allows for the collection of IMS data into 200 “bins”. Each bin collects data sequentially until all 200 bins are filled. In this way all of the data associated with a separation can be collected prior to the ISD resulting in acquisition rates of > 20 Hz. For this work the IMS data acquisition architectures along with new firmware were used to collect HSCE-ESI-MS data as opposed to IMS data. Collecting MS data in this way did not limit the mass range over which MS data were acquired nor decrease the spectral resolution of the instrument.

For high speed detection the LabVIEW program used to control the voltages applied to the microchip was synchronized with the control voltages of the mass spectrometer known as the scan in progress (SIP) signal. When the instrument is in high speed detection mode the SIP determines when data is collected by the on board memory bins, when the 200 bins are written to memory, and is also synchronized with the TOF. Additionally the SIP signal initiates CE injections and determine the temporal length of the injection. A schematic of the effect that this synchronized voltage system has on the microchip as well as high speed MS data collection using the IMS memory is shown in Figure 4.2

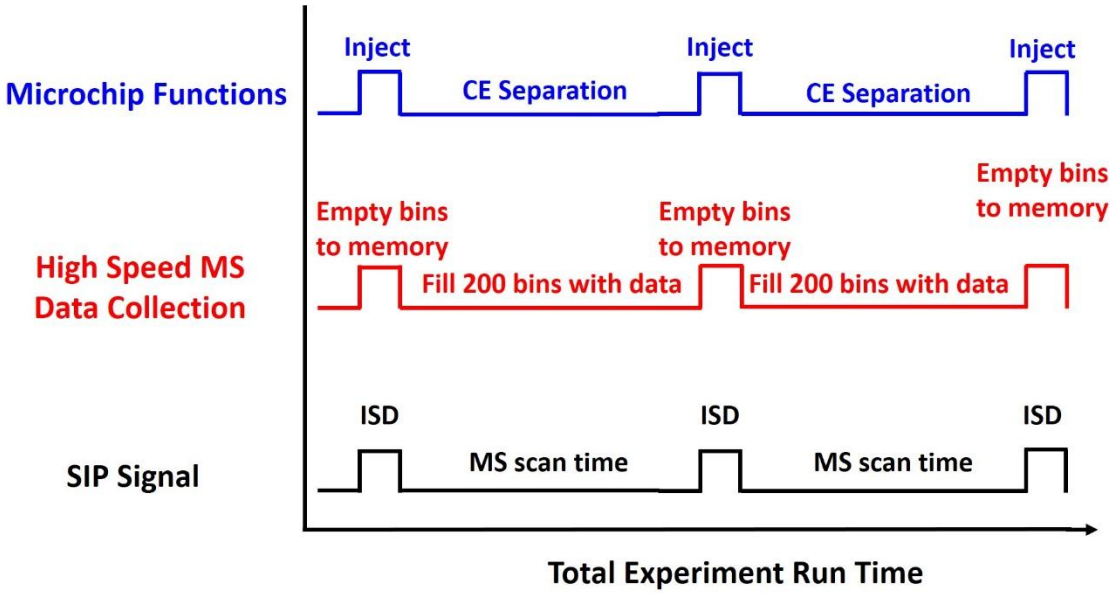

Figure 4.2 Schematic of the MS instrument SIP signal voltage pattern, the timing of high speed MS detection, and synchronized functions of the microchip. The user programs the instrument with an MS scan time to match the CE separation window. The ISD determines the total CE injection time and is also user controlled. The user also programs the total experiment run time. By varying the run time the user can capture a single CE injection or multiple CE injections that are summed into a single file at the end of the run time.

The SIP signal initiates data collection for a duration called the MS scan time which is programmed by the user. Once the MS scan time has completed, the data is written to memory during the ISD. The duration of the ISD is also programmed by the user but can be no shorter than 24 ms, the minimum time required to write 200 bins of data to memory. The MS, operating

in high speed detection mode, performs analysis for the duration of the MS scan time. Once the MS scan time is completed the SIP signal changes. This causes the microchip to perform another injection and for the data from the previous analysis to be written to memory. The total duration of the experiment was also programmed by the user such that one CE injection or multiple CE injections could be collected in rapid succession. When multiple HSCE-ESI-MS experiments are recorded, the data is summed into a single file. Each CE injection results in an electropherogram collected in 200 data bins which are combined to form an MS spectrum. When the experiment run time is longer than the duration for one injection the data is combined into one file in which all of the electropherograms and MS spectra are summed. The individual HSCE-ESI-MS experiments within this file, representing a single HSCE injection each, can be retrieved from the data file after the experiment run time has completed.

With this data acquisition scheme each data bin represents an MS spectrum summed from multiple TOF ion pushes and observed as a single data point in the electropherogram. If MS data were collected for 1 s then the data acquisition rate would be 200 Hz. If data were collected over a 5 s scan time then the data acquisition rate would be 40 Hz. To maximize the acquisition rate the instrument is configured to collect MS data during the separation window only, excluding the CE dead time from the MS scan time. In this way the 200 data bins are allocated across only the time in which CE peaks are present resulting in improved sampling rates. All of the data presented in this chapter were acquired using the high speed MS data acquisition mode with acquisition rates from 40 – 222 Hz. Where noted, the dead time exclusion method was used to achieve increased data acquisition rates to ensure > 5 MS data points per peak. When this dead time exclusion method is used the microchip is triggered to inject more frequently than the full

CE separation time such that more than one injection of analyte is present in the separation channel at one time (overlapping CE injections).

A HSCE-ESI microfluidic device with a 3 cm separation channel was used for the analysis of an intact protein mixture. A schematic of this device is shown in Figure 4.1A. Note that the HSCE-ESI device designs use two EO channels whereas previous iterations of CE devices with integrated ESI emitters used only one EO channel. The dual EO channels were used to improve the symmetry of the electric field in the EO pump region of the device in an effort to minimize band broadening. The 3 cm device was operated at an electric field strength of 1,500 V/cm according to the voltage profile listed in Table 4.1. Data for this separation were collected with the high speed MS data acquisition scheme both with and without using dead time exclusion.

A mixture of intact proteins including β-lactoglobulin and lysozyme in pH 2.8 BGE (50% acetonitrile, 0.1% formic acid) was analyzed. The results of these analyses are shown in Figure 4.3. In Figure 4.3A total ion count electropherograms acquired at different data acquisition rates are stacked for comparison. These data were collected across the range of 50-2000 m/z. Note that the same device was used with the same applied field strength (1,500 V/cm) for each trace in Figure 4.3. The total CE separation time (3.8 s) was also the same for each trace however the MS scan times were different. The bottom trace in black is the result of collecting MS data for the full 3.8 s CE separation time yielding an acquisition rate of 53 Hz. The red trace (top) is the result of excluding the dead-time from the MS scan time: MS data were acquired for only 0.9 s resulting in MS data acquisition at 222 Hz. The MS scan time could not be minimized further without excluding peaks from the electropherogram. The inset in Figure 4.3A shows a close-up image of the β-lactoglobulin peak for each trace with the MS data points across each peak noted.

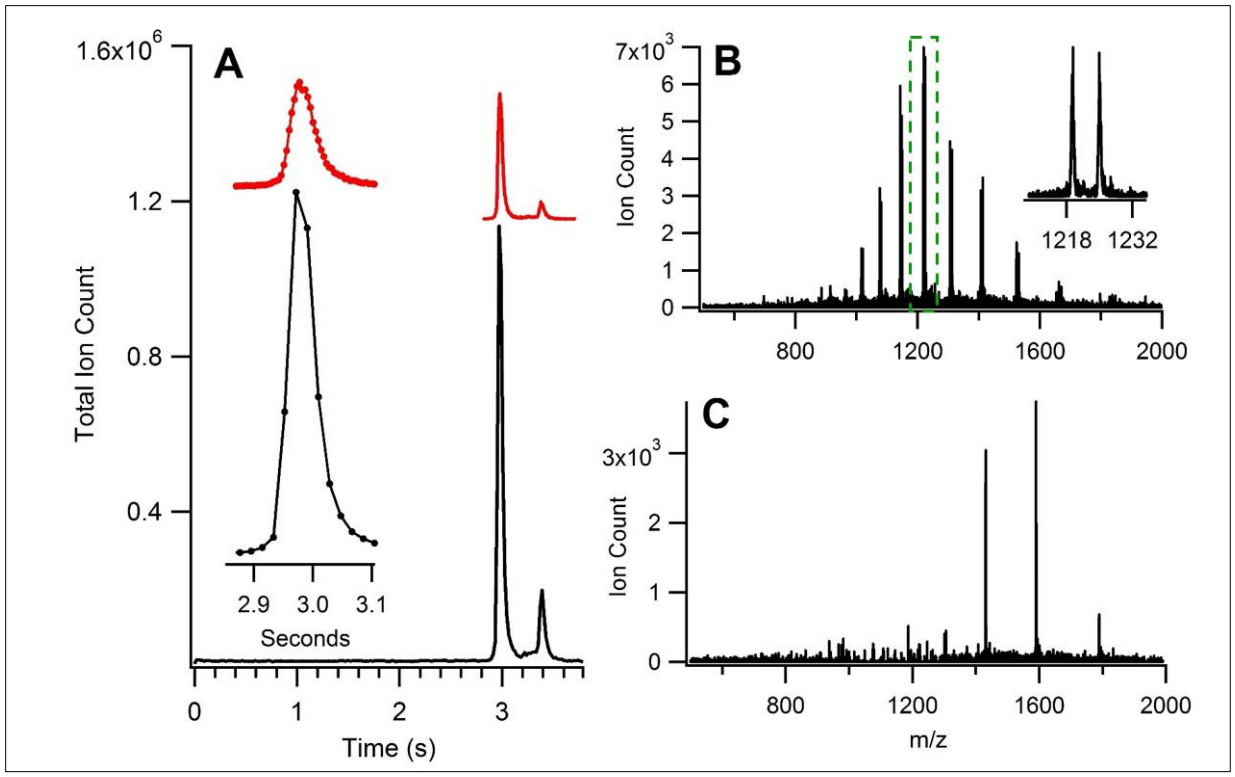

Figure 4.3 HSCE-ESI-MS separation of two intact proteins, β-lactoglobulin and lysozyme. Separations were performed on a HSCE device with a 3 cm separation channel using 10 μM sample in 50% acetonitrile, 0.1% formic acid. Approximately 2 femtomoles of each protein were injected. A) Total ion count electropherograms with varying data acquisition rates; 222 Hz (red, top) and 53 Hz (black, bottom). The inset highlights the sampling across the β-lactoglobulin peak. B) Mass spectrum acquired by summing data across the β-lactoglobulin peak. The inset in panel B is zoomed in on the most intense β-lactoglobulin charge state, highlighted with a green dashed box, showing the presence of two variants of the protein. C) Mass spectrum acquired by summing data across the lysozyme peak.

Scan time, acquisition rate, peak width at base (W_b), MS data points per peak, and number of theoretical plates (N) for both β-lactoglobulin and lysozyme are listed in Table 4.2. MS data acquisition at 222 Hz produced narrower peak widths for each protein than acquisition at 53 Hz as seen in Table 4.2, due to the increased sampling rate afforded by dead time exclusion. These differences in calculated peak widths are also apparent when considering the theoretical plate counts (N) for each protein under the different acquisition conditions. Despite the CE conditions

being exactly the same for each electropherogram, protein peaks collected with 222 Hz MS acquisition resulted in higher plate counts than those collected at 53 Hz.

Table 4.2 Data Acquisition Parameters and Sampling

		β-lactoglobulin			lysozyme		
Scan Time (s)	**Rate (Hz)**	**[a]W_b (ms)**	**[b]Points per Peak**	**[c]Plates (N)**	**[a]W_b (ms)**	**[b]Points per Peak**	**[c]Plates (N)**
0.9	222	92.2	20.5	16,673	102.1	22.7	17,544
3.8	53	92.4	4.9	16,601	116.5	6.2	13,486

[a]Average W_b (n = 3)
[b]Computed from W_b and rate
[c]Average N (n = 3)

For both the data acquired at 53 Hz and 222 Hz the same amount of each protein was injected (~2 femtomoles) but the signal intensity as seen in Figure 4.3A, is lower for the data collected at 222 Hz. This is a result of the ion signal being distributed across more data points for the data acquired at 222 Hz than for the data acquired at 53 Hz. The β-lactoglobulin peak intensity is 4.2x greater when acquired at 53 Hz than at 222 Hz because the signal is distributed across 4.2x less data points. Both sets of data result in the same total ion count when the signal is summed across each peak. The total ion count across the β-lactoglobulin and lysozyme peaks are shown in Figure 4.3B and C respectively. From these mass spectra the accurate mass of each protein was determined using deconvolution software. The inset in Figure 4.3B shows a zoomed in view of the most intense β-lactoglobulin charge state indicated by the green dashed box and clearly shows two variant peaks. The deconvoluted masses (18,277 Da and 18,362 Da) correspond to the A and B variants of the protein, which have been observed previously.[18] The mass spectrum in Figure 4.3C deconvolutes to a single mass of 14,303 Da. All masses are in good agreement with the known masses of each protein[19] indicating that the HSCE-ESI microchips can be used for the rapid analysis of simple protein mixtures. For all runs the migration times for each protein were highly reproducible (≤ 0.06% RSD, n = 3). The high

speed data acquisition firmware provides adequate sampling of temporally narrow protein peaks such that the high speed capabilities of microchip CE can be realized in conjunction with MS.

4.3.2 HSCE-ESI-MS of peptide standards with high speed and efficiency

HSCE-ESI-MS microchips were used to separate a mixture containing four peptide standards as well as the neutral dead-time marker fluorescein. These separations were performed on a device with a 3 cm separation channel. A schematic of the device is shown in Figure 4.1A. The HSCE-ESI device was operated at a field strength of 1,500 V/cm using the voltage profile shown in Table 4.1. Data were collected from 300-1600 m/z with the nominal MS resolution set at 20,000. The experimental MS resolution with high speed detection was comparable to that obtained when operating the MS under normal acquisition mode (> 17,000). Figure 4.4A shows a base peak index electropherogram from a single injection of the peptide mixture. The dead time exclusion method was used to increase the MS data sampling rate to adequately sample the temporally narrow peaks. The average peptide W_b for this separation was 55 ms. If MS data were collected across the entire CE run time the 200 data bins would be distributed across a 3.4 s MS scan time resulting in a data acquisition rate of 59 Hz. At 59 Hz an average of only 3.2 MS data points per peak would be collected. Using dead time exclusion the 200 bins were distributed over a 1.7 s MS scan time resulting in acquisition at 118 Hz. This approach improved the MS sampling and resulted in an average of 6.5 MS data points per peak.

The efficiency of separations performed on the 3 cm device, quantified using Δ values as well as the traditional efficiency metric of theoretical plates (N), can be found in Table 4.3. These data correspond to peptide peaks collected at 118 Hz. At 1,500 V/cm the 3 cm device generated an average efficiency of > 40,000 theoretical plates (N) and fully resolved all components of the peptide mixture in less than 4 s. These separative metrics indicate moderate

efficiency when compared to microchip CE-ESI-MS on the minutes time scale,[4] as shown in Chapter 2, but compares favorably to other high speed CE-ESI-MS reports.[15] The metric Δ, defined as the ratio of the apparent diffusion coefficient to the molecular diffusion coefficient, can be used to compare our work to the theoretically achievable separative performance.[4] As defined, a value of Δ = 1 represents the theoretical limit for separative performance in CE (i.e. diffusion-limited separation). The average Δ value for peptides on the 3 cm device operated at 1,500 V/cm is 12.6 indicating significant room for improvement and highlighting the practical challenges associated with maintaining high efficiency separations at high separation speeds.

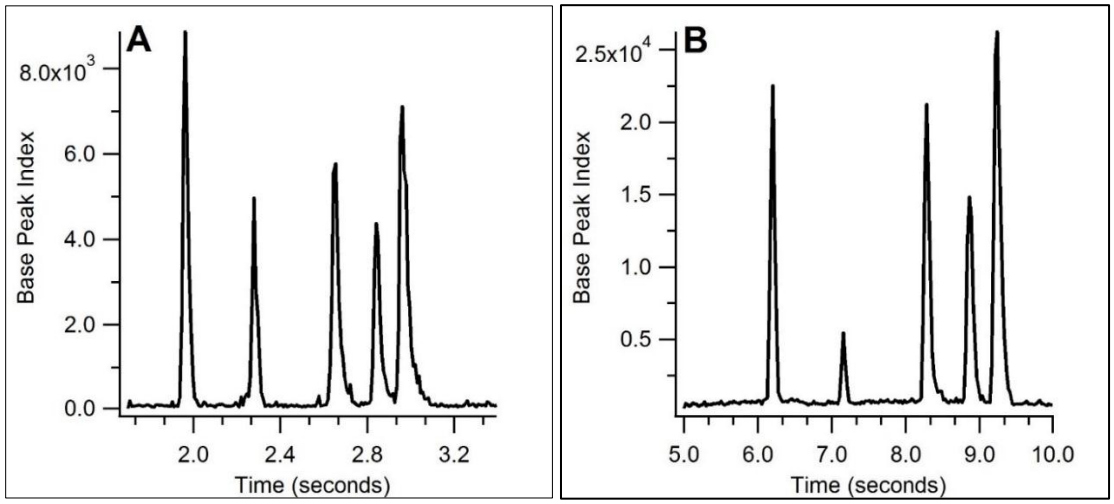

Figure 4.4 Base peak index electropherogram for the HSCE-ESI-MS separation of a mixture containing fluorescein, methionine enkephalin, angiotensin II, bradykinin and thymopentin (listed from shortest to longest migration time). Data were obtained using a 3 cm device at an electric field strength of A) 1,500 V/cm and B) 500 V/cm.

Table 4.3. HSCE-ESI-MS Performance for Peptide Mixture

	4 s Analysis			10 s Analysis		
Compound	**Δ**	**N**	**[a]W_b (ms)**	**Δ**	**N**	**[a]W_b (ms)**
fluorescein	14.5	29,240	48.6	2.9	46,267	115.3
methionine enkephalin	14.5	41,243	44.9	2.3	83,294	99.2
angiotensin II	14.7	37,125	60.2	3.0	57,606	138.1
bradykinin	9.3	51,684	59.5	2.7	56,694	149.0
thymopentin	12.0	31,576	77.9	2.5	49,364	166.3

[a]Average 4σ peak width at base (n = 3)

Reducing the analysis speed by decreasing the field-strength applied to the 3 cm device from 1,500 V/cm to 500 V/cm resulted in improvements in both efficiency and resolution for the five-component mixture. Figure 4.4B shows a base peak index electropherogram obtained on a 3 cm device operated at 500 V/cm. The dead time exclusion method was used which resulted in a data acquisition rate of 40 Hz and an average of 5.5 MS data points per peak. The analysis time increased from 3.4 s at 1,500 V/cm to 10 s at 500 V/cm. The average Δ value for peptide standards was improved from 12.6 at 1,500 V/cm to 2.6 at 500 V/cm denoting a significant improvement in separative performance as compared to the theoretical ideal. The average theoretical plate count also improved to > 61,000 as seen in Table 4.2. Comparing the results from different field strengths highlights the effect that high separation speed has on separative performance. For HSCE-ESI-MS applications in which minimum analysis time is paramount, separations can be performed in a few seconds or less using microchips. For applications requiring maximum separative performance with short analysis times, such as complex mixture analysis, it is advisable to reduce the speed of the analysis. Analysis times of 10 s are still achievable and non-diffusional band broadening is greatly reduced.

4.3.3 HSCE-ESI-MS/MS of BSA tryptic digest

Tryptic digest of the protein bovine serum albumin was analyzed to demonstrate the capabilities of HSCE-ESI microchips for the analysis of complex samples. In order to maximize CE separative performance a HSCE-ESI-MS microchip with a 3 cm separation channel was operated at 500 V/cm resulting in a CE separation time of 10 s. For the analysis of BSA tryptic digest, data independent tandem MS was used in which two CE injections were required for each MS/MS experiment. Because this approach requires two analyses to be performed the total HSCE-ESI-MS/MS analysis time was 20 s.

Data from the HSCE-ESI-MS/MS analysis of BSA tryptic digest is shown in Figure 4.5. The dead time exclusion method was used and data were collected at 40 Hz across the range of 50-3000 m/z. Multiple b-type and y-type ions were detected for each tryptic peptide of BSA. Figure 4.5A shows a base peak index electropherogram acquired using a low collision energy. Low-collision energy MS data were summed across the peak annotated with a green star.

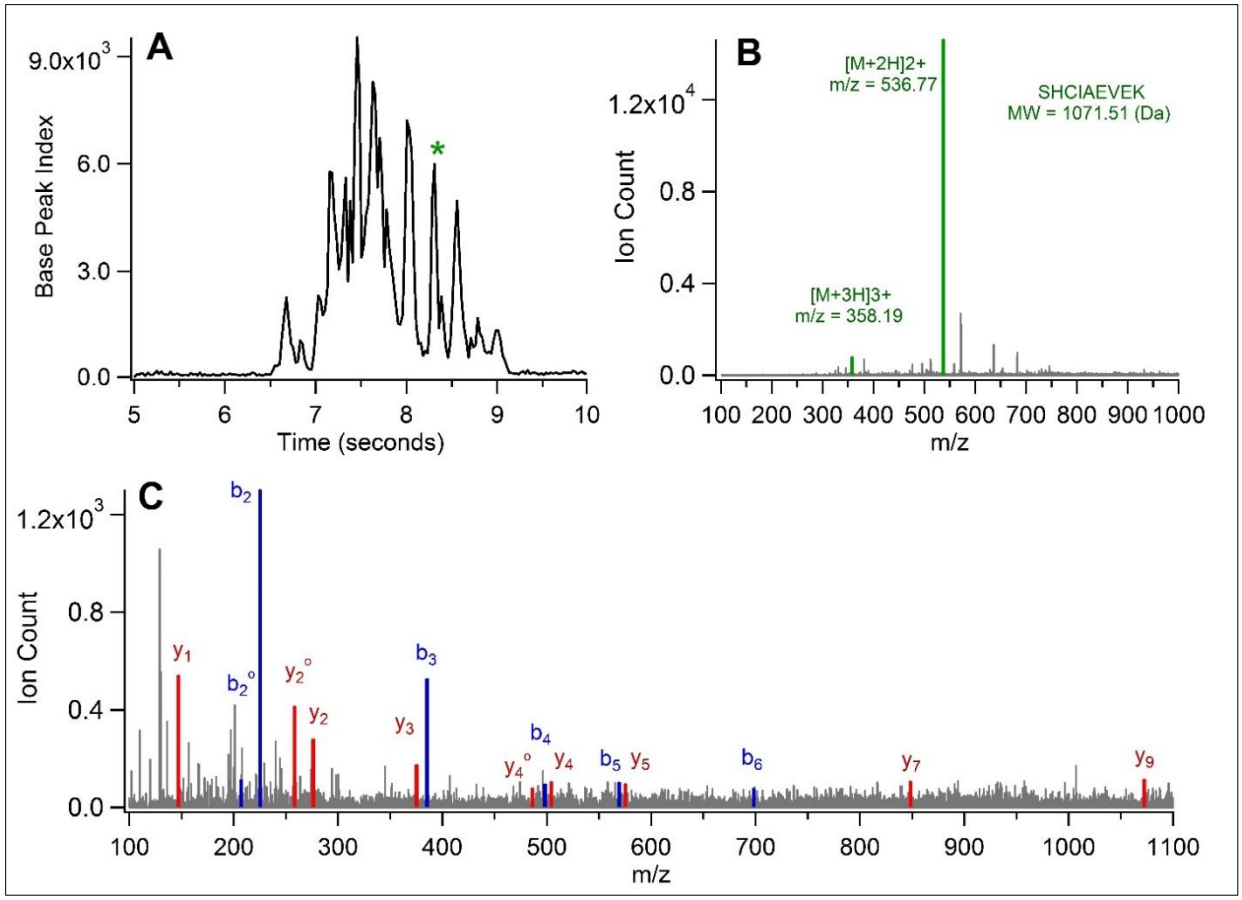

Figure 4.5 A) HSCE-ESI-MS/MS low energy, base peak index electropherogram of a 10 μM BSA tryptic digest in 50% acetonitrile, 0.1% formic acid acquired on a device featuring a 3 cm separation channel. The separation was performed at a field strength of 500 V/cm (< 1 femtomole injected) with an acquisition rate of 40 Hz using the dead time exclusion method. B) Low energy mass spectrum of peak highlighted in panel A; green peaks correspond to the +3 and +2 charge states of the selected BSA tryptic fragment. C) High energy mass spectrum of peak highlighted in panel A; b-type ions in blue, y-type ions in red. Fragments exhibiting a mass shift of -18 Da, corresponding to water loss, are noted with a superscript "o".

The low energy summed MS spectrum is displayed in Figure 4.5B in which the doubly and singly-protonated tryptic peptide signals are highlighted in green along with their m/z values. A single tryptic peptide dominates the low energy summed MS spectrum in Figure 4.5B. The nine residues associated with this peptide are annotated in green. The molecular weight assigned to this sequence by Protein Lynx Global Server (PLGS) is also listed. This value includes a single modification of the cysteine residue (C) resulting from the use of iodoacetimide during the trypsin digestion procedure (+57 Da carbamidomethylation). Figure 4.5C displays the summed mass spectrum associated with the high energy dissociation of the tryptic peptide highlighted in Figure 4.5B. The b-type and y-type ions identified by PLGS are shown in blue and red, respectively. Overall, the software identified 45 tryptic peptides of BSA resulting in 69% sequence coverage from a 20 s HSCE-ESI-MS/MS analysis with < 2 femtomoles of protein injected. This data was sufficient for PLGS to correctly identify the source protein as BSA when searching against the entire SwissProt database with no false positives.

4.3.4 Future directions

Increased MS data acquisition rates enabled the use of microchips to perform HSCE-ESI-MS analyses of biological analytes. Figure 4.6 displays HSCE-ESI-MS data acquired using a 1 cm device (design in Figure 4.1B) and represents the limits of our current surface coating, microchip, and MS data acquisition technologies. The device was operated at 2,400 V/cm according to the voltage profile in Table 4.1. MS data were acquired over a 1 s time period resulting in an MS acquisition rate of 200 Hz and an average of 13.2 MS data points per peak. These data were collected over the range of 300 – 1600 m/z. The average Δ value for the peptides over three injections was $\Delta = 239$ and the average theoretical plate count for peptides was N = 1,075. Given the sub-second separation time, the efficiency in terms of theoretical plates

is quite good especially when compared to previous HSCE-ESI work.[15] However the Δ value indicates excess non-diffusional band broadening and room for significant improvement.

Greater than baseline resolution between neutral fluorescein (red) and methionine enkephalin ($M+H^+$, green) ($R_s = 1.6$) as well as between methionine enkephalin and the remaining three peptides ($R_s \geq 2.6$) was achieved. The late migrating peptides, which exist in primarily the +2 charge state in solution, are less resolved. Angiotensin II (blue), bradykinin (magenta), and thymopentin (black) have electrophoretic mobility differences that are less than the other components of the mixture and are thus expected to be more difficult to resolve. In addition to mobility differences that are small it is evident from the extracted ion electropherogram in Figure 4.6 that these peaks are less efficient due to peak tailing, further reducing their resolution. Peak tailing that appears to affect the late migrating peptides more so than other components of the mixture was observed on the 3 cm device as well but appears to be exacerbated when performing a faster analysis using the 1 cm device. This is evident when considering that the average W_b ($n = 3$) on the 3 cm device (55 ms) was less than that observed on the 1 cm device (65 ms) despite the differences in analysis time. The band broadening observed is attributable to multiple sources including surface charge heterogeneities that are more deleterious to performance at high speeds as was seen with the HSCE-ESI device with a 3 cm separation channel previously. Also, because these data were acquired using a shorter, 1 cm separation channel the potential for band broadening effects associated with the ESI emitter must be considered.

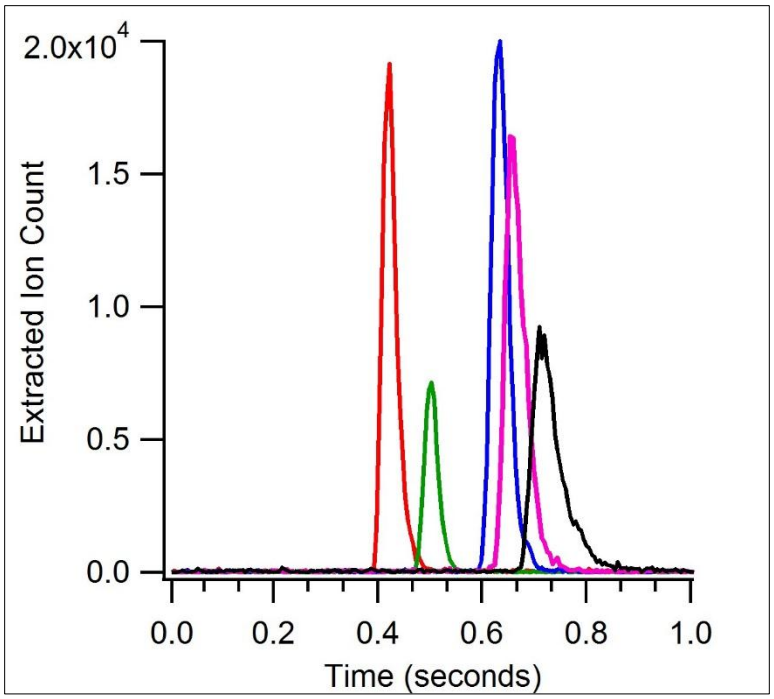

Figure 4.6 HSCE-ESI-MS of peptides in record speed. The extracted ion electropherogram was obtained using a 1 cm device operated at an electric field strength of 2,400 V/cm.

ESI requires that the fluid from the EOF pump region be exposed to the atmosphere which results in surface tension at the fluid-atmosphere interface. This interface is different than the interfaces found at all other orifices of the chip which terminate at reservoirs containing bulk solution. As such the ESI emitter gives rise to pressure effects in the separation channel. Given the reduced hydrodynamic resistance of the 1 cm separation channel relative to the longer 3 cm channel it is feasible that non-diffusional band broadening would occur to a greater extent in the shorter channel. Effects from the ESI emitter with respect to channel length warrant further study. CE-ESI-MS on the sub-second time scale sacrifices separation performance in order to maximize analysis speed. The observed Δ values indicate that far greater separative performance is theoretically possible. Work towards the development of improved, sub-second separations is ongoing.

4.4 Conclusions

The analysis of a protein digest via CE-ESI-MS using a traditional capillary in approximately 60 s has been reported as "ultrafast" CE in the literature.[20] The separations demonstrated in this report using HSCE-ESI microchips were performed with greater speed and efficiency. These separations highlight the benefits of using the integrated microchip platform to perform CE-ESI-MS as compared to traditional capillaries. To demonstrate the performance of HSCE-ESI microfluidic devices an alternative MS detection scheme was used to increase data acquisition rates and improve MS sampling. A five-component mixture of peptide standards and fluorescein was fully resolved in < 4 s with good efficiency and signal to noise (Δ = 12.6). Improved efficiency and resolution was observed when the analysis time was increased to 10 s (Δ = 2.6). A mixture of tryptic peptides from BSA was analyzed via HSCE-ESI-MS/MS. The entire analysis time was 20 s; two CE injections, with run times of 10 s each, were required to perform MS/MS. A single HSCE-ESI-MS/MS analysis resulted in the correct identification of BSA against the entire SwissProt database with no false positives highlighting the utility of the method. By performing the analysis in triplicate 73% sequence coverage was obtained with a total analysis time of 60 s. These results show the benefits of HSCE-ESI-MS for rapid screening in 20 s as well as the potential for more thorough analysis when needed, while maintaining analysis times on the order of 1 min.

To demonstrate the limits of our current microchip technologies a device with a 1 cm separation channel was operated at 2,400 V/cm to separate a five-component mixture. The separation time for this sample was < 1 s and represents the fastest liquid-phase separation coupled with MS detection ever reported.[15] This device produced higher separation efficiencies and shorter analysis times than previously reported HSCE-ESI microchips.[15] As indicated by Δ

values there is room for further improvement of the method. The integrated HSCE-ESI microchip is a powerful platform for the rapid analysis of biological analytes and could be useful for analyses in which speed is paramount. Such applications may include hydrogen/deuterium exchange experiments, in which fast analysis times are crucial for limiting back exchange, as well as 2D experiments. Previously our group has published CE-ESI microchips coupled to liquid chromatography (LC) for comprehensive separations of biological mixtures coupled with MS.[13] This work was MS limited and the CE separations were performed on the 20 s time scale. The high speed analyses shown here offer great promise for improvement of the LC-CE-ESI-MS method when coupled with fast MS data acquisition.

4.5 References

1. Culbertson, C. T., Jacobson, S. C., Ramsey, J. M., *Anal. Chem.* **1998**, *70*. 3781-3789.

2. Culbertson, C. T., Jacobson, S. C., Ramsey, J. M., *Anal. Chem.* **2000**, *72*. 5814-5819.

3. Mellors, J. S., Gorbounov, V., Ramsey, R. S., Ramsey, J. M., *Anal. Chem.* **2008**, *80*. 6881-6887.

4. Batz, N. G., Mellors, J. S., Alarie, J. P., Ramsey, J. M., *Anal. Chem.* **2014**, *86*. 3493-3500.

5. Culbertson, C. T., Jacobson, S. C., Ramsey, J. M., *Anal. Chem.* **2000**, *72*. 5814-5819.

6. Culbertson, C. T., Jacobson, S. C., Ramsey, J. M., *High efficiency separations on microchip devices*. 2000; p 221-224.

7. Jacobson, S. C., Hergenroder, R., Koutny, L. B., Ramsey, J. M., *Anal. Chem.* **1994**, *66*. 1114-1118.

8. Jacobson, S. C., Hergenroder, R., Koutny, L. B., Warmack, R. J., Ramsey, J. M., *Anal. Chem.* **1994**, *66*. 1107-1113.

9. Haselberg, R., de Jong, G. J., Somsen, G. W., *Electrophoresis* **2013**, *34*. 99-112.

10. Whitmore, C. D., Gennaro, L. A., *Electrophoresis* **2012**, *33*. 1550-1556.

11. Ramautar, R., Heemskerk, A. A. M., Hensbergen, P. J., Deelder, A. M., Busnel, J.-M., Mayboroda, O. A., *J. Proteomics* **2012**, *75*.

12. Mellors, J. S., Jorabchi, K., Smith, L. M., Ramsey, J. M., *Anal. Chem.* **2010**, *82*. 967-973.

13. Mellors, J. S., Black, W. A., Chambers, A. G., Starkey, J. A., Lacher, N. A., Ramsey, J. M., *Anal. Chem.* **2013**, *85*. 4100-4106.

14. Chambers, A. G., Mellors, J. S., Henley, W. H., Ramsey, J. M., *Anal. Chem.* **2011**, *83*. 842-849.

15. Fritzsche, S., Hoffmann, P., Belder, D., *Lab Chip* **2010**, *10*. 1227-1230.

16. Ghosal, S., *Electrophoresis* **2004**, *25*. 214-228.

17. Ghosal, S., *Anal. Chem.* **2002**, *74*. 4198-4203.

18. Vallejo-Cordoba, B., Gonzalez-Cordova, A. F., Olguin-Arredondo, H. A., *J. Cap. Electroph. Microchip Tech.* **2008**, *10*. 87-92.

19. Magrane, M., Consortium, U., *Database* **2011**, *2011*.

20. Moini, M., Martinez, B., *Rapid Comm. Mass Spectrom.* **2014**, *28*. 305-310.

CHAPTER 5: RESULTS SUMMARY, MOST RECENT WORK, AND FUTURE WORK

5.1 High efficiency CVD surface coatings

Much work has been done in the Ramsey group to develop highly efficient CE-ESI-MS using integrated microfluidic chip technology. Microchips have provided an excellent platform for high efficiency CE-ESI and have been applied to peptides, proteins, and other biological analytes. The successful implementation of microchip CE-ESI-MS relies on the use of surface coatings for inhibiting analyte-wall interactions while maintaining MS compatibility. Previously the polymeric surface coating PolyE-323 had been used with our microchip technology to produce highly efficient separations generating 1 million plates/m.[1] However, when compared to the theoretical performance expectations for CE using the metric Δ, the work using PolyE-323 was found to have significant room for improvement. In order to realize the full potential of CE new surface coating methods, beyond those previously published in the literature, were developed.

A Chemical Vapor Deposition (CVD) method based on previous work for the silanization of silica wafers was used to coat microfluidic devices for CE.[2-4] CVD coatings improved the separation performance of CE-ESI devices over previous work using PolyE-323 coatings. Prior separations achieved an average of 200,000 theoretical plates for a series of peptide standards using PolyE-323 whereas the CVD coated devices achieved an average of 680,000 theoretical plates. CE-ESI microchips with 23 cm separation channels coated via CVD were used to analyze tryptic digests of the protein enolase. These devices generated a sequence coverage of 85% and a peak capacity of 64 with an analysis time of only 90 s. More recent work has been done to

investigate the limits of the CVD method with regard to coating long microfluidic channels. A microfluidic device with a 1 m separation channel was coated via CVD and achieved a separation efficiency of > 1.4 million theoretical plates with a Δ value of 2.3. This data is shown in Figure 5.1.

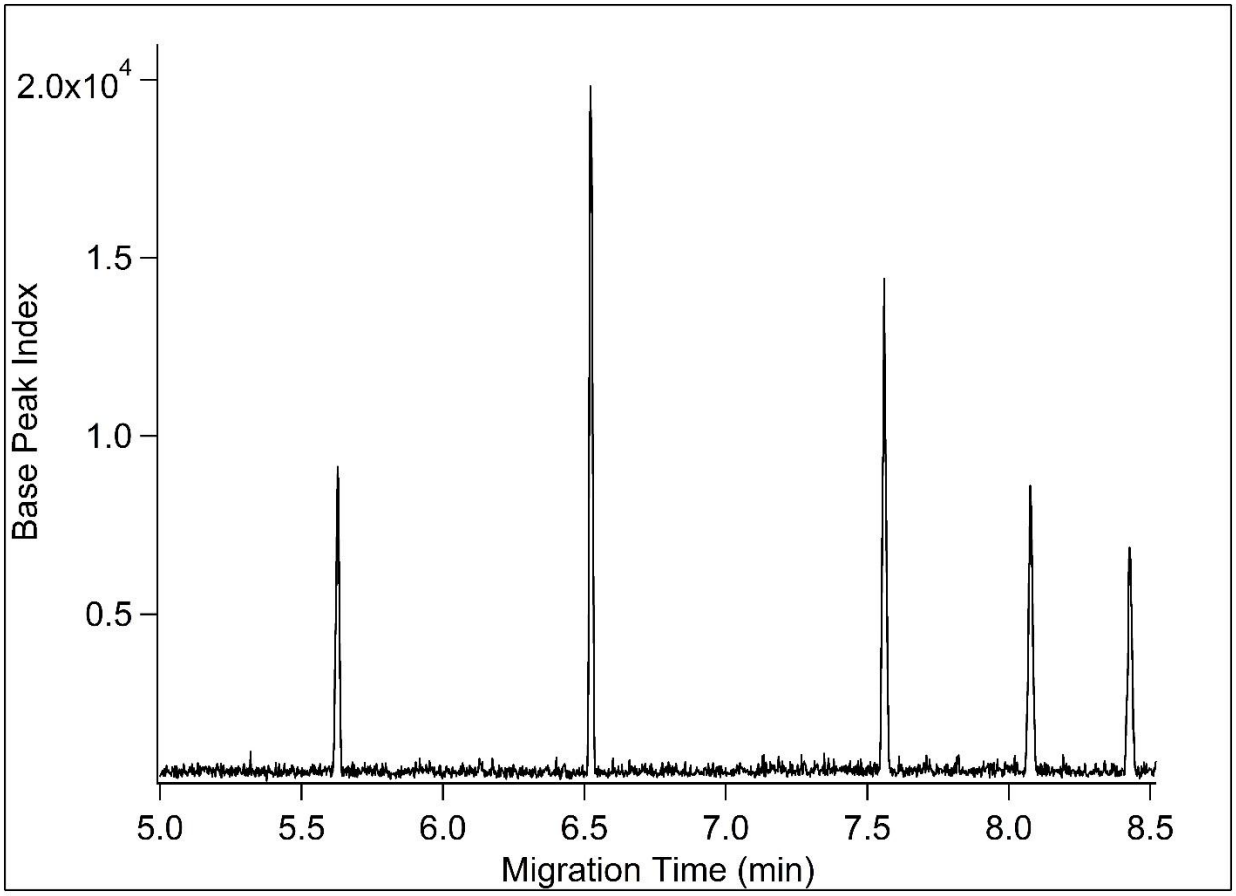

Figure 5.1 Peptide standards plus fluorescein separated on a CE-ESI microchip with a 1 m separation channel. The applied field strength was 300 V/cm with 50% acetonitrile, 0.1% formic acid BGE.

The EOF of the APDIPES coating is high such that even though the separation channel is 1 m long and the field strength (300 V/cm) was low relative to previous work, the entire analysis took less than 8.5 min. The field strength was limited by electrical arcing of the high voltage leads at the separation cross. With improved shielding greater applied voltages should be possible and 2 million theoretical plates could be achievable with this CVD coated CE-ESI device. The CVD

method enables long separation channels to be coated promoting high separative performance and offering great promise for application of microchip CE-ESI-MS to biological samples of greater complexity. Alternatively these coatings are well suited to serve as a base layer for subsequent modifications which can be used to improve separative performance with separation channels that are shorter than 1 m.

5.2 Tunable EOF surface coatings

The APDIPES CVD coatings described in Chapter 2 were modified with NHS-PEG reagents of varying PEG chain length to improve separative performance. These coatings produced efficient ESI-MS compatible separations with a range of EOF magnitudes. An NHS-PEG coating with medium length PEG was used to separate a tryptic digest of the protein enolase. This coating method nearly doubled the peak capacity over separations using only APDIPES (n_c = 128 versus 71) while maintaining near diffusion-limited performance (Δ = 1.8). An NHS-PEG reagent with the longest PEG chain (PEG_{450}) resulted in a near-zero EOF and was used to separate a mixture of intact proteins. This coating improved resolution of an intact protein mixture and resolved subunits of hemoglobin that were not resolved when using an APDIPES coating.

Improvements to the application of pressure during the PEGylation procedure have been made recently. This has led to improved separative performance of PEG_{450} for peptides than that reported in Chapter 3 (Δ = 1.6 versus 2.3). A PEG_{450} coating generated with the improved coating method was used to analyze tryptic digests of the protein enolase. Separations were performed on a CE-ESI device with a 23 cm separation channel using 50% acetonitrile, 0.1% formic acid BGE. Due to the near-zero EOF the PEG_{450} coating resulted in a separation window that was > 5 min wide for this sample. The increased separation window and high efficiency

resulted in a peak capacity of 182 with an analysis time of < 7.5 min. A representative electropherogram for the separation of 5 μM enolase tryptic digest using PEG_{450} can be seen in Figure 5.2.

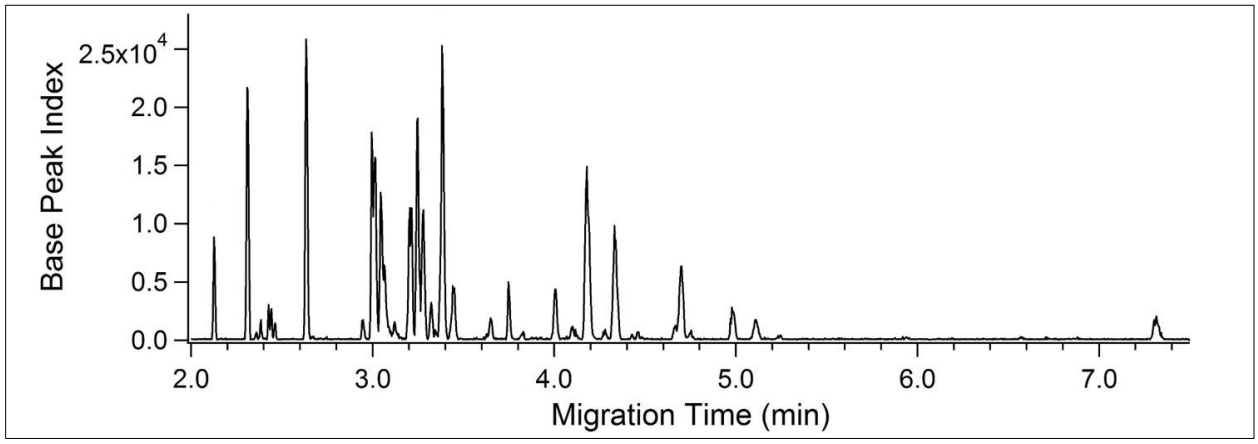

Figure 5.2 Enolase tryptic digest separated on a CE-ESI microchip with a 23 cm separation channel. The applied field strength was 600 V/cm with 50% acetonitrile, 0.1% formic acid BGE.

The work in Chapter 3 demonstrated the utility of CVD to form base layers for subsequent modification. NHS-PEGylation of APS was found to generate efficient separations with a range of EOF magnitudes. The increased peak capacity afforded by the PEG coatings, especially the PEG_{450} coating, improved the performance of CE-ESI microchips. Future work will explore the capabilities of PEG_{450} coated devices for the analysis of peptide samples of even greater complexity such as multiple protein digests. Additionally, complex proteins such as monoclonal antibodies will be analyzed as fully digested, partially digested, and intact protein samples.

5.3 PEG_{450} coatings for intact monoclonal antibody analysis

Monoclonal antibodies are large proteins which have steadily grown as analytes of interest due to their successful application as biotherapeutic agents.[5-6] Antibodies currently represent the fastest growing class of drugs and are considerably more complex than other biological analytes investigated via CE-ESI-MS previously.[7-9] Monoclonal antibodies or

immunoglobulins, are divided into subclasses of which the gamma subclass (IgGs) are most commonly used as biotherapeutics. IgGs are Y-shaped antibodies consisting of two nearly identical heavy chains of approximately 50 kDa each and two light chains of approximately 25 kDa. All four of these chains are connected by disulfide bonds to form the intact protein with an approximate mass of 150 kDa.[5, 9] A cartoon of a generic IgG-type antibody is shown in Figure 5.3.

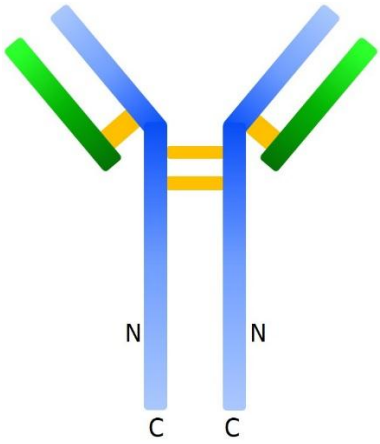

Figure 5.3 Cartoon of the typical IgG structure containing two light chains (green) and two heavy chains (blue) connected via disulfide bonds (yellow). A conserved site for glycosylation which occurs at an arginine residue common to most IgGs is annotated with the letter "N". The C-termini of each heavy chain, where the addition or subtraction of a lysine residue is common, are annotated with the letter "C".

The mass can vary across different IgGs as well as within the population of the same protein due to minor differences in amino acid sequence as well as post translational modifications. These post-translational modifications can arise during cell culture production as well as during protein purification or storage.[5-6] These structural changes such as C-terminal lysine addition/subtraction or glycosylation, among others, can alter both the efficacy and toxicity of the protein drug.[10] Because of this monoclonal antibodies must be rigorously characterized during both the drug development stage and during the production stage after drug approval by regulatory agencies. Currently monoclonal antibodies are analyzed using multiple analytical methods because no one

method is capable of providing all of the necessary information for characterization. Chromatographic methods are commonly used including size exclusion chromatography, ion exchange chromatography and reverse-phase chromatography.[11-12] In addition to chromatographic techniques electrokinetic methods, such as isoelectric focusing and electrophoresis, are particularly effective for separating antibody variants.[13-14] This is because many of the structural modifications that affect monoclonal antibody drug heterogeneity give rise to charge variants to which electrokinetic separation methods are sensitive. A current and future direction for integrated microfluidic CE-ESI microchips coupled with newly developed surface coating methods is to provide a powerful analytical platform for the analysis of monoclonal antibodies.

The most successful example to date for the analysis of biotherapeutic proteins via CE-ESI-MS has been the analysis of the commercial drug Infliximab in its intact form. Infliximab is an IgG that contains nearly equal abundances of C-terminal lysine variants on the two heavy chains.[15] This means that approximately one third of the protein population has zero C-terminal lysine residues, one third has only one C-terminal lysine residue, and a final third has two C-terminal lysine residues. This residue profile makes Infliximab an excellent candidate for analysis via CE-ESI-MS because the addition of each lysine residue, in addition to changing the mass of the protein by +128 Da, also changes the total charge on the protein (+1) resulting in a change in μ_{ep}. For the analysis of monoclonal antibodies the PEG_{450} surface coating was used in conjunction with a CE-ESI device with a 23 cm separation channel operated at 600 V/cm using a 10% 2-propanol, 0.2% acetic acid (pH 3.2) BGE. An electropherogram for the separation of Infliximab is shown in Figure 5.4A. Figure 5.4B shows the deconvoluted spectrum from each lysine variant.

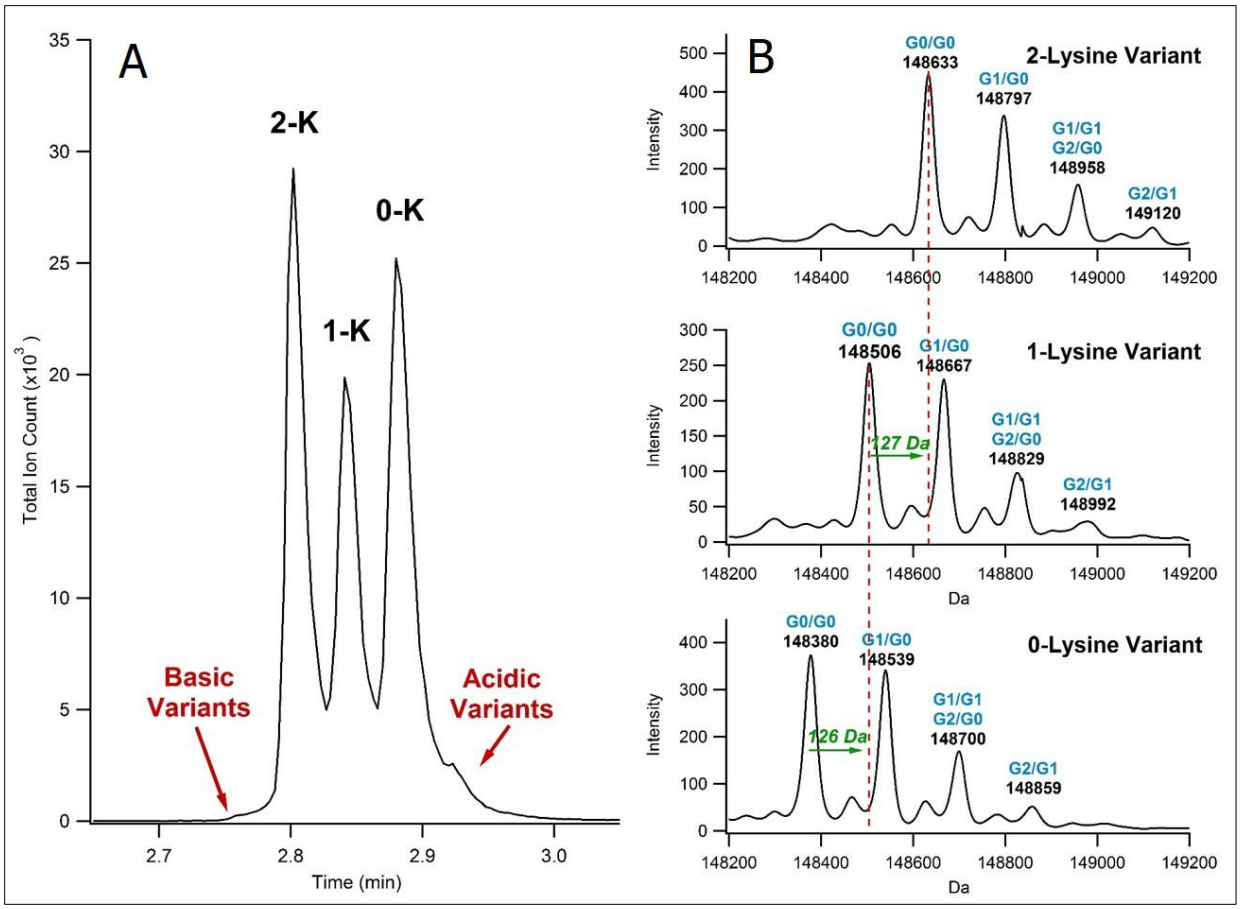

Figure 5.4 Enolase tryptic digest separated on a CE-ESI microchip with a 23 cm separation channel coated with PEG_{450}. The applied field strength was 600 V/cm with 10% 2-propanol, 0.2% acetic acid BGE. A) The protein variant containing two C-terminal lysines is annotated as 2-K, one lysine as 1-K, and zero lysines as 0-K. B) Deconvoluted summed MS spectra for each lysine variant peak. (Figure and data analysis courtesy of E.A. Redman and J.S. Mellors)

The electropherogram in Figure 5.4A shows three major peaks corresponding to the expected lysine variants. These peaks are nearly baseline resolved and smaller peaks to both the left and right of the main peaks are detectable. These smaller peaks indicate proteins with higher pI values (basic variants) and lower pI values (acidic variants) based on the shift in their apparent mobility relative to the main protein peaks. Summed mass spectra were collected for each of the three main peaks by summing data across 2 s for each peak. These mass spectra were deconvoluted using software to generate each mass spectrum shown in Figure 5.4B. The deconvoluted mass spectra generated multiple masses for each lysine variant peak. The most

abundant protein mass for each of the three variants is shifted by the approximate mass of a lysine residue; these mass shifts are shown in green. The mass variations within each lysine variant correspond to differences in the sugar groups (glycans) attached to Infliximab at the conserved arginine residue located on each heavy chain during protein production through glycosylation. These masses are listed in black in Figure 5.3B.The glycan variants are shifted by the addition of a galactose residue (+162 Da). The addition of a galactose residue to one of the N-linked glycans or both of the N-linked glycans for a given protein population are annotated in light blue. The most abundant peak is labeled G0/G0 and structural variants with one additional galactose residue on one N-linked glycan are listed as G1/G0. From these data it is not possible to interpret whether one additional galactose residue has been added to each N-linked glycan on each heavy chain of the molecule or if two additional galactose residues are present on only one of the N-linked glycans. Because of this, annotations listed as both G1/G1 and G2/G0 are provided. The data presented here represents the first time intact mAb charge variants have been separated and identified by MS analysis using a single experiment. The integrated CE-ESI microchip coupled with improved surface coating methods provides a powerful platform for the analysis of intact monoclonal antibodies and holds great promise for the analysis of digested and partially digested antibodies as well. Future work aims to provide evidence for the use of microfluidic CE-ESI-MS as a universal analytical tool for the characterization of biotherapeutic proteins.

5.4 On-chip sample cleanup for CE-ESI-MS of ESI-MS incompatible fluids

The PEG_{450} surface coating requires that the device be operated with a positive high voltage at the injection cross and a lower voltage applied to the EO pump channel. With this configuration the low anodic EOF produced by the coating (3.2×10^{-5} cm^2/Vs) flows from the

ESI pump region up the separation channel toward the injection. A schematic of a PEG_{450} coated device is shown in Figure 5.4.

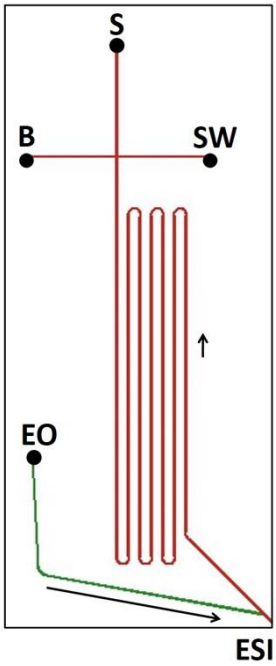

Figure 5.5 A schematic of a CE-ESI microchip with a 23 cm separation channel showing the coating strategy used for analysis of samples with ESI-MS incompatible matrix components. Channels coated with APDIPES are in green, channels coated with PEG_{450} are in red. Black arrows denote EOF direction and relative magnitude.

The direction of the EOF means that bulk flow will proceed into the sample reservoir and only ions of sufficient electrophoretic mobility will migrate towards the injection cross and enter the separation channel upon injection. Positively charged analytes with values of μ_{ep} greater than the EOF, such as peptides and intact proteins, migrate against this weak EOF under the dominant effect of electrophoresis. Negatively charged molecules, neutrals, and low mobility cations will not enter the microchannel network from the reservoir. This mobility bias is beneficial when studying biological samples that are found in matrices with ESI-MS incompatible components.

In the Ramsey lab we have utilized the mobility bias of PEG_{450} coatings to inhibit unwanted components from entering the microchannels for the analysis of intact monoclonal

antibodies as well as hemoglobin digests. Antibody drugs, such as Infliximab, are often stored in a formulation of ESI-MS incompatible salts and surfactants. Using the PEG_{450} coating neutral surfactants, such as Polysorbate 80 which is commonly present in antibody formulations, do not enter the separation channel. Previous work analyzing antibodies in formulation using APDIPES coatings showed that the presence of nonionic surfactants decreased the ESI-MS sensitivity. Use of the PEG_{450} coating alleviates the sensitivity issue without the need for off-chip sample preparation prior to analysis.

Hemoglobin digests have been analyzed recently by our group during the development of CE-ESI-MS procedures for hydrogen/deuterium exchange (HDx) experiments. The main goal of this work is to use high speed, high efficiency CE to generate separations of protein digests that have been deuterated. It is thought that CE could replace LC as a separation method because CE can be carried out more quickly, limiting the amount of back exchange of deuterium labels during analysis. For HDx the enzyme pepsin is used which posed an analytical problem for our APDIPES surface coatings because pepsin is negatively charged at low pH. Pepsin, present in the sample, adhered to the positively charged APDIPES surfaces effectively killing the EOF such that the injection cross of our CE-ESI microchips would fail. Switching to the PEG_{450} coating alleviated this issue because the pepsin cannot enter the separation channel due to its negative charge and electrophoretic mobility toward the anode (sample reservoir).

The use of PEG_{450} coatings for the analysis of hemoglobin digests as well as antibodies in formulation is ongoing. Many questions still remain as to what the limits of the mobility-based sample clean-up are with respect to salts and other ESI-MS incompatible matrix components. Future work will investigate the amount of neutral and anionic species that can be present in samples. One interesting phenomenon that has been observed when using PEG_{450} surface

coatings is a change in analyte signal intensity associated with samples of the same concentration but with different conductivities. The interdependence between sample conductivity and amount of sample injected suggests that the balance of ion flow into the sample reservoir and analyte flow out of the sample reservoir can be manipulated. We have previously observed a decrease in analyte signal when the conductivity of the sample reservoir fluid has been increased, indicating that flux of mobile matrix cations can inhibit the flux of analyte cations from the sample reservoir into the microchannels of the device. It remains to be seen if this effect can be manipulated in order to increase the amount of analyte ion flux into the microchannels to increase signal intensity.

5.5 References

1. Mellors, J. S., Gorbounov, V., Ramsey, R. S., Ramsey, J. M., *Anal. Chem.* **2008**, *80*. 6881-6887.

2. Batz, N. G., Mellors, J. S., Alarie, J. P., Ramsey, J. M., *Anal. Chem.* **2014**, *86*. 3493-3500.

3. Zhu, M. J., Lerum, M. Z., Chen, W., *Langmuir* **2012**, *28*. 416-423.

4. Zhang, F., Sautter, K., Larsen, A. M., Findley, D. A., Davis, R. C., Samha, H., Linford, M. R., *Langmuir* **2010**, *26*. 14648-14654.

5. Reichert, J. M., *mAbs* **2011**, *3*. 76-99.

6. Reichert, J. M., *mAbs* **2010**, *2*. 695-700.

7. Liu, H. C., Gaza-Bulseco, G., Faldu, D., Chumsae, C., Sun, J., *J. Pharm. Sci.* **2008**, *97*. 2426-2447.

8. Arnold, J. N., Wormald, M. R., Sim, R. B., Rudd, P. M., Dwek, R. A., in *Ann. Rev. Immunol.* Annual Reviews: Palo Alto, 2007, vol. 25, pp 21-50.

9. Jones, L. M., Zhang, H., Cui, W. D., Kumar, S., Sperry, J. B., Carroll, J. A., Gross, M. L., *J. Am. Soc. Mass Spectrom.* **2013**, *24*. 835-845.

10. Wang, B., Gucinski, A. C., Keire, D. A., Buhse, L. F., Boyne, M. T., *Analyst* **2013**, *138*. 3058-3065.

11. van den Broek, I., Niessen, W. M. A., van Dongen, W. D., *J. Chromatogr. B* **2013**, *929*. 161-179.

12. Wakankar, A., Chen, Y., Gokarn, Y., Jacobson, F. S., *mAbs* **2011**, *3*. 161-172.

13. Haselberg, R., de Jong, G. J., Somsen, G. W., *Anal. Chem.* **2013**, *85*. 2289-2296.

14. Haselberg, R., de Jong, G. J., Somsen, G. W., *Electrophoresis* **2013**, *34*. 99-112.

15. Shion, H.; Chen, W. *Structural Comparison of Infliximab and a Biosimilar via Subunit* 449 *Analysis Using the Waters Biopharmaceutical Platform with UNIFI*; Waters Corporation 450 Application Note, 2013.